Alma Mater Studiorum – Università di Bologna

DOTTORATO DI RICERCA IN

Ingegneria Chimica dell' Ambiente e delle Sicurezza

Ciclo XXVIII

Settore Concorsuale di afferenza:09/D3-Impianti e processi industriali chimici

Settore Scientifico disciplinare:ING-IND/25-Impianti chimici

Thermal processes for biomass to energy conversion

Ing. Mahsa Baniasadi

Coordinatore Dottorato   *Relatore:*
Prof.ssa Ing. Serena Bandini   Prof. Ing. Valerio Cozzani

                                                                                          Correlatore:
                                                                         Prof. Ing. Alessandro Tugnoli

Esame finale anno 2016

Dedicated to my dearest parents
and Vahid

Abstract

Production of energy from biomassis an attractive alternative to conventional fossil fuels, effectively contribute to reduce problems like resource depletion and greenhouse gas emission. Use of solid feedstock and organic wastes to produce biofuel is seen as a promising route from the economical and sustainability point of view. When using animal waste as biomass, an environmentally safe manner to solve the current problems about disposal of this waste is obtained. Pyrolysis is one of the possible thermochemical methods to convert solid biomasses to valuable liquid and gas products.

In this study, the slow pyrolysis process of poultry litter was investigated using different experimental and analytical techniques. A fixed bed reactor was used for the simulation of the slow pyrolysis process up to a constant temperature (400-800°C) under nitrogen flow. Yields of the different product fractions were determined. Several analytic methods were used to characterise the products. On-line FTIR techniques were used to detect the most significant compounds in the evolved gas (carbon dioxide, carbon monoxide and methane). GC-MS results allowed the identification of the most important categories of compounds in the liquid condensate (phenols, fatty acids, sterols, N-containing compounds). HCNS composition of the products was revealed by elemental analysis and the fate of nitrogen and sulphur, present in relevant amounts in the original substrate, was studied. The energy transfer from the original biomass substrate to the different product fractions was also investigated. The fraction of biomass energy transferred to non-condensable gases raises with pyrolysis temperature and was estimated to be able to thermally sustain the process.

However, the bio-oil obtained from pyrolysis can be used as biofuel only after an upgrading step. In facts, raw bio-oil contains various oxygenated organic compounds, which make it instable, and has high average molecular weight, high viscosity, and low heating value. A suitable method for upgrading bio-oil is catalytic cracking of the pyrolysis products, which converts high molecular weight compounds of the bio-oil into lower-weight molecules. Therefore, in the following step of the present study in-situ catalytic pyrolysis of poultry litter was studied by zeolites (zsm-5) catalyst. In order to study the effect of influential factors (temperature and catalyst to biomass ratio) on the obtained products, experimental design techniques were used.

The results of catalytic and non-catalytic process were then compared and were optimized statistically with the aim of obtaining a compromise between the quality of the products of pyrolysis process and the energy requirement of the process.

Overall, the results achieved shed some light on the potential use of the slow pyrolysis process for sanitation and waste-to-energy valorization of poultry litter.

Contents

b

List of the Figures

e

List of Tables

1-Introduction

1-1-Renewable energy

Due to the increase of the world population and to global warming phenomena, fossil fuels are no more suitable to supply the energy demand of the world. Therefore, new and renewable energy to replace fossil fuel resources are getting more attractive (Isahak et al., 2012). Availability of the low cost fossil fuels probably will continue only for considerable period. In addition, geopolitical issues lower the security of their supply. On the other hand, high greenhouse gas emission urges the need to weaken our reliance on fossil fuels. This would allow a great improvement in sustainability considering natural resource management. This involves operational efficiency, reduction of environmental impact and socio-economic considerations, which are all interdependent (Brennan and Owende, 2010).

Considering the threat of global climate change, most is attributed to the greenhouse gas emission arousing from fossil fuel usage. Climate change has negative consequences for nature and human system. Fossil fuels are the largest contributors (65%) of (GHGs) to the biosphere as it can be seen in Figure 1- 1a. In 2010, around 9500 million metric tons CO_2 was emitted, while the nature has the ability to remove only 12 million tones ("USAenvironmentprotection agency, EPA," n.d.).Therefore, the excess CO_2 must be mitigated by different strategies to neutralize the excess CO_2. The greenhouse gas emitted to atmosphere come mostly from industry, electricity and heat production, transportation, agriculture and land use and etc., as it can be seen in Figure 1- 1b.
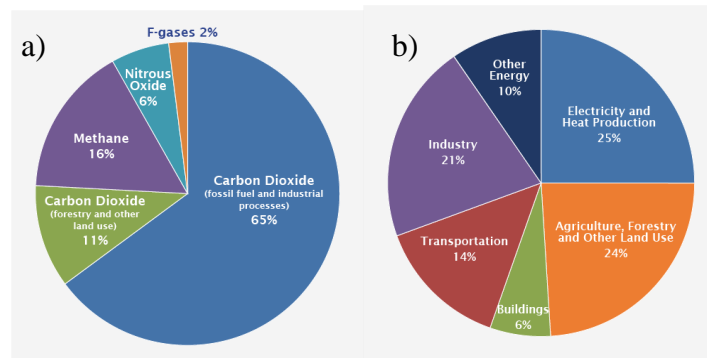
*Figure 1- 1- Global greenhouse gas emission **a)** by gas **b)** by economic sector("USA environmentprotection agency, EPA," n.d.)*

Various effective technologies, including chemical and biological are used for CO_2 mitigation and meeting the agreed target of Kyoto protocol. A selection of a range of effective technologies, including chemical and biological CO_2 mitigation possibilities, has been a focus of several researches. The global strategies are following several targets including (Brennan and Owende, 2010):

✓ Increasing energy efficiency by decreasing energy use per unit of product, process or service

✓ Increasing the use of clean fossil energy by use of fossil fuels coupled with CO_2 separation from flue gases and injection into underground reservoir for gradual release

✓ Increasing the use of renewable energy by development of CO_2-neutral energy resources

With all this, the role of biomass as a part of renewable energy in future of world energy system is not negligible, and there are vigorous energy initiatives in order to find alternative, carbon neutral energy resources.

1-2-Energy from biomass

The most well-known renewable energies are biomass, geothermal, hydropower, ocean, solar PV and concentrated solar thermal power. According to "renewables 2015 global status report" considering traditional use, biomass had the greatest share among global final renewable energy consumption in 2013 ("Renewable 2015 global status report,"n.d).

According to Eurostat, in 2013 more than 60% renewable energy production in the EU was from biomass including (wood and other solid biomass, biogas and liquid biofuels). Excluding wood and other solid biomass, the share would be much smaller (around 13%), and hydropower would have the largest share (around 16%) ("Eurostat, n.d.). This is shown in Figure 1- 2.
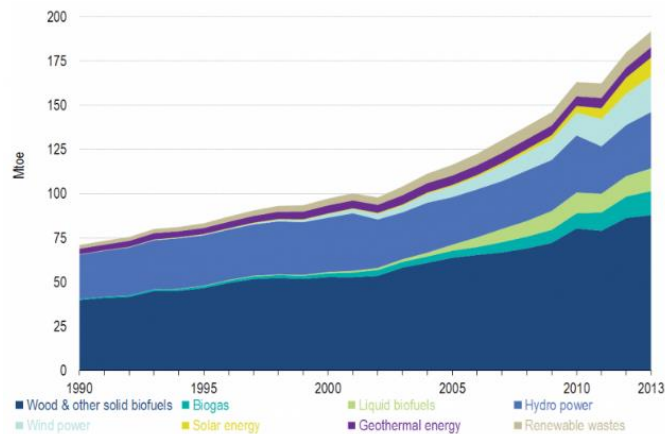
Figure 1-2- Share of different types of renewable energy in the year 2013 ("Energy from renewable sources - Statistics Explained," n.d.)

According to 2014 U.S. renewable energy databook, (n.d.), biomass composed 49% of total renewable energy production in U.S in 2014 which is the largest share among the others (following by hydropower 25% and wind 18.1 %).

However, the use of biomass as an energy source varies in different countries depending on the level of development. Prior to biomass utilization different cultural, socio-economic and technological factors in a given locality must be analyzed. This way, biomass resources could play determining role in meeting future energy requirement (Capareda, 2011).

1-3-Biomass nature and structure

The most general definition of the word biomass, which was invented in the early 1970s, refers to all living matter with particular use as source of energy and fuel. Biomasses are composed primarily of cellulose, hemicellulose and lignin and several extractives such as tannin (Gaur and Reed, 1995). Virgin biomass comes directly from plants or animals (Basu 2013).

Another definition of biomass is a mass that is naturally produced by photosynthesis from water and CO_2. They are organic matters including agricultural crops and trees, wood and wood residues, grasses, animal manure, municipal residues and other residue materials as defined by US department of energy ("Glossary - Biomass Energy Data Book," n.d.).

Biomass is mostly composed of carbohydrate compounds (cellulose, hemicellulose, lignin) and minor amounts of other organics. From elemental composition, they mostly contain carbon, hydrogen and oxygen and quit high energy content (Isahak et al., 2012).

1-3-1-Cellulose

Cellulose is the most common component of biomass and constitutes 30-100% of plants. This material is synthesized by marine and terrestrial plant and by bacteria, animals and fungi. The generic formula of cellulose is $(C_6H_{10}O_5)_n$. Cellulose is a long chain polymer with high degree of polymerization (10000) and large molecular weight (500,000) molecule of d-glucose with the range of units from 1000 (for wood) to 3000 (for cotton). The crystalline structure of cellulose contains thousands of units, which are made up of many glucose molecules. All these, give cellulose a high strength and as a result, cellulose forms skeletal structure of most terrestrial biomass. The major part of glucose in cellulose is composed of D-glucose, which is made of six carbons or hexose sugars. Cellulose is highly insoluble and composed high percentage of wood (40-44%) by dry weight. Cellulose is responsible for tar formation during gasification of biomass (Basu 2013) (Guar and Reed, 1995). Figure 1- 3 shows the molecular structure of cellulose.
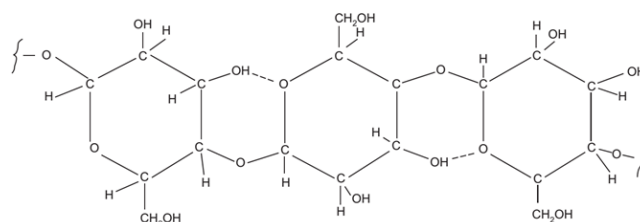
Figure 1-3- Molecular structure of cellulose (Basu 2013)

1-3-2-Hemicellulose

Hemicellulose is a group of carbohydrates with a branched chain structure and a lower degree of polymerization (100-200). The generic formula of hemicellulose may be described by $(C_5H_8O_4)_n$. Hemicellulose generally constitute 12-40% of most of the biomass. Various types of hemicellulose exist, while xylan is the most abundant one. Hemicellulose is the assembly of five and six membered sugar while cellulose is a linear single compound. Hemicellulose is composed of fewer monomers than cellulose, typically 300, and is normally branched and may be attached to other functional units, particularly acetyls (Guar and Reed, 1995). Hemicellulose exists in the cell wall of the plants in addition to cellulose. The structure of hemicellulose is random and amorphous and has little strength in contrast to cellulose, which is resistant to hydrolysis. More gas yield and less tar yield can be obtained from hemicellulose in comparison to cellulose. Hemicellulose is soluble in weak alkaline solutions and can be hydrolysed by dilute acid or base, easily (Basu 2013). Figure 1- 4 shows the hemicellulose structure.
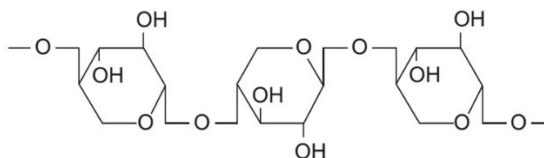
Figure 1-4- Molecular structure of xylan as a typical hemicellulose (Basu 2013)

1-3-3-Lignin

Lignin is three dimensional highly branched polymer of 4-propenyl phenol, 4-propenyl-2 methoxy phenol, and 4-propenyl-2.5-dimethoxyl phenol, which compose 4-35% of the biomass and is the principal non-carbohydrate fraction. Lignin is deposited in an amorphous state surronding the cellulose fibers in wood and is bounded by ether bonds directly to the cellulose and has no exact structure. Lignin is an integral part of secondary cell wall of plants and acts as a cementing agent for holding adjacent cells of cellulose fibers together. After cellulose lignin is the most abundant polymer on earth (Guar and Reed, 1995) (Basu 2013). Figure 1- 5 shows some structural units of lignin.
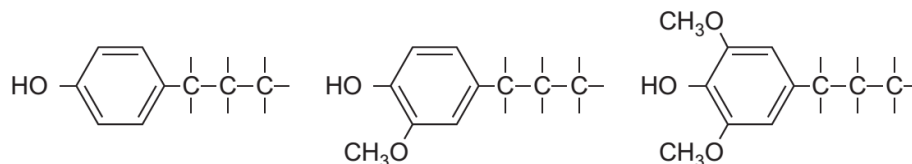
Figure 1-5- Structural units of lignin (Basu 2013)
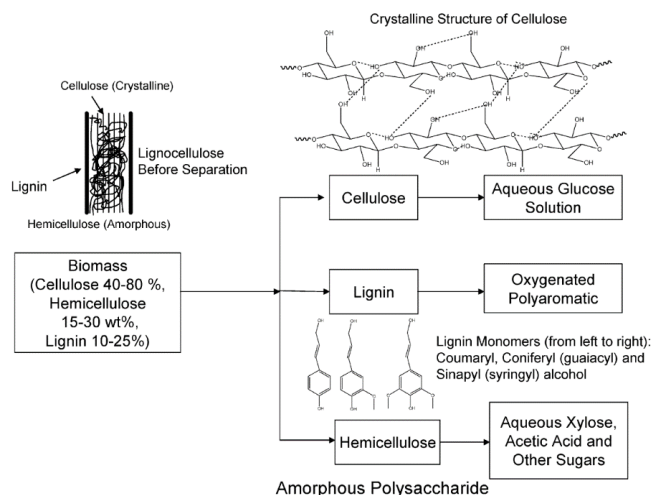
Figure 1-6- Structure of Lignocellulosic material (Huber et al., 2006)

Figure 1- 6 shows the biomass structure including cellulose, hemicellulos and lignin. In addition to these components, most of biomass contains extractive such as terpenes, tannin, fragrances and etc. These extractive usually evaporates during heating at relatively low temperatures and therefore do not ususally show up in thermal analysis (Guar and Reed, 1995).

The most important characteristics of biomass that must be known prior to use are proximate and ultimate analysis. HHV of biomass is usually estimated (which is in the range of 15 – 25 MJ/kg) and is compared with coal (Capareda, 2011). Figure 1- 7 shows the characteristics of biomass that are important to be known. Proximate analysis data are usually obtained by thermogravimetric analysis under nitrogen atmosphere, with a ramp of 10 °C/min up to 800 °C (ASTM E1755, EN 15148, ISO 17246) and then changing the carrier gas to air in order to obtain the ash and fixed carbon. Ash is equal to the weight of the residue at the end of the test (after combustion). The volatile fraction is the weight percentage change during thermal degradation up to the final isotherm (at 800 °C) in nitrogen

flow. The fixed carbon is the amount of carbon losses during combustion process on moisture free basis. Figure 1- 7 shows well the concept of elemental analysis and proximate analysis of biomass.

Wet biomass				
Dry matter (total soilds)				Moisture
Volatile solids / Elemental composition			Ash (metals, materials, adventitious materials)	
Cl, ... / N, S, ... / O / H / C			Elemental composition (Si, Al, Ti, Fe, Ca, Mg, Na, K, P, S, Cl, C, H, O,....)	
Volatile Matter		Fixed Carbon		
Structural components		Extractives (sugars, starch, lipids, protein, inorganics,....)		
Cellulose / Hemi-cellulose / Lignin / Pectin,...				

Figure 1- 7- Biomass composition (Van Alfen, 2014)

1-4-Biomass types

Biomass are usually categorized in primary, secondary and tertiary ("Glossary - Biomass Energy Data Book," n.d.). First generation of biomass used for energy valorization, which have now attained economic levels of conversion by conventional technology, and are from food and oil crops including rapeseed oil, sugarcane, sugar beet, and maize, as well as vegetable oils and animal fats (Brennan and Owende, 2010). These are composed mostly from carbohydrates and dissolve easily. They are relatively easy to derive liquid fuels from fermentation or other processes. Most commercial ethanol plants use crops as feedstock. Natural crops and vegetables are a good source of starch and sugars and, therefore can be hydrolyzed. Some vegetables and crops (e.g., coconut, sunflower, mustard, and canola) contain fat, providing a good source of vegetable oil (Basu 2013). The use of these types of biomass remains limited due to several issues including competition with food and fiber production, use of arable land, high water and fertilizer requirements and a need for conservation of bio-diversity (Brennan and Owende, 2010).

Therefore, the second generation of biomass used for energy valorization was intended to produce energy products from the whole plant matter of dedicated energy crops or agricultural residues, forest

harvesting residues or wood processing waste, rather than from food crops. However, this generation has not reached the commercial exploitation scale (Brennan and Owende 2010). These biomasses are lignocellulosic material and are non-starch, fibrous part of plant materials, with major composition to be cellulose, hemicellulose, and lignin. These kinds of biomass are not easily digestible by humans; therefore they are not part of human food chain. There are defined "energy crops" which are the plants that are cultivated exclusively for energy production. Short growing period, high yields and little or no fertilizer requirement are the characteristics of these plants. Woody crops such as miscanthus, willow, switchgrass, and poplar are the examples of these biomasses (Basu 2013). However, there are still some concerns regarding their use, such as land use and required land use change (Brennan and Owende 2010).

Third generation of fuels are from microalgae and are free from the drawbacks of previous generations (Brennan and Owende 2010).

Another classification is according to European committee for standardization, by two standards for classification and specification (EN 14961) and quality assurance (EN 15234) of biomass. The biomass is classified under four broad categories based on its origin, which are (Basu 2013):

- ✓ Woody biomass
- ✓ Herbaceous biomass
- ✓ Fruit biomass
- ✓ Blend and mixtures

By this classification, trees, bushes, and shrubs fall under woody biomass. Plants that die at the end of the growing season are among herbaceous biomasses. This group also includes grains and cereals that grow on such plants. However, fruits are classified as a separate group. When biomass are mixed intentionally, it is called blends while, when they are mixed unintentionally they are called mixture (Basu 2013).

Another classification which done by Basu, 2013 classifies the biomass in two groups of virgin biomass and waste biomass according to Figure 1- 8.

A. Virgin biomass	A.1 Terrestrial biomass	i. Forest biomass ii. Grasses iii. Energy crops iv. Cultivated crops
	A.2 Aquatic biomass	i. Algae ii. Water plant
B. Waste biomass	B.1 Municipal waste	i. MSW ii. Biosolids, sewage iii. Landfill gas
	B.2 Agricultural solid waste	i. Livestock and manures ii. Agricultural crop residue
	B.3 Forestry residues	i. Bark, leaves, floor residues
	B.4 Industrial wastes	i. Demolition wood, sawdust ii. Waste oil/fat

Figure 1-8- Biomass classification to virgin and waste biomass (Basu 2013)

In this classification, waste biomasses are derived from virgin biomass like trees, vegetables, meat during the different stages of their production or use. An important source of waste biomass are municipal solid waste (MSW) which contains some renewables like food scraps, lawn clippings, leaves, and papers. It also contains, nonrenewable components such as plastics, glass, and metals which are not considered biomass. Refuse derived fuel (RDF) are the combustible part of MSW which is usually separated and sold. Sewage sludge usually contains human excreta, fat, grease, and food wastes and is an important biomass source. Waste produced in sawmills during the production of lumber from wood is another important waste biomass. Landfilling is a new method, which has basis of traditional disposing of garbage. The land is filled with waste, which decomposes and methane gas is produced. However, for modern landfilling techniques careful lining of the containment must be considered (Basu 2013).

Talking about biomass types for energy purposes, sustainability means an ecosystem condition in which biodiversity, renewability, and resource productivity are maintained over time ("Glossary - Biomass Energy Data Book," n.d.). When a biomass is used for energy valorization purposes, it should (Brennan and Owende 2010):

✓ Be competitive or cost less than petroleum fuel

✓ Require low to no additional land use

✓ Enable air quality improvement (e.g. CO_2 sequestration)

✓ Require minimal water use

1-5-Poultry litter as biomass

The definition and composition of poultry litter is usually different from source to source. However, generally talking, poultry litter means a composite mixture of bedding material, manure, feathers, and spilled feed obtained from of hatcheries, broiler, turkey and egg laying (Mante and Agblevor, 2010). Poultry litter or animal manure in general is a low cost and indispensable by-product of feedlots. On the other hand, the safe and sustainable disposal of this waste is a major industrial problem, which is getting more sever every year as a result of the need for more animal meat production to feed the growing population of the earth (Agblevor et al., 2010). The estimated amount of poultry litter manure produced in Italy in 2010 was 2472000 ton per year ("European commission directorate general environment" n.d.). The amount of poultry meat production worldwide increased 1.4% from 2013 to 2014 (2015 annual report of Association of Poultry Processors and Poultry Trade in the EU Countries – ASBL, n.d.). Therefore, the use of animal manure as a biomass to be converted to energy products is doubly beneficial, since, it provide a safe disposal method by which the organic matters contained in it are reutilized (Zhang et al., 2011).

Animal manure like the other biomasses is composed of celluloses, hemicelluloses, lignin plus having lipids, proteins, simple sugars, starches, water, hydrocarbons, phosphatase, ash, and other compounds. As it was mentioned before, the conversion of hemicelluloses and celluloses takes place mush easier than the conversion of lignin (Zhang et al., 2010).

New regulation for waste disposal and management requires more sustainable strategies with the aim of waste minimization, separation and re-use of materials and potential production of biofuels and bioproducts from biomass waste. By these strategies, the volume of waste that needs to be disposed decreases largely and creates sustainable economic opportunities (Schnitzer et al., 2007).

Conventionally the litter is used as a valuable source of plant nutrients and can substitute the use of inorganic fertilizers and also as a protein source for cattle feeding. However, these conventional methods are no more environmentally accepted and are under pressure. Land application of poultry litter may provide valuable organic matter and nutrients, which are good for crop growth, but if they over-applied to the land, they will enter water resources and lead to excessive level of phosphorus (P) and nitrogen (N) and finally eutrophication of lakes and rivers (Agblevor et al., 2010). Nitrate (NO_3) contamination of groundwater may also occur, which if be present in drinking water may cause methaemoglobinaemia (blue baby syndrome), cancer, and respiratory illness in humans and fetal abortions. Spread of pathogens, production of phytotoxic substances, air pollution and emission of greenhouse gases (methane emission) are all negative consequence of poultry litter land filling (Kelleher et al., 2002).

Use of chicken litter for cattle feeding, will lead to mad cow disease and contamination of the food chain. Usually around 20% or higher amount of poultry litter is added to cattle feed which was found to be beneficial and cheap source of proteins for the animals. However, the recent concerns about bovine spongiform encephalopathy (BSE) hindered the continued use of the poultry litter for cattle feeding (Agblevor et al., 2010).

The use of poultry litter for energy application and conversion of biomass into biofuels is the more efficient method for waste disposal. The production of energy products from poultry manure is sustainable strategy in comparison to the available methods such as composting, incineration, land application, and landfill of the animal residue (Schnitzer et al., 2007).

Using poultry litter for energy application, some factors must be considered, such as low calorific value (10–16 MJ/kg) of that biomass, which is even less by increasing moisture content (Agblevor et al., 2010). High nitrogen content (in the form of protein and urea) and high amount of ash (alkali metals mainly K and Na) differs poultry litter from other types of biomasses and limits their commercial application for thermochemical conversion. The high (15–20 wt%) ash content and low fusion temperature of poultry litter may cause fouling, slagging, corrosion and loss of fluidization may

occur during their industrial use (Giuntoli et al., 2009). This high ash amount, remains in the char after conversion. This way, the obtained char has the potential to be used as fertilizer (Ro et al., 2010). In addition, there is need for deep investigation of the fate of nitrogen to avoid the excessive emission of NO_x and N_2O (Giuntoli et al., 2009). The possible release of phosphorus as phosphine gas during gasification must be also investigated (Sheth and Bagchi, 2005).

1-6-Biomass conversion to energy

Biomass can be converted to the fuels of different states including liquid fuels (ethanol, methanol, biodiesel, Fischer-Tropsch diesel) and gaseous fuels (hydrogen and methane), which are all called biofuels. Liquid biofuel can be used as fuel for vehicles, but also for fuel engines or fuel cells for electricity generation. However, more advanced research and development is needed to produce a bio-oil with the quality to be used for transportation applications (Wright et al., 2006).

Biomass conversion methods can be classified in three major groups (thermochemical, biochemical, physicochemical), with the first two to be the most important. Figure 1- 9 shows the biomass processing options and utilizations.

No significant advantage of one group of technologies over the other was reported. However, thermochemical process yields longer chain hydrocarbons, which are favorable for transportation fuel. Combination of biochemical and thermochemical technologies synergistically in integrated biorefineries was suggested with the added benefit of increased flexibility and efficiency (Butler et al., 2011). In the following thermochemical and biochemical biomass conversions are explained since they are the major conversion methods.
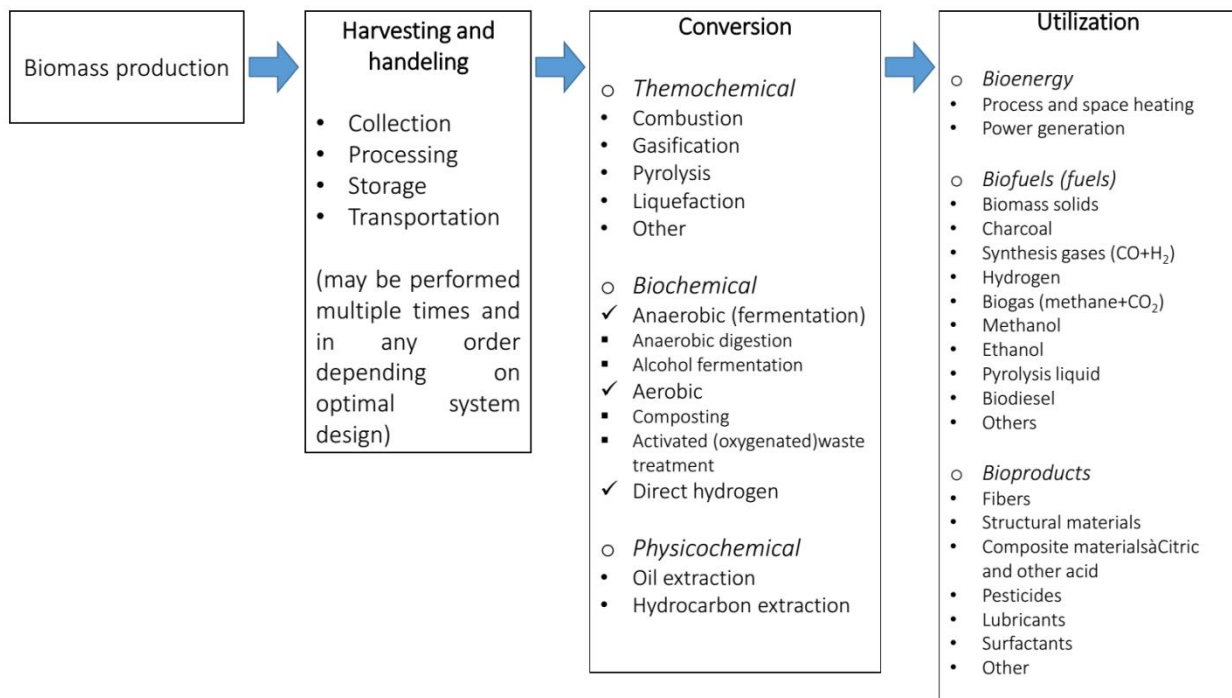
Figure 1-9- Biomass processing options (Van Alfen, 2014)

1-6-1- Biochemical methods

Anaerobic digestion is the most common biomass biochemical conversion method. Therefore, this process is described in the following.

Anaerobic digestion is a process in which the biomass is treated by naturally occurring microorganisms in the absence of air (oxygen). Apart from energy generation, anaerobic digestion is beneficial from pollution control aspects. The products are combustible gaseous fuel comprising mostly from methane (CH_4) and carbon dioxide (CO_2). Some traces of other gases such as nitrogen (N_2) and hydrogen sulphide (H_2S) may be also present. The term "biogas" is usually referred to the gaseous products of this process. All the nitrogen, phosphorus and potassium content remain in the digested biomass (Capareda, 2011).

Anaerobic digestion process contains three steps, which are conversion of complex organic solids into soluble compounds by enzymatic hydrolysis, conversion of formed soluble organic material into mainly short-chain acids and alcohols during the acidogenesis step and finally the conversion of

second step products into gases by different species of strictly anaerobic bacteria (methanogenic bacteria) which is methanogenesis step (Capareda, 2011).

Biogas obtained from anaerobic digestion contains between 50-80% methane. Methanogenic bacteria require a pH range of 6.4 to 7.2 for growth, while acid producing bacteria can tolerate low pH. During the second step, the acid producing bacteria lower the pH and accumulate acids and salts of organic acids. Methane-forming organisms should rapidly convert the products of the second step; otherwise the condition would become adverse to methane formers. Therefore, long retention time is needed in reactors to obtain equilibrium to convert biomass wastes into methane. The most suitable types of biomass for anaerobic digestion are municipal wastes and livestock manures. In addition, aquatic biomass and micro algae have potential to be used as valuable sources for anaerobic digestion. Ability to use high water content biomass (up to 99%), potential of biomass residue to be used as a fertilizer, smaller unit requirement are the other advantages, while disposal of large quantity of sludge and high cost of biogas storage are disadvantageous of this process. Usually, a significant fraction of biogas is consumed for maintaining the reactor temperature otherwise the microorganism with the ability to tolerate lower or moderate temperatures must be used (Capareda, 2011).

1-6-2-Thermochemical conversion

During thermochemical conversion methods, at high temperatures biomass easily converts to other forms of energy products since the molecules break down to smaller and less complex molecules in the form of liquid and gaseous and some solid products. The oldest thermochemical biomass conversion is combustion by which the complete oxidation to carbon dioxide (CO_2) and water (H_2O) occurs. The most important thermochemical conversion methods are combustion, pyrolysis, gasification, liquefaction and torrefaction. Using thermochemical conversion processes some advantageous can be obtained as follows (Capareda, 2011):

✓ Rapid completion of reactions

✓ Large volume reduction of biomass

✓ Production of range of liquid, solid and gaseous products

✓ No need for additional heat to complete the process in some processes

Biomass pyrolysis is a technology to partially oxidize the biomass and is older (1980s) than gasification (Butler et al. 2011). The most important thermochemical technologies to convert biomass to energy are pyrolysis and gasification. Since pyrolysis is the main scope of this work, it is explained in separate section.

1-7- Pyrolysis

The word pyrolysis has Greek origin which is combination of pyr "π΄ υρ-fire" and lysis "λ΄ υσις-breakdown/separation" and therefore it specifies the process which is disintegration of material due to heat (Dahlquist, 2013).

Pyrolysis is the thermochemical conversion of biomass in the total absence of oxygen, for thermal decomposition of biomass at high temperature (above 300-400 °C) into useful products in the form of gas, liquid, and solid. During pyrolysis, the large hydrocarbon molecules of biomass are broken down into smaller hydrocarbon molecules, gases such as (CO, CO_2, CH_4…) and solid carbon as char. The high temperature is called the pyrolysis temperature and the biomass is hold for a specific time at that temperature. This process is not exothermic unlike combustion (Basu 2013).

Figure 1- 10, shows the thermal decomposition path that the biomass goes through during pyrolysis process. The primary products of pyrolysis are condensable gases (tars) and solid char. The condensable gas goes through further secondary reactions and break down into non-condensable gases (CO, CO_2, H_2, and CH_4), liquid, and char. The secondary reactions occurs in gas-phase homogeneously and a part of it through gas-solid phase heterogeneous thermal reactions (Basu 2013).
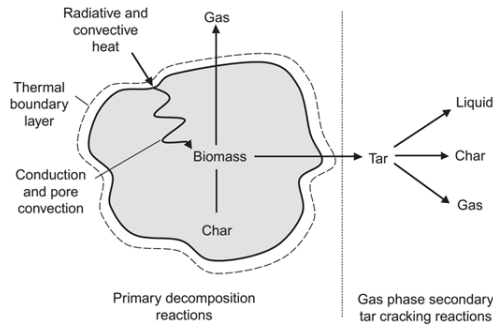
Figure 1-10- Thermal decomposition of biomass to energy products during pyrolysis (Basu 2013)

Pyrolysis is similar and a mixture of processes such as cracking, devolatilization, carbonization, torrefaction, dry distillation, destructive distillation, and thermolysis. However, it is far from gasification process in which chemical reactions take place in the presence of an external agent known as gasification agent. Pyrolysis temperature is usually in the range of 300-650 °C, while the gasification temperature is in the range of 800-1000 °C. However, pyrolysis is usually considered as a primary step in gasification (Basu 2013).

Pyrolysis process can be described by Equation 1-1, which is a generic formula to describe biomass pyrolysis (Basu 2013).

$$C_nH_mO_p + heat \rightarrow \sum_{Liquid} C_aH_bO_c + \sum_{Gas} C_xH_yO_z + \sum_{Solid} C + H_2O \qquad \text{Equation 1-1}$$
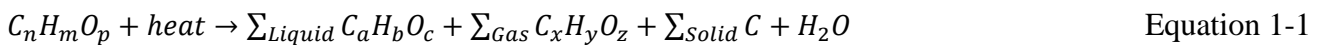
The general products of pyrolysis process are as follows (Basu 2013) (Dahlquist,2013):

✓ Liquid bio-oil also called bio-crude (oxygenates, aromatics, water, products of low degree of polymerization, tars, etc)

✓ Solid called char (mostly char or carbon, and ash)

✓ Gas (e.g., CO_2, H_2O, CO, C_2H_2, C_2H_4, C_2H_6, C_6H_6)

The products of pyrolysis process are described more in detail in section 1-7-6.

Pyrolysis process can be divided in to four stages thermally. However, there are always overlap between the stages (Dahlquist, 2013).

Drying step: During the initial phase of biomass heating at low temperature (around 100°C), the free moisture which is bounded loosely evaporates. Then the heat is conducted into biomass interior part.

When the humidity is high, the water promotes melting of lignitic fraction, which solidifies after cooling (Dahlquist, 2013).

Initial stage: In the initial stage, (100-300 °C) dehydration of biomass takes place exothermically. Water and low-molecular-weight gases like CO and CO_2 are released at this stage (Dahlquist, 2013).

Intermediate stage: Primary pyrolysis takes place in this step in the temperature range of (200-600 °C). Most of bio-oil precursors are produced at this stage in addition to primary char and non-condensable gases (Dahlquist, 2013).

Final stage: which takes place at higher temperatures (300-900 °C) involves secondary cracking of volatiles into char and non-condensable gases and the formation of secondary char. If the volatile exit rapidly the process, it will condense as bio-oil or tar. Above 600 °C, hydrogen production increases quickly (Dahlquist, 2013).

1-7-1- Pyrolysis types

Pyrolysis products and their characteristics depend strongly on the operating parameters, since they can affect the nature of process, in the following ways (Dahlquist, 2013):

- Heat transfer to the biomass particles

- Beginning of the primary endothermic reactions and volatile release

- Transfer of hot volatile to cold non-pyrolyzed part of biomass

- Deposition of volatiles in cold part of particle and secondary reactions that yields to secondary char formation

- Initiation of secondary pyrolysis reactions while primary pyrolytic reactions are going on simultaneously in competition

- Occurrence of further thermal decomposition, recombination of radicals

All the above mentioned mechanisms depend on vapors residence time, temperature, pressure profile and etc. The effects of these factors are discussed more in details in the following section (section 1-7-2- to 1-7-4).

These factors have influential role on the distribution of the products. Char production is enhanced at lower process temperatures and long residence time, while long residence time and high temperature favors gas production. Liquid yield improves at moderate temperature and short residence time (Dahlquist, 2013).

Based on operating conditions (specially heating rate), pyrolysis process can be divided into fast and slow, each of which with specific products characteristics and applications. However, the terms fast and slow pyrolysis cannot be defined precisely. Slow pyrolysis is the process in which the vapor residence time is in the order of minutes and promotes the production of char and gas. The production of the secondary char enhances during the slow pyrolysis, since adequate time is available for condensable vapor to react with primary char and produce non-condensable gases and secondary char. In the slow pyrolysis, the heating rate is slow (0.1–1 °C/s) and the residence time is quite long. Char coal is the major product at these conditions and the process is called also carbonization (Dahlquist, 2013).

Fast pyrolysis, instead is a process in which the vapor residence time is on the order of seconds or milliseconds, and favors the production of liquid product (bio-oil) (Dahlquist, 2013)(Lima et al., 2009). During the fast pyrolysis, the biomass is heated rapidly in the absence of oxygen at moderate temperatures (450-600°C). In this process, the pyrolysis products, both condensables and non-condensable gases, stay in the reactor for very short residence time (30-1500 ms). By these conditions, the highest yield of bio-oil is achievable 70-75% (Dahlquist, 2013).

1-7-2-Effect of temperature on pyrolysis products

During pyrolysis, the sample is heated from the ambient temperature to the pyrolysis temperature with a specific rate and is held at that temperature up to the completion of the process. This temperature can affect both yield and characteristic of the products. The char yield usually decreases with temperature increase, while, the heating value of the char product increases as a results of presence of

more fraction of fixed carbon, which has a high heating value in char after volatile removal. The non-condensable gas (CO_2, CO, H_2, CH_4) yield increases with temperature (Dahlquist, 2013).

At lower temperature, CO_2 yield is high and declines at higher temperatures. Hydrocarbon production reaches a peak at 450 °C and declines above 500 °C (Dahlquist, 2013).

1-7-3- Effect of heating rate on pyrolysis products

The heating rate can affect the yields and characteristics of the products as well. Rapid heating rate yields more condensable volatiles and bio-oil. At slower heating rate, more char and gas product are obtained (Dahlquist, 2013).

1-7-4- Effect of residence time on pyrolysis products

In addition to heating rate, the residence time of the product in the reactor can be influential in pyrolysis. By slow or gradual removal of volatiles from the reactor and higher residence time, secondary reactions between char particles and volatiles are promoted and leads to secondary char formation (Dahlquist, 2013).

1-7-5- Pyrolysis model

A large number of models have been proposed to explain decomposition of biomass during pyrolysis process. These models can be classified in three categories (Patwardhan, 2010):

- ✓ First category models describe pyrolysis as a set of single step multiple reactions.
- ✓ Second category, which is known, also as "global decomposition models" are the models in which thermal decomposition is expressed as a single first order irreversible reaction.
- ✓ Third category are the models in which pyrolysis is described as a two step process and accounts for primary and secondary reactions.

Table 1- 1 summarized different models proposed by different researchers for pyrolysis process. The first four do not considering the secondary reactions. Among these four models Broido-Shafizadeh
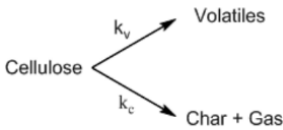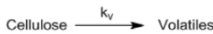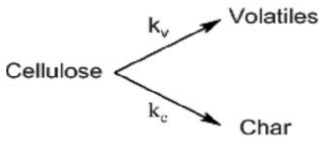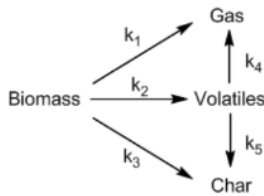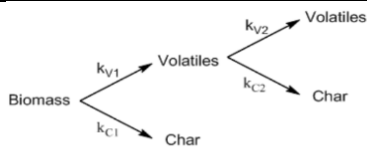
model is the most accepted model, which can be applied qualitatively to the all biomasses. This model involves four step reactions:

- Reaction 1 is the step in which the biomass is converted to active intermediates. Reaction 1 products undergo two different reaction (first order) paths in parallel which are path 1, dehydration and path 2 depolymerization. Path 1 is dominated at low temperatures (<300 °C) and slow heating rates and path 2 at fast heating rate and higher temperature (>300 °C).

- Dehydration path involves also decarboxylation, and carbonization through several steps and produces char and non-condensable gases including water vapor, carbon dioxide, and carbon monoxide.

- Depolymerization path involves scission, which leads to formation of vapors including tar and condensable gases. In this path, levoglucosan is formed as an important intermediate product.

- Secondary reactions (reaction 4) are the cracking of primary volatiles to secondary products (secondary char, tar and gases) (Dahlquist, 2013).

Reaction 2 and 3, which are in parallel are in competition. The activation energy of reaction 3 (depolymerization) is more than reaction 2 (dehydration). Therefore, the condition, in which low temperature and long residence time exist, favors reaction 2 and produce primarily char, water, and carbon dioxide and at higher temperatures reaction 3 is favored and yields to mainly gas. If the temperature would be moderate and the residence time would be short, it will avoid secondary cracking, and the final product will be the condensable volatiles and promote bio-oil production (Dahlquist, 2013).

Table 1- 1- Models proposed for biomass (or cellulose) pyrolysis (Patwardhan 2010)

Model Name	Category	Explanation	Scheme
Broido and Nelson	First	At low temperatures (<250 °C) char and low molecular weight volatiles At high temperatures (>250 °C) competing reaction for tar formation	 Broido and Nelson (1975)
Broido and Shafizadeh	Third	First formation of intermediate (active cellulose) Then 2 path of dehydration or depolymerisation	 Broido and Shafizadeh (B-S model) (1979)
Cooley and Antal	Second	Single first order reaction with activation energy 193 kj/mol	 Cooley and Antal (1988)
Sunberg and coworkers	First	Transition from high activation energy to low activation energy ✓ Two single step competing reaction: Endothermic of tar evaporation at high temperatures ✓ Exothermic reactions of char formation favored at low temperature	 Suuberg and co-workers (1996)
Modified Broido-shafizadeh	Third	Production of char, gas and bio-oil through three competing reactions Secondary decomposition of bio-oil to secondary char and gas	 Modified B-S model (1979)
Koufopanous	Third	Two competing reactions producing primary volatiles and char which react to produce secondary volatiles and char	 Koufopanos (1991)

1-7-6-Pyrolysis products

During pyrolysis, biomass decomposes to condensable and non-condensablegases, which are called primary gas. Condensable fraction of volatiles is made of heavier molecules, condense by cooling, while the non-condensable fraction contains lower-molecular-weight gases like carbon dioxide, carbon monoxide, methane, ethane, and ethylene, and do not condense by cooling. By further secondary cracking of condensable fraction, which happens at higher temperatures, new non-condensable fraction of gases is produced which is called secondary gases. The secondary gas has much higher heating value in comparison to primary gases. However, the final gas product is the mixture of both gases (Dahlquist, 2013).

During pyrolysis, the biomass constituents make varying contributions to the products. As mentioned before, volatiles are come mostly from cellulose and hemicellulose. However, cellulose decomposition yields mostly to condensable vapor and hemicellulose yields to more non-condensable gases and less tar. As a result of high aromatic content, lignin makes a large contribution to char yield. Among the biomass constituents, hemicellulose is the least stable and decomposes within 200-300 °C as a result of lack of crystallinity. Cellulose decomposes at higher temperatures around 300-400°C and pyrolyzes to a monomer called levoglucosan. This monomer vaporize above 500 °C to gas and oil and therefore form low char. Lignin decomposition takes place over a wide temperature range (280-500°C) and maximum decomposition rate takes place at 350-450 °C and produces more aromatic and char in comparison to cellulose. Around 40% of lignin weights yield in char. Lignin also contributes to bio-oil yield around 35%. Linkage of ether and carbon-carbon bands yields some phenols. Only around 10 % of lignin weight contributes to gas (Dahlquist, 2013). The three products of the pyrolysis are described in the following.

1-7-6-1-Char

Char is a stabilized material obtained from biomass in which carbon is stored mainly in a highly recalcitrant chemical form (Shackley et al., 2010). In general, char comprise mainly from stable aromatic forms of organic carbon. This carbon cannot be readily returned to atmosphere even under desirable environmental and biological condition opposite of carbon in original biomass (Sohi et al., 2010). Therefore, char production is a good carbon sequestration method in which large part of carbon is retained in char in stable solid form and can be stored in the soil for centuries, instead of carbon release to atmosphere (Dahlquist, 2013). Apart from pyrolysis, char can be produced by other processes such as carbonisation, charcoal retorts and gasification (Bakhshi et al. 1999).

Temperature can affect the characteristics of the produced char. At low pyrolysis temperatures (<400 °C) the obtained char is acidic (pH <7). By raising the temperature the produced char is alkaline (pH>7). At very high temperature, (800 °C) char can reach even the pH of 12. The surface area of the char can be affected by temperature as well. Higher temperature yields to more surface area due to the development of micropores structure (Shackley et al., 2010). The energy content of char can vary between 30 and 35 MJ kg^{-1}, according to the original biomass. For this energy, char is usually used to provide the heat driving the primary pyrolysis through burning or gasification, or to dry incoming feedstock (Sohi et al., 2010).

Char is composed from mostly carbon, but it can also contain hydrogen and oxygen. Large pore surface area is the characteristic of the char. Char contains inorganic materials and organic solids (ash) and carbonaceous residues. Char is formed mostly as a result of lignin decomposition. Char is a very flammable material with auto ignition temperature in the range of 200 and 250 °C, which is in the range of powdered coal. The ash content of char is 6–8 times larger than the original biomass. High alkali content of char may cause problems in combustion application (Dahlquist, 2013).

Important characteristics of char that must be considered before application are as follows (Tang et al., 2013) (Dahlquist, 2013) (Bakhshi et al. 1999):

- Internal surface area (BET)
- Porosity

- Amount of functional group
- pH
- Cation exchange capacity (CEC)
- Carbon recovery
- Density
- Ash content
- Elemental composition (CHN analysis)
- Methylene blue number
- Iodine number

High porosity and surface area gives char high sorption capacity. Chars can be more than 90% pore space and can exhibit surface areas higher than 400 m^2/g. All the above-mentioned characteristics can be changed by the original biomass used and by pyrolysis conditions. As an example the values reported for the surface area of char obtained from rice straw pyrolysis were (234.9 m^2/g), porosity (0.4392 ml/g) and the amount of functional groups (2.995 mmol/g). The high ash amount of char may cause fouling problems, but it gives the char the potential to be used in addition to fertilisers to enhance fertiliser use efficiency. The presence of Ca complexes on the surface, such as hydroxides, oxides and carbonates give acid neutralising capacity to char (Tang et al., 2013).

Char produced from some biomasses may contain contaminants such as heavy metals and organic compounds. During conversion process, these materials undergo changes and may destroy or convert to benign compounds. However, sometimes they remain unchanged or give rise to potentially harmful substances such as polycyclic aromatic hydrocarbons (PAH) and in some cases, dioxins (Shackley et al., 2010).

The contaminants available in char are two types: the group that is coming from the original biomass (heavy metals, dioxins, polycyclic aromatic hydrocarbons (PAHs), etc) and the contaminants produced through pyrolysis (PAHs).

The first type of contaminants can be avoided by careful selection of biomass. They can also be separated and removed during char production. By appropriate selection of operating conditions, specifically temperature range, the reduction of char PAH is possible (Shackley et al., 2010).

However, two methods such as steam activation, magnetization and oxidization of char are available to improve char properties (Tang et al., 2013).

1-7-6-2-Bio-oil

The liquid product of biomass pyrolysis is considered most of the time as the most desirable product of biomass pyrolysis. High energy density, easier store and transport and de-coupling of production and utilization processes makes this product very interesting (Dahlquist, 2013).

There are several names available for liquid product of pyrolysis process such as tar, bio-oil, or biocrude. Several definitions are available for bio-oil as well. However, there is no universally accepted definition for that. Bio-oil is a complex mixture of condensable hydrocarbons, containing high oxygen, 1- to 5-ring aromatic, phenols and complex polyaromatic hydrocarbons (PAHs). Another definition is the mixture of materials with a molecular weight larger than 78, which is the molecular weight of benzene and can be condensed in the downstream of pyrolysis or gasification unit (Basu, 2013). These molecules are derived from depolymerization and fragmentation of biomass building blocks (cellulose, hemicellulose and lignin). Most of the produced bio-oil is the contribution of cellulose, which produce anhydrocellulose and levoglucosan after decomposition. The most of acetic acid available in bio-oil is the result of hemicellulose decomposition. The bio-oil, which is produced from lignin decomposition, has lower oxygen content and higher calorific value. However, high viscosity and resistance to cracking are the characteristic as consequences (Dahlquist, 2013).

Characterisation of available compounds in bio-oil is very important, since it gives insights into its properties and suitability for upgrading, handling, environmental consideration, etc. Bio-oil has high molecular weight, which exceed 500 Daltons (Dahlquist, 2013). In the temperature range of 200 to 500 °C, the biomass constituents (cellulose, hemicellulose, and lignin components) break down into primary tar, which is also known as wood oil or wood syrup and contains oxygenates and primary organic condensable molecules. At higher temperatures (>500 °C), primary tar molecules reform and convert to smaller and non-condensable gases (such as CO_2, CO, and H_2O) in addition to heavier tar

components called secondary tar which mostly contains phenols and olefins. When the temperature goes even higher, primary tar products crack to tertiary products which contains methyl derivatives of aromatics, such as methyl acenaphthylene, methylnaphthalene, toluene, and indene, while condensed tertiary aromatics make up a polynuclear aromatic hydrocarbon (PAH) series without substituents (atoms or a group of atoms substituted for hydrogen in the parent chain of hydrocarbon). This series contains benzene, naphthalene, acenaphthylene, anthracene/phenanthrene, and pyrene. Table 1- 2 shows the list of typical compounds available in bio-oil. In addition to these compounds, the oxygen-containing compounds such as derivatives of phenol, guaiacol, veratrol, syringol, free fatty acids, and esters of fatty acids are present in bio-oil. Generally, bio-oil is a microemulsion, with the continuous phase to be aqueous solution of the products of cellulose and hemicellulose decomposition, which contains small molecules from lignin decomposition. Pyrolytic lignin macromolecules are the major composition of discontinuous phase (Basu, 2013).

Another classification of the compound available in bio-oil is: hydroxyaldehydes, hydroxyketones, sugars and dehydrosugars, carboxylic acids, and phenols.

Several analytical techniques are available for characterization of bio-oil compounds. By gas chromatography mass spectrometry (GC-MS) up to 40% of compounds available in bio-oil are detectable. Around 15–20 % wt of the compounds available in bio-oil are HPLC (High Performance Liquid Chromatography) detectable. Still 15 wt% of bio-oil compounds is undetectable which is mostly composed of high molecular weight compounds. Gel permeation chromatography (GPC) and Fourier Transform Infrared Spectroscopy (FTIR) are also the analytic methods, which can be used (Dahlquist, 2013).

Table 1- 2- Typical bio-oil compounds (Basu, 2013)

Benzene
Toluene
Other 1-ring aromatic hydrocarbon
Naphthalene
Other 2-ring aromatic hydrocarbon
3- ring aromatic hydrocarbon
4- ring aromatic hydrocarbon
Phenolic compounds
Heterocyclic compounds
Others

The bio-oil compounds can be divided into following categories: (Dahlquist, 2013)

- Hydroxyaldehydes

- Hydroxyketones

- Sugars and dehydrosugars

- Carboxylic acids

- Phenolic compounds

1-7-6-3-Biogas

The non-condensable gaseous product can be called by different names such as biogas, producer gas, pyrolytic gas and syngas. However, the difference of these terms must be considered.

✓ Biogas is produced from anaerobic decomposition of organic matter in an oxygen-free environment and composed mostly from CH_4 (50-75 vol%)and a fraction of CO_2 (25-40 vol%), N_2 (0–10%)and small traces of H_2O, O_2, H_2, and hydrogen sulfide. Biogas can contain

also contaminants such as volatile organic compounds, sulfur compounds, siloxanes, halogenated hydrocarbons, ammonia, etc. However, the term biogas can also be used for the product of pyrolysis and gasification processes (Dahlquist, 2013).

✓ Producer gas or pyrolytic gas is the best term to be allocated to gaseous product of pyrolysis and gasification of organic materials such as biomass, which contains CO, H_2, CH_4, CO_2, H_2. Pyrolytic gas can be of low or medium value since it is combination of combustible and non-combustible gases and may also contain some tar content. When the gas is used for direct heat applications, the presence of tar is not a major problem. When the producer gas is used in internal combustion engines for the generation of mechanical power or on-site electricity, purification is necessary (Basu, 2013) (Samy Sadaka and Eng, n.d.).

✓ Syngas is the mixture of (CO and H_2) with several applications in chemical industry by Fischer-Tropsch or conversion to methane a substitute natural gas (CH_4).

1-7-7-Application of pyrolysis products

Pyrolysis is a zero waste process since all the products have potentially commercial value. Even though bio-oil is more of interest in most of the cases, char can not be considered as the byproduct of process, since it has several value added application. Gas product can be used for electricity and heat production. The applications of different pyrolysis products are discussed in the following.

1-7-7-1-Char applications

In the pyrolysis process, the main objective is maximizing the energy efficiency of the process. However, another important factor that must be considered is the carbon abatement of this process, which is the summation of two aspects: one, the substitute of fossil fuels with biofuels and two, the carbon storage in the char instead of release in the atmosphere. Considering these two facts, slow pyrolysis is optimum process rather than fast pyrolysis in carbon abatement. Considering the large yield of char in the slow pyrolysis process and high operational expenses, it is not feasible to consider char as an unwanted product.

In the most of the pyrolysis processes char is considered as a low value added by product and there are efforts to minimize its yields. However, the most conventional application of char is as a fertilizer and soil conditioner. Considering the current price of pyrolytic char, that higher value added applications are more likely to be economically feasible. Char can be used for different applications including (Dahlquist, 2013):

- Carbon sequestration and climate change mitigation

- Replace nutrient losses in soil

- Reduce fertilizer use

- Enhance marginal soil productivity

- Reducing contaminate runoff and improve water quality

- Soil remediation

- Decrease NO_x and methane emission from solids

a) Use of char for soil amendment and carbon sequestration: Use of char for soil amendment purposes is a beneficial task, which at the same time yields to carbon sequestration. These two aspects of char application are interconnected. Char is stabilized form of biomass, and can be stored in soil on a very large scale. The physical and chemical properties of char give char the potential to improve crop productivity through dynamic or reversible interactions with nutrients and soil mineral particles (Sohi et al., 2010). Terra Preta in Amazon proves the char possibilities to improve soil fertility for long time after application whilst surrounding soils remain poor. In addition, char is resistant to rapid microbial degradation which enables the carbon storage in char to remain for hundreds of years (Quirk et al., 2012).

On the other hand, it has also been suggested that char can enhance crop resistance to disease and can be used as a disease control agent in agriculture. This may be another reason to improve crop productivity (Tang et al., 2013). The chemical impact of char application in soil are temporary or long term and are the results of leachable ash and modification of soil pH, promotion of short-term

microbial activity including the effect of small labile fractions. Char can have also physical impact on soil properties, which arise from modification of soil bulk density, water holding capacity and promoting soil aggregation (possibly in combination with soil biological effects). The char application can affect the soil in the case of cation exchange capacity (CEC) and specific surface area (SSA), biological associations (with micro-organisms, fungi and with plant roots), and bio-physical benefits (mediating the connection of micro-organisms and microbial substrate, promotion of meso-faunal activity, including earthworms) (Shackley et al., 2010).

The summarized effect of char application in soil amendment suggested by Pragoyo et al., (2014) and Shackley et al. (2010) are as follows:

- Char has high resistant toward microbial decay and therefore it would be a long term sink of carbon and therefore mitigate climate change

- Char can impact on soil physicochemical properties and promote soil fertility and crop growth

- Char changes the microbial enzyme activity as a result of enzyme sorption to char

- Toxic compounds available in char such as dioxin and PAHs reduces microbial activity in soil and as a consequence, reduces decomposition of soil organic matters (SOM) and protects soil carbon

- Provision of labile organic mater

- Supply of plant available nutrients

- Modification of soil pH

- Modification of soil physical characteristics

- Cation exchange capacity and sorption

- Microbial activity

b) Use of char for soil and water remediation: Char can act as efficient sorbent of various organic and inorganic contaminants because of its huge surface area and special structure. This way char can be used as a cost effective and environmental friendly tool for remediation of heavy metals and

organic pollutants. The soil remediation was reported for both heavy metal and organic pollutants. The mechanism is electrostatic interaction and precipitation in the case of heavy metal, and the surface adsorption, partition and sequestration in the case of organic contaminants (Tang et al., 2013). Figure 1- 11 shows the pathway for heavy metal removal from soil by char.
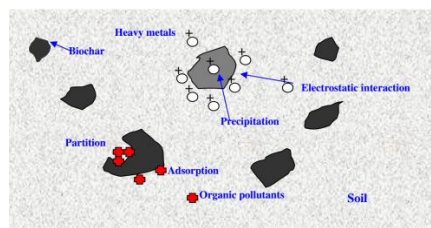
Figure 1-11- Mechanism ofchareffectivenessin soil remediation (Tang et al., 2013)

In many other studies, the char ability to remediate organic pollutants such as dioxins, PAHs, pesticides, and other contaminants was reported. This way char can remove organic pollutants from soil, water and sediments, and thus lowering their bioavailability and preventing toxic substances transferring from environment to plant and further to organisms including human (Tang et al., 2013).

Char can be used for water and wastewater treatment as well. Removal of high molecular weight polycyclic aromatic hydrocarbons (PAHs), herbicides, pesticides, and other organic contaminates from water, heavy metals including copper, cadmium, lead, … is also possible by the use of char. The ability of char to adsorb sulphur compounds and reduce odors was also observed. Removal of nitrate, phosphate and ammonia was also reported for char. Char properties such as porous structure, high surface to volume ratio and presence of functional group (specially oxygen containing functional groups such as carboxyl (-COOH), lactone (C=O) and hydroxyl groups), irregular surface with high BET surface area, makes char to work so well in water filtration. The presence of oxygen rich organic compounds on the char surface add substantial cation exchange capacity and enhance char sorbent properties. The role of char in water treatment is based on adsorption process, which is the surface interaction between dissolved materials and the char. However, the reactive sites of char can also bind non-problematic dissolved organic matter and the targeted hazardous contaminants such as pesticides). Therefore, a compromise must be achieved before their usage. When there is a specific

pollutant to be removed a proper system must be designed as follows ("International char initiative," n.d.):

- Ammonia - char with an additive of steel wool

- Nitrates - char with an additive of iron rust

- Phosphates - combinations of char, iron rust, steel wool, and oyster shells

- Copper and zinc - char blended with compost

c) Use of char for cattle feeding: The use of char for cattle feeding was reported to be beneficial as well. The productivity of cows and thus production units are greatly dependent on the proper nutrition. This is the reason why diseases of the digestive tract and the corresponding treatment strategies play a key role in commercial livestock farming. Hormonal, chelating, antibiotic, teratogenic, carcinogenic and neural effects are the main symptoms of the cattle diseases. The advantage of activated carbon in adsorbing pathogenic clostridial toxins such as C. tetani and C. botulinum was proved. Char can have the same effect by its adsorption potentials, which cause a wide range of toxic substances to be bound in the gastrointestinal tract. Detoxification of already resorbed toxins (in particular lipophilic toxins) in the plasma via "enteral dialysis" is also takes place by use of char for animal feeding as a result of adsorption power of the huge surface area of char which interacts with the beneficial permeability properties of the intestine. The char can also influence dysbiosis. Also eubiosis can be influenced and be maintained much longer despite environmental fluctuations in the digestive tract. The adsorption takes place both for lipophilic and hydrophilic substances. However, the presence and amount of heavy metals, dibenzodioxins and dibenzofurans should be studied as limiting factors before use. Char affect the digestion on the following mechanisms: adsorption, coadsorption, competition, chemisorption, adsorption followed by a chemical reaction, desorption. The effect of char on bacteria and their toxins in the gastrointestinal tract are as follows ("Ithaka-Journal for ecology, winegrowing and climate farming" n.d.):

- Adsorption of proteins, amines, amino-acids

- Adsorption of digestive tract enzymes, as well as concentration of bacterial exoenzymes in the activated carbon

- Adsorption, via chemotaxis, of mobile germs disposing of special attachment mechanisms

Another important effect to be considered is the specific colonisation of the char with gram-negative germs with increased metabolic activity, which results on one hand, in a decrease in endotoxins needing to be resorbed and on the other hand, in the adsorption of the toxins in the char ("Ithaka-Journal for ecology, winegrowing and climate farming, 55 use of char" n.d.).

d) Use of char as an immobilization surface in fermentation: Char can be also used as an immobilization surface for fermentation process. During fermentation, the organic matters breakdown by microbial consortia in organised and layered biofilm communities. The effect of immobilization surface on the process yield is now well recognized (Intapaniya 2012). Char can play the role of support media for development of biofilm in the biodigester and would as a result increase the yield of biogas. The large surface area to weight ratio of char functions as a focal point for attachment of microbes and the formation of structured microbial consortia enclosed in a biofilm matrix increasing the efficiency of microbial fermentation. Some hypotheses are available for the effect of char on fermentation process, which are as follows (Intapaniya 2012):

- Char will enhance the biofilm development in biodigesters and increase the rate of mineralisation of organic matter and the production of biogas

- By providing habitat for methanogenic and/or methanotrophic microbial consortia, char application can change the potential utilization of end products

e) Catalytic role of char in gasification process: Char can be used as a catalyst for gasification process as well. The catalytic effect of alkali cations on the gasification process is proved by decreasing both the tar and methane contents in the products. Most of the biomass types have the high concentrations of alkali, which can be effective catalysts for tar decomposition. As an example, potassium is usually available inherently in the ash of biomass (Sutton et al., 2001).

f) Use of char in building sector: Char can be used also in the building sector, which is carbon negative and offers unique and promising properties as well. Two of char's key properties are its low thermal conductivity and its ability to absorb water up to 5 times its weight. These properties suggest that char is a suitable material for insulating buildings and regulating humidity. It can be used also for enhancing fire safety specially when used in roof and ceiling ("IthakaJournal for ecology, winegrowing and climate change , The use of char in cattle farming," n.d.).

In pyrolysis process and in some metallurgical processes char can be used as a heat supply and as a substitute for coke (Dahlquist, 2013).

1-7-7-2-Bio-oil applications

Pyrolysis product (bio-oil) can be used in engines and turbines and also used as a feedstock for refineries for light fuels and/or chemicals production (Dahlquist 2013). However, several weakness of bio-oil, restrict the use of bio-oil for industrial applications and urge the need for upgrading. The adverse characteristics of bio-oil and upgrading methods are discussed in details in section 1-8 and 1-9. However, the available applications of bio-oil are mentioned below:

- Using bio-oil as substitute for hydrocarbon fuels in conventional prime movers to produce electricity or generate steam has been demonstrated but has not been commercially adopted (Ringer et al., 2006). Design and study of specialized bio-oil burners at CanmetENERGY and the Combustion Research Laboratory, at the University of Toronto was performed. Existing oil-fired burners can work with relatively minor or even no modifications of the existing equipment in order to run on bio-oil. It is economically feasible to use bio-oil to substitute for fuel oil in burners and boilers for heat and power generation. With all these, there are still limitations and challenges for use of bio-oil for heat and power applications even though it has reached commercial scale (Dahlquist, 2013).

- Direct combustion in purposely-built boilers for heat generation was done commercially by Red Arrow (Wisconsin, USA), a chemical company that operates fast pyrolysis plants for the

production of food additives. By-products from these processes are combusted in 5 MWt industrial boilers. Burners and boilers intended to operate on pyrolysis bio-oil need to be adapted to its corrosive nature, particle content and high viscosity. Nozzles, pumps, fuel lines, tanks or any other part of the equipment in contact with the fuel needs to be made of corrosion proof material (San Miguel, 2012). Bio-oil prior to be directly burned needs preheating to 70–80 °C to reduce the viscosity without recirculation of heated product back to the storage tank. Furthermore, like the conventional fuels startup and shutdown must be done to avoid deposition and coking of nozzles (Dahlquist, 2013).

- Co-firing of bio-oil has been tested at various plants including the 20 MWe coal power station at Manitowac (Wisconsin, USA) and the 350 MWe combined cycle natural gas power plant in Harculo (The Netherlands) (San Miguel, 2012). Both bio-oil and char can be co-combusted in coal-fired power stations with 85% biomass-to-fuel energy efficiency (Dahlquist, 2013).

- Various companies tried to use bio-oil in slow speed diesel engines, which are robust and can operate on low-grade fuels (Dahlquist, 2013). These companies are include Finish Wärtsila and the British Ormrod (San Miguel, 2012). In this case, an auxiliary fuel should be used during start-up since bio-oil has poor ignition properties. However, after ignition, bio-oil is combusted readily. The level of emission (CO, NO_x, THC and smoke) is same as conventional fuels. Since bio-oil is immiscible with hydrocarbons by use of surfactants, it can be emulsified. However, it must be considered that the use of surfactants may be expensive. Emulsified bio-oil is more stable, less viscose and less corrosive than the original bio-oil (Dahlquist, 2013).

- The use of bio-oil in gas turbines was also tested, which have demonstrated that the engines and turbines are able to run on bio-oil but notable deficiencies and damage to the equipment were detected owing to the corrosive properties, abrasive nature and thermal instability of the bio-oils (San Miguel, 2012).

The only commercial application of fast pyrolysis technology at present is the production of flavoring agents. The American company Red Arrow Products has been using Ensyn technology to produce smoke flavorings and food additives for over 20 years (San Miguel, 2012).

The use of bio-oil as replacement for petroleum-based phenolic resins, which are employed in the production of wood panels was investigated (San Miguel, 2012).

Corporate Development at Suncor Energy has confirmed that the use of bio-oil in refining operations could be of long-term strategic interest. However, the state of the technology today does not support imminent commercialization. The commercial potential of this technology is being assessed against other potential technologies in the renewable energy area (Marshal,2013).

The most economically sound approach to developing products from bio-oil may be to extract valuable chemicals and material building blocks from the oil first, and then to utilize the remaining bio-oil as a crude fuel. This residual bio-oil could be upgraded and fractionated into conventional fuels as required (Marshal, 2013).

1-7-7-3-Biogas applications

The gas product of the pyrolysis and gasification process can be low or medium energy. Figure 1- 12 shows the classification of the obtained gas from energy level and shows well the operational condition leads to their production.

The use of pyrolysis gas differs according to its energy level. The gas product of pyrolysis and/or gasification can be used for electricity and heat, fuel and syngas production. These applications are discussed in the following.
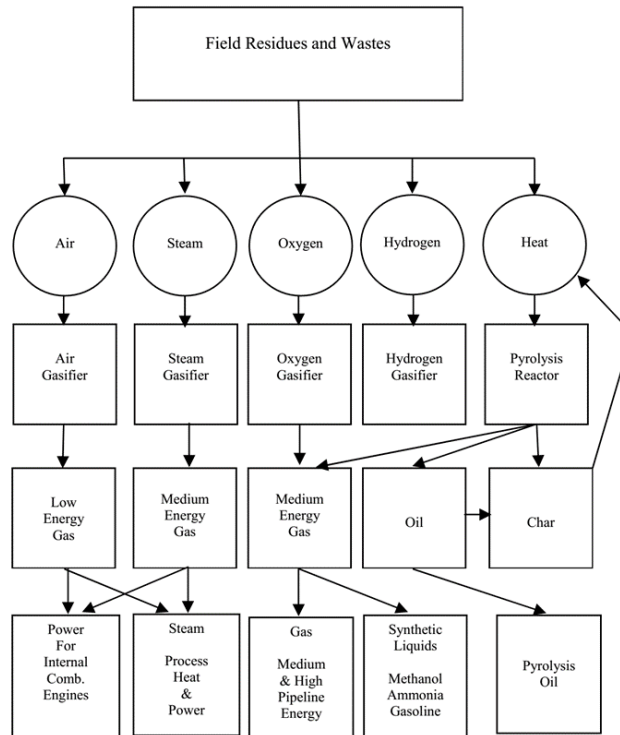
Figure 1-12- Gaseous products of thermochemical conversion processes (Samy Sadaka and Eng, n.d.)

a) Gas application for electricity and heat production: The most conventional use of biogas is conversion of the gas into electricity and heat in the place of origin. Heat and electricity production are inter related. Combined heat and power plant (CHP) is an approach to use biogas in combustion engine, which runs a generator for producing electric power and can even obtain the efficiency of 30-40%. The use of other kinds of engines and gas turbines or power generation by fuel cells is also possible. Natural gas combustion is thoroughly studied nowadays and all aspects including ignition, extinction, flammability limits, flame speeds, cellular instabilities, emission and detailed thermo-transport and kinetic models for simulating and analyzing flames in a variety of configurations are clarified. All the obtained results on natural gas combustion can be applied for biogas combustion since it mainly composed of CH_4 and CO_2 with small traces of H_2O, and N_2. It must be considered that biogas has much lower energy content in comparison to natural gas. Therefore, higher feeding rate must be applied and lower flame temperature is obtained when the biogas is used. Some of the generated heat is consumed for the domestic use of the plant and buildings. Another portion of thermal energy is used through organic Rankine cycle (ORC) technology, where the heat loss is used

for vaporization of an organically working fluid, which runs a turbine and electric power generator. The excess biogas, which is not consumed directly in the plant, can be used in micro-gas grids to transport the raw biogas to satellite CHPs. In general, the biogas must be used on-site or be distributed in energy grids such as district heating systems, gas pipes, and electrical grids. For gas use in turbine engines an IGCC facility is an efficient, low-emission power generation, and for carbon capture and storage approach. Use of produced gas in natural gas-fired combustors, spark ignition (SI) and compression ignition (CI) engines were all proved to be promising in researches. Diesel engine operating in a dual-fuel mode which using a combination of diesel pilot injection and syngas fumigation in the intake air was tested. In dual fuel CI engines diesel and biogas are used. This is a good approach for fuels with low energy content like biogas (Dahlquist, 2013).

b) Use of gas as fuel: Biogas can also be used as a substitute for natural gas. However, it has to be heavily conditioned to reach the quality of natural gas. The conditioned biogas (bio natural gas or biomethane) can be used everywhere that natural gas is used. Sweden and Switzerland were forerunners in using biogas as fuels in cars, buses, trucks and rail cars (Dahlquist, 2013).

c) Syngas production from gas product: Producer gas can be reformed to produce syngas (mixture of carbon monoxide CO and hydrogen H_2). The conditioning required for steam reforming is similar to that required for a biomass gasification-derived syngas (Dahlquist, 2013). This way the producer gas composition is manipulated. Syngas is the product of high temperature steam or oxygen gasification of organic material such as biomass. Any impurities such as tars must be removed then the syngas can be used to produce organic molecules such as synthetic natural gas (SNG-methane (CH_4)) or liquid biofuels such as synthetic diesel (via Fischer-Tropsch synthesis) (Samy Sadaka and Eng, n.d.).

Production of commercial methanol can be done by the produced syngas. Methanol synthesis involves reacting CO, H_2 and steam over a copper-zinc oxide catalyst in the presence of a small amount of CO_2 at a temperature of about 600° C and a pressure of about 70 bar. The syngas with H_2/CO of at least 2 and CO_2/CO ratio of about 0.6 is desirable to prevent catalyst deactivation and to keep the catalyst in

an active reduced state. Extensive treatment and tar, acid and particulates removal must be done before methanol production. CO_2 must be also removed. Methanol synthesis reaction is as follows (Samy Sadaka and Eng, n.d.):

$$CO + 2 H_2 \rightarrow CH_3OH \qquad\qquad\qquad\qquad \text{Equation 1-2}$$

$$CO_2 + 3 H_2 \rightarrow CH_3OH + H_2O \qquad\qquad\qquad \text{Equation 1-3}$$

According to the equations, methanol can be produced by means of the catalytic reaction of carbon monoxide and some carbon dioxide with hydrogen. The reactions are exothermic and as a consequence are favored at low temperature and high pressure (Samy Sadaka and Eng, n.d.).

Gasoline and diesel gasoline and diesel (synthetic fuels) can be obtained from syngas via a Fischer-Tropsch (Samy Sadaka and Eng, n.d.).

Fischer-Tropsch synthesis is the catalytic reaction of H_2 and CO to form hydrocarbon chains of various lengths (CH_4, C_2H_6, C_3H_8, ...). The H_2/CO ratio around 0.5 to 0.7 is desirable for Fischer-Tropsch when iron is used as the catalyst (Samy Sadaka and Eng, n.d.).

1-8- Necessity of upgrading pyrolysis products

Although bio-oil is one of the most valuable products of biomass pyrolysis, it can be used as a biofuel only after upgrading.

Bio-oil undesirability comes from high amounts of oxygenated compounds. These oxygenated organic compounds are in the form of carboxylic acids, ketones, and aldehydes and some other unfavourable compounds. All these weaknesses make several operational problems in the use of bio-oil as a fuel. Oxygenated compounds usually form more than 35% in of bio-oil and are available in more than 300 different compounds (Dahlquist, 2013).

One of the adverse characteristics of bio-oil is instability since bio-oil has non-equilibrium composition and tends to reach thermodynamic equilibrium by time and changes its composition and properties during storage. High reactive moieties in the bio-oil, yield to further reaction and degradation. Therefore, over time, the increase of water content and viscosity of bio-oil takes place,

which is called aging of bio-oil. In general, the aging of bio-oil lead to increase the average molecular mass of the oil, the viscosity, and the water content and ultimately separation of bio-oil in two phases (Mortensen et al., 2011) (Dahlquist, 2013).

Some examples of aging reactions are repolymerization reactions, which occur in the presence of air, and are mostly due to the presence of olefins. Ethers, acetales, and hemiacetals may also form as a result of presences of ketones, aldehydes, and organic acids, respectively. Some of the suggested reactions by Nguyen et al. 2013, which may be responsible for instability of bio-oil are as following:

- Organic acids with alcohols forming ester and water

- Aldehydes and alcohols forming hemiacetals or acetals and water

- Aldehydes forming oligomers and resins

- Aldehydes and phenols forming resins and water

Another problem when using bio-oil for energy applications is its low calorific value. Bio-oil cannot compete with petroleum oils regarding to energy content, which is again as a result of high water and oxygen content. The water content also cause ignition difficulties and decrease of the flame temperature of bio-oil (Güngör et al. 2012). Another problem with high water content is the polar nature it gives to bio-oil and as a consequence makes it immiscible with crude oil (Mortensen et al., 2011). High water content of bio-oil comes from feedstock moisture or also from dehydration reactions during decomposition of mainly cellulose and hemicelluloses. The high water content of bio-oil has some negative effects including lowering heating value, lowering flame temperature, delay in ignition, and decrease in combustion rate. On the other hand, it can also affect the bio-oil flow characteristics in positive way by reducing the oil viscosity, which is good for pumping and atomization. High water content leads to more uniform temperature profile in a diesel engine and lower NO_x emissions (Dahlquist, 2013).

Acidity of bio-oil is another serious drawback. Presence of acids and formic acid give bio-oil acidity in the range of pH=2-4. Carboxylic acids are the main responsible of the acidity of bio-oil (60-70%), after that phenols (5-10%) and sugars (20%) are other components responsible for the acidity of bio-

oil. Phenolic components are also troublesome but their high-energy content, makes them more desirable than carboxylic acids (Nguyen et al., 2013). As a result of acidity, problems such as harsh conditions for equipment used for both storage, transport, and processing of bio-oil exist. Corrosion problem was observed working with common construction materials such as carbon steel and aluminum (Nguyen et al., 2013)(Mortensen et al., 2011).

In order to be representable in the market, bio-oil needs to be upgraded. Upgrading in the case of bio-oil means general decrease in the oxygen content (Mortensen et al., 2011).

Pan et al., (2010) reported bio-oil prior to upgrading mainly consisted of long carbon chain compounds with various terminal groups (LCTG), while after upgrading it is consisted of aromatic hydrocarbons. Pütün et al., (2009) reported that long chain of alkanes and alkenes of the pyrolysis oil were converted to lower-weight hydrocarbons. They reported that aliphatics, aromatics, and olefins increased and asphaltenes and polar groups (highly oxygenated groups) had a sharp decrease.

1-9-Available upgrading methods

Bio-oils from biomass pyrolysis could be upgraded to much more valuable products through different methods. One of the possible ways is upgrading bio-oil to produce a refined bio-oil with different application as biofuel or feedstock of chemical industry. The bio-oil can also be gasified to obtain high quality biogas. Several upgrading methods for bio-oil are available. Table 1- 3 classifies available bio-oil upgrading methods, according to their application.

Table 1-3- Available techniques for bio-oil upgrading

With goal of obtaining high quality bio-oil	With goal of high quality biogas production
Esterification	Oxygen/air gasification
Hydrotreating	Steam reforming
Catalytic cracking	

In the following, all the techniques mentioned in Table 1- 3 are described. This study does not concern with esterification and hydrotreating process. Therefore, only a brief overview of these two processes is explained. The other three processes (Catalytic cracking, oxygen/air gasification and steam reforming) instead, are described in details.

1-9-1-Upgrading methods with the aim of high quality bio-oil productions

1-9-1-1- Esterification

As mentioned before a serious problem concerning the bio-oil is its instability and deterioration as consequences of different reactions (the most important are polymerization and condensation). Esterification is a method in which, by addition of small concentrations of alcohols (<10%), stabilization of bio-oil takes place. Bulushev and Ross, 2011 reported that as an example of alcohols, ethanol and methanol would improve the bio-oil stability (more effective was methanol, by which the aging rate was reduced by a factor of nearly 20 times). After esterification, water removal is also much easier from an ester-containing mixture than from the original acidic mixture (because of the lower level of hydrogen bonding). Therefore, in the esterification process, a separate step of water removal is necessary and it is usually done by using distillation or adsorption on a zeolite. Use of alcohols with higher boiling point makes the water separation process easier. Biomass-derived alcohols (ethanol and butanol) can be also used for this process (Bulushev and Ross, 2011).

The reaction involving in the esterification process are as follows (Bulushev and Ross, 2011):

Ester formation: $R_1COOH + R–OH \leftrightarrow R_1COOR + H_2O$ Equation 1-4

Acetal formation: $R_1CHO + 2R–OH \leftrightarrow R_1CH(OR)_2 + H_2O$ Equation 1-5

The added alcohol, reacts with acids and aldehydes and form ester and acetal respectively. This way the bio-oil properties are improved (Bulushev and Ross, 2011).

In the previous study on esterification of bio-oil, GC mass analysis of upgraded bio-oil showed that the concentration of esters as compared to the raw bio-oil increased by a factor of twenty, but the

concentration of aldehydes and ketones decreased considerably. During this process, acidic compounds were converted to esters. Esterification is a suitable approach to change fatty acids into biodiesel. Significant improvement achieved on the chemical and physical properties of bio-oil. The disadvantageous of this process is consumption of valuable alcohols and necessity of an extra water separation stage (Bulushev and Ross, 2011)(Rizzo et al., 2013).

The use of catalysts in the esterification process is also common. Both liquid and solid catalysts can be used for esterification. The most common catalyst for esterification process is sulphuric acid, but it cause corrosivity and difficulty of sulphuric acid separation from the products and there is also environmental concern with the use of liquid acids and necessity of neutralisation or regeneration after the upgrading step (Bulushev and Ross, 2011).

In comparison, solid catalysts are easier to be separated from the products. Solid catalysts possess high acidity and can be used at lower temperatures in comparison with sulphuric acid. Being non-inflammable, non-toxic and environmentally friendly, makes solid acid catalyst more interesting than liquid one. The drawbacks of solid catalysts are deactivation and limited access of some of the reactants to the active sites of typical porous solid acids. Acid sulphated zirconia is the most common in the esterification process. Some other solid acid used in previous research for esterification processes were: SiO_2/TiO_2-SO_4, K_2CO_3/Al_2O_3-NaOH, SiO_2/TiO_2-SO_4, $Pd/SO_42-/ZrO_2/SBA-15$ (Bulushev and Ross, 2011).

1-9-1-2- Hydrotreating

Hydrotreating or hydrodeoxygenation (HDO) is a process in which the hydrogen is added at high pressure in order to remove oxygen from bio-oil in the form of H_2O and Nitrogen in form of NH_3. This way the yield of hydrocarbons increases. Hydrotreating is somehow similar to hydrodesulphurization (HDS) process from the refinery industry for removing sulphur compounds and produce H_2S (Campanella and Harold, 2012) (Mortensen et al., 2011). The upgraded bio-oil can be

described as naphtha equivalent. Generic reaction to describe several deoxygenation reactions could be (Dahlquist, 2013):

$$C_6H_8O_4 + 6H_2 \rightarrow 6CH_2 + 4H_2O \hspace{3cm} \text{Equation 1-6}$$

The reaction suggests that the reaction is limited by the carbon content in bio-oil and the stoichiometric yield is limited to 58.3% of bio-oil on a mass basis without H_2 requirement consideration (Dahlquist, 2013).

During dehydrodeoxygenation, a group of reactions including hydrogenation, cracking and decarboxylation take place. Among them, cracking and hydrogenation are the rate determining steps. The result is production of two-phase liquid, solid coke, and a gas phase containing CO_2, CO, light alkanes, and light olefins. This process is exothermic and temperature range of 250-450 °C is usually required. High pressure in the range of 70-200 bar is also needed (Campanella and Harold, 2012) (Mortensen et al., 2011) (Bulushev and Ross, 2011). The reactions takes place during HDO are exothermic and by equilibrium calculations, temperatures of at least 600 °C was purposed to achieve full conversion. The key factor in the economics of this process is the availability of hydrogen. For lowering the hydrogen consumption, the process must be carried out with minimum or no saturation of the aromatic rings (Dahlquist, 2013).

Catalysts such as Co-Mo and Ni-Mo can be used for improving the process and the presence of hydrogen donor solvents is essential. Reactions such as dehydration, decarboxylation, decarbonylation, and aromatization are promoted in the presence of acidic sites of the catalyst. The drawbacks of this process are the need for high operational pressure in addition to expensive and not easily available hydrogen (Campanella and Harold, 2012) (Mortensen et al., 2011) (Pütün et al., 2009).

1-9-1-3- Catalytic cracking of bio-oil

Since this upgrading method is very important and is the focus of this study, it will be explain later in a separate section 1-9-3.

1-9-2-Upgrading methods with the aim of high quality biogas productions

Upgrading with the aim of high quality biogas production is done through gasification process. In the gasification process, the presence of an oxidizing agent is necessary. Since the main feathers of air/oxygen gasification and steam reforming are more or less the same, they are discussed later in the same section 1-9-4 in detail.

1-9-3- Theory and concept of catalytic cracking of bio-oil

1-9-3-1- Catalytic cracking mechanism

In order to crack high molecular weight compounds available in bio-oil, both thermal and catalytic methods can be used. As a result of cracking, the yield of bio-oil decreases and biogas increases, since some of the heavy organics (mostly high molecular mass oxygenated compounds) are cracked to light organics and gaseous products. The light organics contains mostly formic acid, acetic acid and some other acids plus esters, ketones, alcohols, ethers and phenols (Nguyen et al., 2013).

During the catalytic cracking, high molecular weight organics undergo a number of reactions within the catalyst bed. The first step of the process is deoxygenation and cracking. Products of deoxygenation are water and carbon oxides. The main deoxygenation route is dehydration. Additionally, during the cracking process, chemicals undergo decarboxylation and decarbonylation reactions. These reactions take place on acidic catalysts such as zeolites. Consequently, the nature of the reaction mechanism strongly depends on the nature of the catalyst. The produced carbon fragments then undergo oligomerization reactions, which yield to production of a mixture of C_2-C_6, olefins. The next step is aromatization of olefins to produce benzene followed by alkylation and isomerization to produce various aromatic hydrocarbons, part of which polymerizes to coke. Aromatization process consists of cyclization and hydrogen or hydride transfer. As a result of hydrogen shortage in biomass and absence of external source of hydrogen, most of the hydrocarbons in bio-oil are in aromatic forms. Another pathway for aromatic hydrocarbons production is through

scission of all oxygenate substituents from phenol ring of phenolic compounds (Nguyen et al., 2013)(Güngör et al., 2012)(Srinivas et al., 2000) . Figure 1- 13 shows example of reactions that takes place during catalytic cracking of bio-oil.
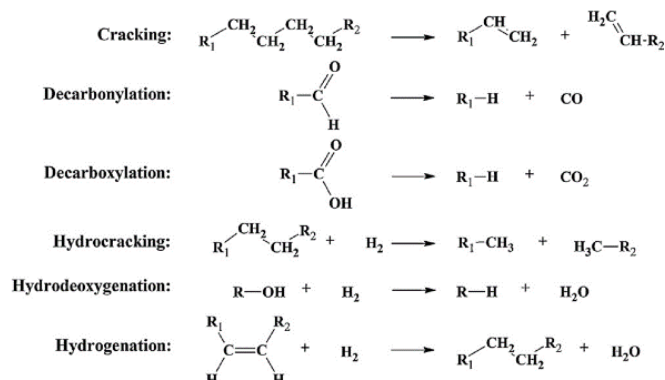
Figure 1-13-Examples of reactions taking place during catalytic cracking of bio-oil(Mortensen et al., 2011)

Mortensen et al. (2011) describe the overall process by following equations:

$$CH_{1.4}O_{0.4} \rightarrow 0.9\text{"}CH_{1.2}\text{"} + 0.1CO_2 + 0.2H_2O \hspace{3cm} \text{Equation 1-7}$$

In which, "$CH_{1.2}$" is an unspecified hydrocarbon product.

The gaseous product of the process usually contains CO_2, CO, light alkanes, and light olefins. By further refining processes, gasoline or diesel hydrocarbons can be produced from upgraded bio-oil (Bulushev and Ross, 2011) (Campanella and Harold, 2012).

1-9-3-2- Catalyst type for catalytic cracking

In the recent years, microporous and mesoporous materials have been employed to study the catalytic upgrading of bio-oils. Zeolites, MCMs and nano metal oxides have been used for this purpose (Bulushev and Ross, 2011) (Campanella and Harold, 2012) (Mortensen et al., 2011).

a) Zeolite catalyst: Zeolites are microporous, aluminosilicate minerals with three-dimensional porous structures. Zeolites are commonly used as commercial adsorbents and catalysts. By adsorption of bio-oil on the acid sites of zeolite catalyst, bio-oil cracking occurs through one of the two paths: decomposition route and bimolecular monomer dehydration. The most important factor in the choice

of catalyst is the availability of acid sites. For aluminosilicate zeolites, the availability of acid sites depends on the Si/Al ratio. Pore structure of the zeolite is determinative of which of the two routes is more significant and it is therefore responsible for product distribution. Presence of small pore structures yields to the less bulky ethylene product. In the presence of medium pore size zeolites, deoxygenation of bio-oil gives increased production of C_6–C_9, while larger pores gives increased production of C_9–C_{12} (Mortensen et al., 2011).

The most common zeolite catalyst is ZSM-5 (a type of zeolite Si/Al=24), due to its balance between acid strength and shape selectivity. Other type of zeolite catalyst such as GaHZSM-5, H-mordenite, H-Y, MgAPO-36, SAPO-11, SApO-5 and ZnHZSM-5 were also used in previous studies (Campanella and Harold, 2012) (Bulushev and Ross, 2011) (Mortensen et al., 2011).

Disadvantages of zeolite catalyst usage are fast deactivation of the catalysts by coke deposition, the low yields of organic liquids and the formation of polycyclic aromatic hydrocarbons (PAHs) (Lu et al., 2010b).

b) MCMs catalysts: MCMs are a series of mesoporous materials. Two of the most popular mesoporous molecular sieves that are studied by researchers are MCM-41 and MCM-48. Although these catalysts are composed of amorphous silica wall, they possess long range ordered framework with uniform mesopores. Another characteristic of these catalysts is possession of large surface area (>1000 m^2g^{-1}). The pore diameter of these materials within mesoporous, range between 1.5 to 20 nm and depends on synthesis conditions as well as the employing surfactants with different chain lengths. Medium acidity is another characteristic of these catalysts. Usage of these catalysts yields to an increase in the concentration of phenolic compounds which is important in the production of adhesives. The phenols could also be hydrodeoxygenated and form aromatics and cyclohexanes which are important in fuel applications. Previously SBA-15, MSU and their modified ones were investigated apart from MCM-4 (Lu et al., 2010a).

In the choice of MCMs one must consider that, high Si/Al ratios had a negative effect on both the activity and the catalyst stability. The strongest catalytic effect was observed for Si/Al ratio of 20 (Adam et al., 2005).

In comparison with ZSM-5, this catalyst possesses low hydrothermal stability (leading to dealumination). Poor hydrothermal stability and high production cost, limits the industrial use of these catalysts at this moment (Lu et al., 2010a) (Bulushev and Ross, 2011).

c) Nano metal oxide: Nano metal oxides have unique properties which make them wildly attractive. In the work of Lu, et al. (2010b) six nano metal catalyst: MgO, CaO, TiO2, Fe_2O_3, NiO and ZnO were investigated. Different catalytic capabilities in the case of pyrolytic products were observed for these catalysts. Use of CaO significantly reduced the levels of phenols and anhydrosugars, and eliminated the acids and increased the formation of cyclopentanones, hydrocarbons and several light compounds. Use of ZnO slightly altered the pyrolytic products and can be considered as a decarboxylation catalyst. The other four catalysts all decreased the linear aldehydes dramatically and increased the ketones and cyclopentanones. All of the catalysts except NiO reduced the anhydrosugars. On the other hand, the catalysis by Fe_2O_3 resulted in the formation of various hydrocarbons. By use of these catalysts, the bio-oil yields were not substantially reduced. Only CaO was able to reduce significantly the acids, which could be a problem for the use of catalytic bio-oils as liquid fuels. Deactivation happens also for these types of catalysts (Lu, et al. 2010b) (Bulushev and Ross, 2011).

1-9-3-3- Coke formation and catalyst deactivation

As mentioned in previous section, a big operational problem with catalytic cracking is deposition of coke, which leads to catalyst deactivation. The coke is the product of cracking of oxygenated compounds such as acetic acid, acetaldehyde or acetone as well as different phenols and complex aromatics. The presence of oligomers is also responsible for the fast catalyst deactivation and low organic yield. Coke may block the active sites of the catalysts and lead to catalyst deactivation (Bulushev and Ross, 2011) (Lu, et al. 2010a).

Coke is the carbon formed from catalytic cracking and may deposit in the micropores, and strongly block to the acidic sides of the zeolite. Catalytic carbon leads more strongly to catalyst deactivation in comparison to thermal carbon (Mortensen et al., 2011).

Regeneration is a method to remove the coke and make the possibility to reuse the catalyst. However, a lower catalyst lifetime and deoxygenation degree was found after regeneration comparing to new catalyst. The situation deteriorates by repeating regeneration cycles. After each deactivation and regeneration, the amount of active sites on the catalyst decrease. Regeneration is done through, catalyst wash with acetone and heating it in an oven at 500°C for 12 hour (Mortensen et al., 2011).

1-9-3-4- Operational condition and parameters for catalytic cracking

Important operational parameters that may influence the products of catalytic cracking process are:

✓ In-situ or separate position of catalyst (one stage or two stage upgrading)

Catalytic cracking of bio-oil can be done in two different modes, which are called primary methods and secondary methods. Primary conversion processes or in-situ catalytic cracking is a process in which, pyrolysis and catalytic cracking of the produced volatiles are carried out simultaneously in one reactor. Instead, in secondary methods, volatiles upgrading is conducted in a separate reactor in downstream of the pyrolysis reactor.

In primary or single-step catalytic pyrolysis, the catalyst is in contact with solid biomass. So the degradation of biomass is influenced itself by presence of catalyst. On the other hand, in the case of secondary or two-step catalytic pyrolysis, the catalyst is in contact not with the biomass but with volatiles from degradation of biomass and it effects volatiles composition (Güngör et al., 2012). In the secondary method, the first reactor only involves with thermal reactions of bio-oil without a catalyst. This way, less coking and deactivation of the catalyst in the second reactor occurs and thus enhancing catalyst life (Bulushev and Ross, 2011) (Srinivas et al., 2000). Another advantage of the secondary methods is the possibility to investigate thermal and catalytic cracking processes separately. This way,

the effect of temperature on each process can be studied separately, and the optimum parameters would be obtained accordingly.

The problem with primary methods is the high coke formation, which cannot be solved easily. However, in these methods, the need for addition of second reactor is eliminated. Although secondary methods are beneficial from reducing catalyst deactivation point of view, they need additional equipment and investment cost (Xie et al., 2012).

✓ Catalyst bed temperature

The temperature of catalyst bed may influence the product distribution. Working in two stage catalytic reactor paves the way for obtaining the optimum temperature of the catalytic bed. While for in-situ catalytic upgrading, the temperature of catalyst bed is equivalent to pyrolysis temperature and cannot be studied separately.

✓ Amount of catalyst

The amount of catalyst can definitely change the yields and characteristics of the products. Therefore, the optimal amount of catalyst must be investigated.

Decision about the above mentioned operational conditions can be done through a comprehensive literature review which is reported in the Chapter 2.

1-9-4-Theory and concept of gasification of pyrolysis products process

1-9-4-1- Mechanism of gasification process

During pyrolysis the conversion of biomass takes place in the absent of oxidizing medium. Figure 1-14 shows the pyrolysis process and its product, which undergo a further gasification step. In the gasification step by introduction of catalyst and an oxidizing agent (air, oxygen or steam) the decomposition of char and tar to gases occur. The scheme of gasification of pyrolysis product process is represented comprehensively in Figure 1- 14. As it can be seen, pyrolysis is an internal step in gasification process. The gasification temperature is usually in the range of 600 to 1000 °C. The most

important reactions involved in gasification of pyrolysis products are mentioned in the following (Dahlquist 2013) (Rezaiyan and Cheremisinoff 2005):
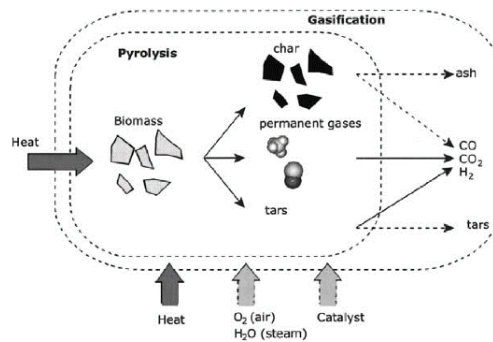
Figure 1-14- Representation of pyrolysis and gasification of biomass (Dahlquist 2013)

Feedstock→char+tars+CO_2+H_2O+CH_4+CO+H_2+(C_2−C_5)+impurities (pyrolysis reaction) Equation 1-8

$C+\frac{1}{2}O_2 \rightarrow CO$ (partial oxidation)   Equation 1-9

$C+CO_2 \leftrightarrow 2CO$ (reverse Boudouard)   Equation 1-10

$C+H_2O \leftrightarrow CO+H_2$ (water gas reaction)   Equation 1-11

$CH_4+H_2O \leftrightarrow CO+3H_2$ (steam reforming)   Equation 1-12

$CO+H_2O \leftrightarrow CO_2+H_2$ (water gas shift)   Equation 1-13

$C + 2H_2 \rightarrow CH_4$ (Hydro-gasification)   Equation 1-14

$CO + 3H_2 \rightarrow CH_4 + H_2O$ (Methanation reaction)   Equation 1-15

The principle gasification reaction is water-gas shift reaction. Boudourd reaction is endothermic and at the same temperature in the absence of a catalyst, takes place much slower than the combustion reaction. Hydro-gasification is also very slow except at high pressures. When the aim of process is H_2 production, the water-gas shift reaction becomes important. In the absence of catalysts, methanation reaction proceeds very slowly. Another reaction, which can take place, is as follows:

$C + H_2O \rightarrow 1/2CH_4 + 1/2CO_2$ Equation 1-16

The reaction above is relatively thermal neutral, suggesting that gasification could proceed with little heat input but methane formation is slow relative to other reactions unless catalyzed (Rezaiyan and

Cheremisinoff 2005). The water can be provided by the biomass itself or by supplying in the system in the form of steam.

Cracking of tars may also occur thermally or catalytically in the form of following equations (Dahlquist 2013):

$$pC_nH_x \leftrightarrow qC_mH_y + rH_2 \qquad \text{(thermal conversion)} \qquad \text{Equation 1-17}$$

$$C_nH_x + nH_2O \leftrightarrow (n+x/2)H_2 + nCO \qquad \text{(catalytic steam reforming)} \qquad \text{Equation 1-18}$$

$$C_nH_x + nCO_2 \leftrightarrow (x/2)H_2 + 2nCO \qquad \text{(catalytic dry reforming)} \qquad \text{Equation 1-19}$$
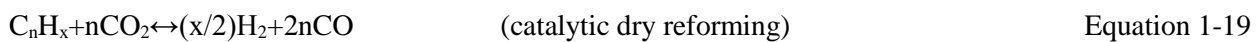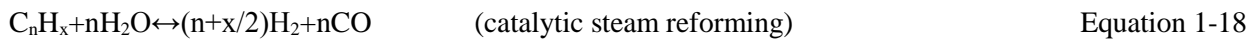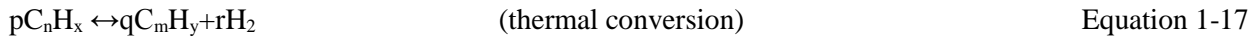
1-9-4-2- Oxidizing agent

Using oxygen or air as an oxidizing agent is called partial oxidation, while use of steam is called steam reforming process. Most of the available literature is on steam reforming.

a) Air/Oxygen

When concerning gasification, air/oxygen is provided in lower amount than the stoichiometric values for complete combustion reactions (Skoulou and Zabaniotou, 2012). The injected oxygen into a gasifier can be pure oxygen or air, and it is consumed in several processes such as combustion, partial oxidation or water formation to provide the heat necessary to dry the solid fuel, break up chemical bonds, and raise the reactor temperature to drive endothermic reactions (Rezaiyan and Cheremisinoff 2005).

b) Steam

Using steam as an oxidizing agent is mostly with the aim of H_2 production, since steam promotes the water-gas shift reaction carried out in the presence of catalysts. By feeding steam as a gasifying agent, the partial pressure of H_2O in the gasifier raises and promote water gas reaction as well as water gas shift and methane reforming reactions, where the last two occur at gasification temperatures above 750–800 °C. Hydrogen production is done conventionally by catalytic steam reforming of methane, light hydrocarbons, and naphtha, partial oxidation of heavy oil residues, and coal gasification. When using biomass as fuel for hydrogen production emissions of SO_2 and NO_x will reduce significantly

and also the process is CO_2 neutral. Biomass content leads to gasification at lower temperatures, which is an advantage over coal in the gasification process. The use of catalyst in biomass steam reforming process is needed. The process is very favourable in syngas and then transport fuels production. By this process adjustment of the H_2/CO ratio and production of syngas for Fischer–Tropsch or methanol synthesis are achieved. It also removes tar and methane. Using steam as oxidizing agent improves the heating value of the product rather than oxygen (Bulushev and Ross, 2011) (Rennard et al., 2010) (Mahmood et al., 2013).

Since the temperature of the added steam is generally lower than the gasification temperature, it leads to lowering the temperature in the gasifier. Therefore, too high steam-to biomass ratio will have negative effect on the process. Preheating the steam or any gasifying agent before introducing it into the gasifier, to induce a higher gasification temperature, is necessary (Dahlquist 2013). Several previous researches are available for steam reforming of biomass in the catalytic process (Mahmood et al., 2013) (Skoulou and Zabaniotou, 2012) (Wu et al., 2013).

1-9-4-3- Catalysts in gasification of pyrolysis products process

The aim of catalytic gasification of pyrolysis products is the elimination of condensable organic compounds and methane in the produced gas. Using this cheap technology will enhance the economic viability of biomass gasification products. Using appropriate catalyst is a solution for the above-mentioned goals.

Tar and condensables, cause operational problems like fouling at the downstream of the process and can takes place even at very high temperature. By using the catalyst, the tar or condensable hydrocarbon can be reformed by passing over the catalyst particles. This happens on the catalyst surface with either steam or carbon dioxide, thus produces additional hydrogen and carbon monoxide. Tar cracking without catalyst can be accomplished only at above 1200 °C. By using catalyst, this happens at moderate temperatures of 750–900 °C. Generally, by using catalyst, both gas yield and the heating value of the product gas improve. The main purpose of catalyst usage is to reduce the tar

content of the product gas but it may also catalyze the gasification reactions (Dahlquist 2013) (Basu, 2013) (Abdoulmoumine et al., 2014).

On the other hand, methane presence in the gas cannot be tolerated when the aim is syngas production. Syngas requires a precise ratio of CO and H_2 to be present in the gas product. During steam reforming process in the presence of a catalyst (metal based), methane reacts with steam at a temperature of 700-1100 °C, and is reformed into CO and H_2 (Sutton et al. 2001) (Basu, 2013).

According to what mentioned above, a good catalyst must meet the following criteria (Sutton et al., 2001) (Dahlquist 2013) (Basu, 2013):

1. Effective in the removal of tars

2. Capable of reforming methane, if the desired product is syngas

3. Capable of providing a suitable syngas ratio

4. Resistant to deactivation as a result of carbon fouling and sintering

5. Easily regenerable

6. Mechanically strong

7. Inexpensive

The three main groups of catalysts, which proved to be suitable for the aims above, are dolomite, alkali metals and noble metal (nickel based) (Sutton et al., 2001) (Bulushev and Ross, 2011).

a) Dolomite

Dolomite ($CaCO_3MgCO_3$) is a magnesium-calcium ore and contains some minerals at trace levels, such as SiO_2, Fe_2O_3 and Al_2O_3. The chemical composition and its characteristics, such as surface area and pore diameter, vary from source to source. Some important characteristics that influence the function of catalysts are the surface area, pore size and pore distribution. Dolomite when calcinated ($MgCO_3 \cdot CaCO_3 = MgO \cdot CaO + 2CO_2$) is more effective than raw dolomite. However neither of them is very useful for methane conversion. Dolomite is mostly effective for tar disposal, and it is inexpensive and widely available. This catalyst can be used as a primary catalyst by mixing with the biomass or as

a secondary catalyst in the downstream of reformer which is called a guard bed. However, the more common is their secondary use (Dahlquist 2013) (Sutton et al. 2001).

When applying suitable ratios of biomass to oxidant agent, in the presence of dolomite, almost 100% elimination of tars can be achieved. Dolomite has potential to decompose all tar compounds except naphthalene, and as a result, naphthalene is usually the most abundant condensable compound in the products of reforming of tars over dolomite at 800–900 °C. This fact restricts dolomite applications as catalysts if the overall aim is the total elimination of all tars from the product gas. An additional drawback with dolomite is its limitation in applications at high pressure conditions. Dolomite must be calcined in order to perform acceptably and calcined dolomites can be re-carbonated depending on the temperature and partial pressure of the carbon dioxide. As an example, if the partial pressure of carbon dioxide exceeds more than 100 kPa at 900 °C, CaO will be carbonated to $CaCO_3$. Besides, dolomite is not enough physically resistant toward erosion. The presence of chlorine in the gas phase is also problematic since it easily forms $CaCl_2$ at the conventional gasifiers temperature. Low melting point of $CaCl_2$ (782 °C) which is lower than the temperature normally used in the gasifier may lead to formation of $CaCl_2$ as a soft outer layer at the bed particles. This layer cause blocking of pores and deactivation of catalyst. Deactivation can be also due to carbon deposition. However, the relatively high amounts of steam, which is normally used in gasification, can be influential in maintaining the activity of the dolomite catalysts (Dahlquist 2013).

b) Alkali metals

Another type of catalysts which are able to act catalytically well in gasification process are alkali salts. The use of NaOH, KOH, Na_2CO_3, K_2CO_3, and $Ca(OH)_2$ as alkali metals is reported in previous researches. Alkali metals are effective in decreasing both the tar and methane contents in the products. Most of biomass inherently contains high concentrations of alkali (like potassium) in their ash which can act as catalysts for tar decomposition. On the other hand, the inherent alkali metals in the catalyst can leads to agglomeration and cause operational problems. Alkali metal catalysts are usually used as primary catalysts, and in situ with biomass, by dry mixing or wet impregnation. These catalysts are

effective in increasing the rate of gasification, reducing the methane content of the product gas and reducing the tar content. The drawback of this type of catalysts is their rapid deactivation. The regeneration of catalyst is a difficult and costly process. These catalysts also have a severe corrosion effect at conventional temperatures of gasification. Unlike dolomite, they are effective also in reduction of methane in the product gas through a reforming reaction (Dahlquist 2013) (Bulushev and Ross, 2011) (Sutton et al. 2001) (Basu, 2013).

c) Nickel based catalysts

Improvement of hydrogen yields in bio-oil steam reforming was reported to be achieved, by use of noble metal catalysts. Ni catalysts are effective not only for the removal of tars and methane but also in the adjustment of the CO/H_2 ratio in synthesis gas by means of water-gas shift reaction. Water-gas shift reaction is one of the reactions in hydrogen production from methane and nickel-based catalysts are very effective in catalyzing this reaction. As long as they are active, nickel based catalysts are able to remove tar totally. The most common catalyst in the catalytic gas cleaning for biomass gasification with steam reforming, are nickel catalysts. These catalysts are resistant and not expensive, although they are more expensive than dolomite.

However further work is needed to optimise the properties of the catalysts such as the Ni content, the average Ni particle size and the support used in the catalyst. Nickel based catalyst are used mostly in a supported form. Materials such as α-alumina, magnesia, magnesium aluminum spinel and calcined zirconia are usually used as a support for nickel based catalysts. Good performance was reported for magnesium-modified and Ni/Al_2O_3 catalysts in previous researches. Good carbon conversion to gas and a hydrogen yield was obtained by use of them (Dahlquist 2013) (Basu, 2013).

The problem with Ni catalysts is their deactivation by sintering and/or coke deposition. Deactivation in Ni catalyst is usually as a result of sulfur poisoning (at higher pressure), carbon fouling and (thermal) sintering of the nickel particles. The best results can be obtained by using them as secondary catalysts at temperature around 780°C, by locating the catalyst bed in a separate reactor downstream. The advantage of using the secondary reactor is the possibility to work at conditions different from

gasifying reactor. It has been reported that when secondary Ni-based catalyst is used, the deactivation is faster and easier in the fixed beds rather than fluidized beds (Dahlquist 2013) (Basu, 2013).

The best choice would be application of nickel catalysts in combination of dolomite guard beds. The optimum choice would be the use of a dolomite as a catalyst support for Ni. This way carbon deposition, may take place in the guard and the Ni catalyst are kept safe from deactivation. It has been reported that by use of a guard bed of dolomite, the removal of tar up to 95% can be achieved. In the Ni catalyst bed the adjustment of the gas composition and final tar cracking using a second catalytic nickel can be obtained (Dahlquist 2013) (Basu, 2013).

1-9-4-4-Coke formation and catalyst deactivation in gasification process

The main problem of catalytic gasification technology and steam reforming process is deactivation of the catalysts by coking. Deposition of coke on alkali metals or poisoning by compounds containing sulphur or nitrogen is responsible for catalyst deactivation. Coke deposition is the major cause of catalyst deactivation, which may block the active sites of the catalysts. Coke may be originated from oxygenated compounds such as acetic acid, acetaldehyde or acetone as well as from different phenols and complex aromatics. Previous researchers reported that by using high heating rates, high catalyst to feed ratios and proper choice of catalyst, the problem of coke formation would be minimized. Generally, when catalyst is used in primary approach, deactivation process is more sever (Dahlquist 2013) (Campanella and Harold, 2012) (Bulushev and Ross, 2011).

1-9-4-5- Operational conditions and parameters for gasification of pyrolysis products

Important operational parameters that may influence the performance of air/oxygen gasification and/or steam reforming process are:

✓ In-situ or separate position of catalyst (one stage or two stage upgrading)

Primary and secondary approach for catalytic gasification and steam reforming process are available same as catalytic cracking. The catalyst, in the gasification process, can be applied primary (in situ) in

contact with biomass or separately in a secondary reactor. Although in-situ application is effective in reducing the tar, it is not effective in reduction of methane amount. The problems like catalyst deactivation, erosion and elutriation are more sever in primary methods. More attention has been paid to secondary catalytic bed approaches. The presence of a secondary reactor in the downstream of the gasification reactor is needed. This gives the possibility to study different process conditions than those of the first (pyrolysis) reactor, since the catalytic bed operates independently. This way, the condition of the second reactor can be held as optimum for the reforming reaction. Gasification catalysts are active in hydrocarbon reforming and often in methane reforming as well. Particles and other impurities may be removed before entrance to the secondary reactor and exposure to catalyst. Considering different type of catalyst, mentioned in previous sections dolomites can be used both as primary and secondary catalysts, nickel-based, mainly as secondary catalyst and alkali metals, as primary catalyst.

- ✓ Catalyst bed temperature

The conventional gasification temperature is in the range of 800–1200 °C which is higher than pyrolysis temperature. The production of syngas usually takes place at high temperatures (over 700 °C). This may be as a result of equilibrium in the water-gas shift reaction. Thermal upgrading without the presence of catalyst can be obtained at high temperature of 1250 °C. The presence of catalyst enables the process to perform at much lower temperature (Mahmood et al., 2013). By raising temperature, higher conversion can be achieved and the product gas yield increases. The tar content also decreases. Naturally, the contents of H_2, CO, CO_2 and CH_4 are also changed by temperature as a result of the gasification reactions kinetic alteration. Since the H_2 production reactions, the water gas reaction and the steam reforming as well as a reverse of the exothermic water-gas shift reaction are all endothermic, at temperatures above 750–800 °C, the H_2 and the CH_4 content will increase and decrease, respectively. By further increase of temperature above 850–900 °C, reverse Boudouard reaction become substantial together with the water gas and steam reforming reactions (Dahlquist 2013) (Skoulou and Zabaniotou, 2012) (Campanella and Harold, 2012) (Bulushev and Ross, 2011).

✓ Amount of catalyst

The optimal amount of catalyst must be investigated to obtain the gaseous products with the desirable conditions. Appropriate range for catalyst amount can be achieved by the comprehensive literature survey.

✓ Steam to feed ratio

The steam ratio is mostly mentioned as steam to biomass ratio or sometimes steam to carbon ratio. More than enough steam may have negative effect on the process, since it will lower the temperature of the system.

✓ Equivalence ratio (ER)

Equivalence ratio (ER) is an important operational parameter when oxygen or air is used as an oxidizing agent. ER is defined as the ratio of airflow to the amount of airflow needed for stoichiometric combustion of the biomass. In the other words, ER is an indication of the extent of partial combustion. ER is defined by the following equation, in which subscripts a and s stand for actual and stoichiometric, respectively (Dahlquist 2013) (Abdoulmoumine et al. 2014).

$$ER = \frac{[\dot{m}_{O2}]_a}{[\dot{m}_{O2}]_s}$$
Equation 1-20

Decision about these operational parameters can be made through a comprehensive literature review, which will be mentioned in the Chapter 2.

1-10- Aim of study

A comprehensive literature review (Chapter 2) shows that most of the previous pyrolysis studies involved with fast pyrolysis with the aim of obtaining a high quality bio-oil. Hence, the characterisation of char and gaseous product of the process is very rare in the literature especially considering the effects of temperature on them. There is a lack of study which considers thoroughly the slow pyrolysis process, by investigating the potential value-added application of all product streams. The research on pyrolysis of chicken manure is even more rare, although it is a demanding type of biomass to be converted to the energy product and be to be disposed safely at the same time.

However, the challenges of this type of biomass are the potential release of nitrogenous and sulphur component which must be investigated from environmental point of view.

What was studied in this work is the slow pyrolysis of the biomass (chicken manure) in a fixed bed reactor and analysis of all the products (biogas, bio-oil and char) for better understanding of their composition, their characterisation and also upgrading possibility for further application. The effect of temperature was also studied in the range of 400- 800 °C on the characteristics of the products. On the other hand, by using elemental analysis the fate of problematic nitrogen and sulphur was investigated. The HHV of all the products, heat demand of the system and mass balance were also performed. The ability of the produced gas to suffice for sustaining a self-sufficient pyrolysis process was observed.

The catalytic cracking of the pyrolysis product was also done to study the effect of catalyst on improving the products.

2- Literature review

2-1- Pyrolysis of biomass

This part of literature review mostly involves with the large scale pyrolysis of biomass in reactors of different types and scales. A suitable reactor configuration must meet three aims (Dahlquist, 2013):

- Operation within the reaction engineering coordinates of temperature, pressure and residence time

- Low risk of implementation

- Ability to be scaled up to economically justified commercial size while maintaining the energy and mass balance efficiencies of bench and laboratory scale systems

In the commercial scale the most used type of the reactor are bubbling fluidized bed, circulating fluidized bed, rotating cone reactors and etc. However, for study of slow pyrolysis in laboratory scale usually fixed bed reactors are used.

Biomass pretreatment and handling system is very similar to the system used in pulp and paper industry. Usually drying and grinding are needed for reactor use. Since the biomass size reduction is very expensive, the size of the biomass must be considered before reactor design (Dahlquist, 2013).

Pyrolysis of biomass in reactor was studied by various researchers for different purposes. However, most of the works were aimed at improving the amount of bio-oil yield and its characteristics. For this purpose, most of the researches were involved with fast pyrolysis in fluidized bed (Miao et al., 2004) (Ngo et al., 2013) (Agblevor et al., 2010). Some of the researchers investigated the upgrading of the obtained bio-oil from fast pyrolysis in a secondary reactor, which was in the most of the cases a catalytic bed (Mahmood et al., 2013) (Rennard et al., 2010) (Xie et al., 2012). This way, the effect of temperature and catalyst type and amount was studied in the work of different researchers.

The works involved with slow pyrolysis in the laboratory scale reactor are quit few and some are mentioned in the following:

In the work of Xiao and Yang, 2013 rice straw was slowly pyrolysed in a tubular reactor at different temperatures and the temperature effect was studied on char and oil characteristics. The yield of bio-oil passes a maximum at 500 °C. By temperature raise, the organic functional group available in biomass semi-char decreased greatly. The major compounds detected by GC-MS in bio-oil were acid, phenol, ketone, alcohol, ester and furan.

In the work of Cozzani et al., 1995, the slow pyrolysis of refuse-derived fuels (RDF) was investigated in a laboratory scale fixed bed reactor at different temperatures (500-900 °C). The gas was analysed by gas chromatography and the influence of gas phase secondary tar cracking reactions on final gas components was studied. The initial results of TGA and DSC in RDF samples demonstrate that the behaviour of RDF during pyrolysis may be considered as the sum of the separate behaviour of each key component. By raising temperature in the range, constant decrease of two phases of bio-oil was observed, which is the evidence of occurrence of tar cracking reactions in homogeneous phase. Temperature has significant effect on the components of the gas. The yield of hydrogen, and CO_2 increased by temperature increase, while the yield of carbon monoxide decreased. Methane and other hydrocarbons were found to be present only at high temperatures. Therefore, it was concluded that, these compounds are arising from secondary homogeneous reactions. Increase of hydrogen and hydrocarbons cause the overall gas heating value increase by temperature raise. High volatile and low char yield pointed out the crucial role of pyrolysis during gasification process.

Grierson et al., 2009 studied the degradation behaviour of six different algal biomass under the condition similar to slow pyrolysis by computer aided thermal analysis and 10 °C/min heating rate, and calculated the necessary heat to achieve thermal conversion of the samples to be equal to 1 MJ/kg. Gas chromatography of gas was done and the combustion heat of gas calculated to be in the range of 1.2-4.8 MJ/kg for different biomasses. The yield of the bio-oil obtained at 550 °C was measured and the average molecular weight of different obtained bio-oil was suggested to be between 240-450 amu, which is an indication of difference in properties and characteristic of the obtained bio-oil from different algal biomass types.

The work of Jena and Das, 2011 is focused on comparison of liquefaction and slow pyrolysis of algal biomass. The pyrolysis was done in an 8 liter mild steel cubical reactor. The yields obtained from the slow pyrolysis at 500 °C were: water phase: 22%, bio-oil: 30%, char: 28% and gas: 30%. The energy content of obtained bio-oil was 33.62 Mj/kg. The bio-oil was analysed by GC-Ms and the major compounds identified were aromatic hydrocarbons, N-hytrocyclics, amides, amines, carboxylic acids, esters, ketons and straight chain hydrocarbons. The high N-hetrocyclic content of the bio-oil is the result of high protein content of the algae, which is also the case for poultry litter. Bio-oil obtained from pyrolysis at higher temperatures showed better stability. The produced gas was also analysed by GC and contained N_2:75-83% (carrier gas), CO_2: 7.0-8.5%, H_2: 0.37-0.73%, 1.2-2.5% CO and 8.2-10.5% hydrocarbons. The list of obtained hydrocarbons is also mentioned in that work and is shown in Table 2-1. Water soluble compounds were also analysed by HPLC and were: formate, acetate, ethanol and propionate. The energy content of char obtained from slow pyrolysis was 26.12 Mj/kg and was alkaline (pH=11). The distribution of the intrinsic nitrogen of biomass was also evaluated and was 18.6 % in bio-oil, 6.95% in water phase, 51.83 in solid char and 22.65 in gas, while for the liquefaction most (98%) of the nitrogen remains in the char and bio-oil and only 0.78% goes to gas. This fact in addition to higher energy recovery in bio-oil and higher stability bio-oil made liquefaction a better process in comparison with slow pyrolysis. It must be mentioned that, the biomass used in this work had a very high moisture content (80%) which must be removed prior to pyrolysis and that is what makes the pyrolysis process economically worse from energy point of view.

Table 2- 1- Composition of gaseous product of liquefaction and pyrolysis by GC-MS (Jena and Das, 2011)

		area, %		
RT^a	compd	$TCL\ 350^b$	$Pyro350^c$	Pyro500
1.37	cyclopentene		0.32	1.20
1.43	propanenitrile		5.45	5.38
1.50	2-butanone	10.81	9.13	12.26
1.56	furan, 2-methyl-		22.64	4.31
1.84	cyclopentene, 4-methyl-	2.76	1.49	
1.92	1-pentanamine		3.62	4.47
1.95	benzene			6.76
2.17	1-heptene		1.45	0.35
2.26	heptane		2.44	1.44
2.28	heptane	1.42		1.90
2.83	1H-pyrrole, 1-ethyl-	10.63		
3.18	toluene	6.85	28.63	55.00
3.82	styrene	3.42		
4.74	ethylbenzene			3.85
4.88	*p*-xylene	0.95		2.99
5.31	1-butylpyrrolidine	2.47		
5.91	2-pyrrolidinone, 1-propyl-	1.97		

[a] RT: retention time. [b] TCL: thermochemical liquefaction. [c] Pyro: pyrolysis.

Cordella et al., 2012, have studied the hazardous components available in the bio-oil obtained from slow pyrolysis of three different biomasses (corn stalk, poplar and switch grass) and found it to be toxic and carcinogenic. GC-MS analysis was done for characterisation of bio-oil and the hazardous compounds available in bio-oil were phenols, furans and PAHs.

The work of Güngör et al., 2012 is the biomass (pine bark) slow pyrolysis in the reactor. The process was studied both in the presence and absence of the catalyst. The catalytic process was done both in situ and in the second stage reactor. Three different types of catalysts were tested. In the in-situ presence of catalyst, the yield of char slightly decreased, while the yield of the aqueous phase increased. When the catalyst was used in the second stage, the gas yield increased by the expense of bio-oil. ZSM5 catalyst was tested only in the second stage and it causes a decrease in the water yield and increase in the yield of water soluble. The effect of temperature was also studied in the process in the range of 300-600 °C. The difference in the yield of products (aqueous, gas, char and bio-oil) between catalytic and non-catalytic process, was observed only at higher temperatures. The catalyst has notable effect on the products distribution in fluidized bed rather than fixed bed. Compounds available in the bio-oil were analysed by GC-MS and were phenols, ketons, aldehydes, aromatic compounds, carboxilyc acids and esters. Phenols had the major quantity. By use of ZSM5 catalyst in

the second stage, the compounds that are mostly affected are aldehydes and aromatics, which decrease and increase respectively. Ketones were also decreased. The other groups were changed only slightly. Produced gas from biomass pyrolysis, is rich in carbon oxides as a consequence of high oxygen content of biomass. CO_2 is the product of the primary pyrolysis of cellulose and hemicellulose, where CH_4 and CO are mainly formed from secondary cracking of volatiles, followed by reduction of CO_2 ($C+CO_2 \leftrightarrow 2\ CO$). Catalyst had no considerable effect on the gas in one step process. However, the gas composition was affected in two step pyrolysis. The aim of catalyst application is the removal of oxygenated compounds, via water, CO_2 and CO formation. In two step catalytic process, using ZSM5, the yield of CO_2 increased, whereas relative amount of CO was almost unchanged, which is the evidence of oxygen removal from volatiles in the form of CO_2 by decarboxylation reaction. The comparison of single-step and two-step process showed that, single-step process produces more CH_4 and H_2 and CO than two step pyrolysis. The use of ZSM5 also decreased the O/C ratio of the obtained bio-oil and improved the calorific value of the fuel.

The combination of pyrolysis and gasification process was done by Xie et al., 2012. In this work, initially the pine saw dust was pyrolysed in a tublar reactor and then the same process was repeated in the presence of steam in order to do gasification with the aim of improving the syngas (H_2+CO) production. The effects of the temperature of the both stages were studied. The optimal temperature were resulted to be 750 ° C for pyrolysis and 850°C for gasification, in order to obtain char of the high quality and maximum yield of syngas production. The maximum syngas produced was reported to be 3.29 Nm^3/kg.

2-2-Thermochemical conversion of poultry litter

The use of poultry litter for energy application and conversion of biomass into biofuels is the more efficient method for waste disposal, which is done via thermochemical routs such as combustion, co-firing, gasification, liquefaction or biochemical route like anaerobic digestion and pyrolysis. The production of energy products from poultry manure is sustainable strategy in comparison to the

available methods such as composting, incineration, land application, and landfill of the animal residue (Schnitzer et al., 2007).

In the last years, co-firing with coal and gasification of poultry litter are investigated totally in the research stage and there are available pilot scale plants and test facilities available (Giuntoli et al., 2009). Pyrolysis was also reported to be an efficient method to convert poultry litter into energy products of high energy density and higher value chemicals (Mante and Agblevor, 2010) (Das et al., 2009).

Combustion of poultry litter in large scale is already done in United Kingdom (UK) with capacities ranging from 13.5 to 38.5MW. Gasification and pyrolysis are not still thoroughly investigated and no commercial system is in operation in either Europe or USA. Considering small farms, pyrolysis may be a suitable option by which liquid fuel may be produced and then be distributed to the near farms for on-farm heating of poultry houses. In addition, the solid product of the process (char) can be used as a fertilizer since it contains most of the inorganic matters of the original biomass (Agblevor et al., 2010). On the other hand, by gasification process, manure can be converted into hydrogen or syn-gas (H_2 and CO) and char. The char combustion feedbacks energy to the gasification process. The catalytic effect of the ash content of the manure may exert a great catalytic effect on the reactivity of the residual char during gasification process (Zhang et al., 2010). During biochemical routs of anaerobic digestion, animal manure produces combustible biogas and residual digested solids. The solids can be stabilized via aerobic composting and produce an odour-free humus material. This method is becoming restricted due to seasonal limitation and economic performance (Zhang et al., 2009). The product of thermochemical conversion methods can be used as energy intermediates for combined heat and power generation (CHP) or feedstock for downstream catalytic conversion processes to produce higher value products such as liquid transportation fuels (Ro et al., 2010).

The biomass may be pre-treated by use of water leaching techniques to remove high amount of ash. In addition, there is need for deep investigation of the fate of nitrogen to avoid the excessive emission of NO_x and N_2O. The nitrogen can release also in the form of ammonia, which favours reduction

reactions and thus actually reduce the needs for NO_x removal technologies (Giuntoli et al., 2009). The concern about NO_x emission is more serious in combustion and air gasification where there is a huge amount of oxygen available. However, it can be controlled by modifying the combustion process (Sheth and Bagchi, 2005). High sulfur content was also reported for poultry litter (Giuntoli et al., 2009). The possible release of phosphorus as phosphine gas during gasification must be also investigated (Sheth and Bagchi, 2005). Poultry litter has lower elemental carbon content in comparison to other biomasses and therefore may produce lower char yields than other plant biomasses (Lima et al., 2009).

The characteristics of the obtained bio-oil are determined by the nature of the biomass from which they originate. The protein and lipid content of poultry litter lead to the production of bio-oil with improved HHVs. During pyrolysis, protein undergoes decarboxylation and nitrogen release and leads to higher hydrocarbon content and as a result higher HHV. The higher amount of hydrocarbon in the bio-oil obtained from poultry litter in comparison to the bio-oil obtained from hardwood (10 times more) is the result of proteins, not lipids (Agblevor et al., 2010). The bio-oil obtained from poultry litter is rich also in nitrogenous compounds such as primary, secondary amides, aromatic amines and N-heterocyclic (Zhang et al., 2011).

Thermochemical conversion of poultry litter to energy products was studied by several researchers. Joseph et al., 2012 have performed the chicken manure and wood shaving gasification and characterisation of different products. Although the energy recovery was very low as a result of low energy efficiency of gasification unit (19.6%), this method was observed to be a suitable method for waste disposal. The gasifier was a pilot scale reactor. Gas chromatography analysis of the gas indicated that the highest calorific value obtained was (2.9 MJ/m^3).

Most of the pyrolysis studies were microscale thermogravimetric analyzers (TGAs). These small-scale studies provide preliminary information on animal manure pyrolysis. Dejong et al. 2007, conducted TG-FTIR analysis of different biomass including chicken manure, and analysed the evolved gas both qualitatively and quantitatively and then, obtained the tar yields by mass balance. Whitely et al. 2006,

studied the kinetic study of poultry litter analysis, and reported the temperature range in which each gas is evolved. Giuntoli et al. 2009, analysed the gas evolved by TG-FTIR. This study is important mostly considering the fate of nitrogenous compounds that form during the process. HNCO was observed at 430°C. Ammonia formation was observed during the whole process. HCN formation was observed at the temperatures around 430 and 472 °C. The kinetic study was also done in this work. Kim et al., 2009, have done one of the few large scale studies of poultry litter which is fast pyrolysis in fluidized bed. In this work the yield of different products were obtained, and the viscosity of bio-oil was measured. The work of Lima et al., 2009 is one of the few slow pyrolysis of poultry litter found in the literature. The aim of this study was the production of char with high potential to absorb metals. However, the gas was also analysed, and the effect of temperature was studied. Major evolved gases were CO, CO_2, low molecular weight hydrocarbon and H_2. By raising the temperature (700-900 °C) all the non-condensable gaseous products were increased except CO. The yield of liquid product was measured in this work by difference.

The work of Ro et al., 2010, is a pilot scale slow pyrolysis at 620 °C, in order to obtain combustible gas and char. The gas was analysed and the presence of s-containing compounds such as dimethyl sulfide and methyl mercaptane was observed more than OSHA limits. The energy of original biomass was recoverd 50% in char and 25% in gas. Quantities of different gaseous compounds were measured and also the H/C ratio of the char was measured and compared to the original biomass. The energetics of the process was also studied, by calculating the energy for drying and sensible heat of biomass. During drying, 80% thermal efficiency was considered, and for sensible heat calculations the heat capacity of wood was considered. The pyrolysis heat was considered to be equal to the pyrolysis heat of cellulosic biomass. The heat demand of the process was huge as a result of high amount of moisture content in the biomass. Only after mixing the biomass with another low moisture content biomass, the energetics of the process became neutral.

The bio-oil obtained from chicken manure is rich in hetrocyclic nitrogen compounds as a consequence of high amount of proteins available in biomass. In the work of Kazi et al., 2010 these compounds

which are valuable because of their application in chemical, pharmaceutical and food industry were separated by column chromatography. In general, seven based structure were identified which were pyrazine, benzoquinoline, carbazole, phenylpyridine, indole, pyrazole and pyridine.

Sheth and Bagchi 2005 studied the fate of problematic nitrogen and phosphorus compounds during catalytic gasificateion of chicken manure and observed that almost all phosphorus remains in char residue and some (20-70%) of nitrogen end up as ammonia in gas.

The complete characterisation of the products, operational problem and feasibility of the process is not yet completely clear, especially for slow pyrolysis. In addition, the effect of temperature on the yield and characteristics of different products is unknown.

2-3- Upgrading of pyrolysis products

Bio-oil, which is considered most of the time as the most valuable product of pyrolysis process, has several drawbacks which make it far from industrial use. The necessity of the upgrading of the pyrolysis product and the available method are described in detail in section 1-8. In these section results of previous attempts of the researchers for upgrading of the products in the secondary reactor are reviewed. The upgrading methods can be classified into catalytic cracking and gasification of pyrolysis products.

2-3-1-Catalytic cracking of pyrolysis products

Srinivas et al., 2000 suggested the mechanism shown in Figure 2-1 for the thermal or catalytic upgrading of the pyrolysis products in the second reactor.
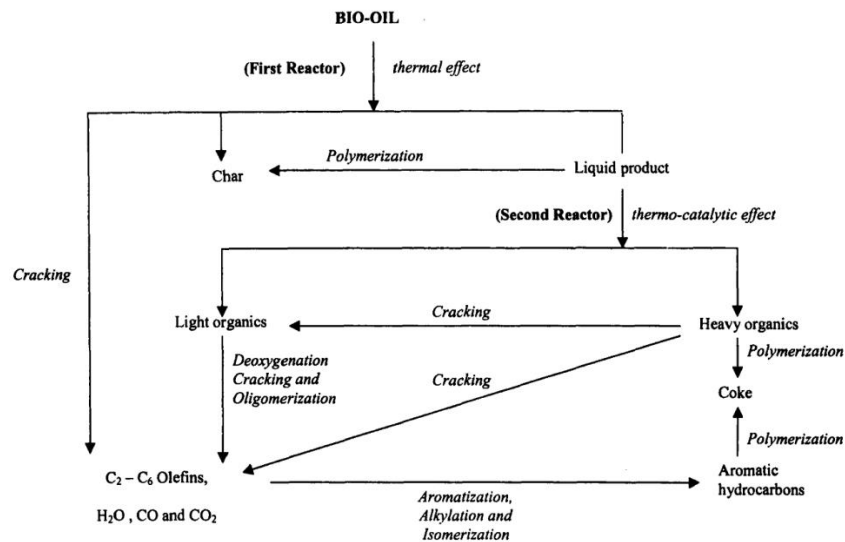
Figure 2- 1- Mechanism of thermal and catalytic cracking takes place in the secondary reactor(Srinivas et al., 2000)

Several researchers have studied upgrading of biomass pyrolysis products in two stage reactor systems (Srinivas et al., 2000) (Güngör et al., 2012) (Iliopoulou et al., 2007) (Choi and Meier, 2013).

Secondary catalytic cracking of bio-oil was done by Güngör et al., (2012). The biomass used was pine bark. The catalyst (ReUS-Y, ZSM-5) was presented in the second reactor, while there was no catalyst in the first reactor. The temperature range of 300-600 °C was studied in the first (pyrolysis reactor). The catalysts decreased the bio-oil yield with a consequent increase in the gas yield. In this work a comparison of the catalytic cracking process and thermal cracking process was done. It was reported that, the difference between thermal and catalytic runs was only observed at high temperatures, the bio-oil yield decreased by the increasing the temperature from 500 to 600 °C in catalytic run, while it did not vary between 500 and 600 °C in thermal run.

In the work of Pan et al., 2010 the catalytic pyrolysis of *Nannochloropsis sp.* was performed in the presence of HZSM-5 catalyst. They obtained lower bio-oil yield and higher biogas yield in the presence of catalyst in comparison to the process without catalyst as well. In their work, the yield of aqueous fraction of bio-oil product was higher in the presence of HZSM-5 catalyst at all pyrolysis temperatures. An interesting result of their work is the lower coke formation at higher temperature since coke on catalyst surface could be easily formed at relatively low temperature, and partly

decomposed at higher temperature over 400°C when *Nannochloropsis sp.* residue is used as pyrolysis material. In this work, biogas composition over temperature was also reported. As it is shown in Table 2- 2 syngas (H_2 and CO) yields reaches a maximum at 450 °C.

Table 2-2- The yields (wt.%) of various gaseous products at different temperature in the catalytic pyrolysis process (Pan et al., 2010)

Temperature	H_2	CO_2	CO	CH_4	C_2H_4	C_2H_6	C_3H_6	C_n^a
300 °C	0.05	9.55	2.58	0.13	tr[b]	tr	tr	0.13
350 °C	0.08	14.78	4.37	0.82	0.20	0.21	tr	1.23
400 °C	0.14	20.40	0.72	2.38	1.42	1.23	0.75	5.78
450 °C	0.18	22.70	1.56	2.67	1.25	0.93	1.04	5.89
500 °C	0.17	27.47	0.63	3.50	1.99	1.21	0.44	7.14

Pan et al., (2010) in the same work also studied the effect of different amount of catalyst ratio on products yields. They tested the catalyst to biomass ratio in the range of 0:1 to 1:1 with 0.2 intervals. The yield of liquid product notably decreased with a simultaneous increase of char as more catalyst HZSM-5 was added into reaction material. It can be explained as the coking trend over catalyst. When the volatile intermediates formed in the primary pyrolysis process passed over the catalyst surface or went deep into its micropores, the high acidity of catalyst might enhance various secondary reactions of the intermediates such as repolymerization and aromatization. As a result, bio-oil reduced. Cokes were remained on the catalyst surface and in its micropores, with more gas and aqueous products produced. The increase of catalyst-to-material ratio enhanced the direct contact between heterogeneous catalyst and solid materials, and promoted the thermal cracking and secondary reactions of reactants to produce more gas and aqueous products. Table 2-3 shows the biogas composition at different catalyst to biomass ratio. Considering the goal to be maximizing CO and H_2 production, the ratio of 0.2/1 of catalyst to biomass seems to be the optimum according to Table 2-3. It must be known, that in this work the catalyst and biomass were in contact in one reactor. According to the work of Pan et al., (2010) by raising the amount of catalyst the liquid product will decrease due to more cracking reactions. Char and gas yield increase instead. Considering the resulted gas composition, H_2 and CO reach a maximum at the ratio of 0.2:1 of catalyst to biomass. Adding more

catalyst, cause a decline in this two gases and rise in CO_2. The CH_4 does not change significantly. Generally the range of 0.2:1 to 1:1 are worth to be examined.

Table 2-3- The yields (wt.%) of various gaseous products at different catalyst-to-material ratios (wt/wt) at 400°C (pan et al. 2010)

Catalyst-to-material ratio	H_2	CO_2	CO	CH_4	C_2H_4	C_2H_6	C_3H_6	C_n[a]
0/1	0.23	18.73	3.68	0.97	tr[b]	0.83	nd[c]	1.80
0.2/1	0.26	18.25	2.94	2.16	tr	0.92	nd	3.08
0.4/1	0.18	18.88	2.38	2.02	0.57	0.75	tr	3.34
0.6/1	0.14	19.97	1.39	1.95	1.05	1.05	0.23	4.28
0.8/1	0.16	20.76	1.17	1.85	0.92	1.10	0.51	4.65
1/1	0.14	20.40	0.72	2.38	1.42	1.23	0.75	5.78

In the work of Pütün et al. 2009, volatile upgrading of olive residue pyrolysis was performed in a two stage fixed bed reactor. Clinoptilolite (a natural zeolite) was used as catalyst. Catalyst bed temperature varied in the range of 350-500 °C. A catalyst bed temperature of >450°C caused improvement of the gas yields and reduction of the oil yields. After application of catalytic treatment, the long chains of alkanes and alkenes of the pyrolysis oil were converted to lower-weight hydrocarbons. An increase of aliphatics, aromatics, and olefins and a sharp decrease of asphaltenes and polar groups (highly oxygenated groups) were observed. Increasing the catalyst bed temperature enhanced the gas yields at the expense of liquid yields. As the temperature of the catalyst bed was increased, the coke yields decreased under the present experimental conditions. Coke formation was decreased for each catalyst, while the catalytic temperature increased from 350 °C to 500°C.

To generalize, the operational conditions of the catalytic cracking of pyrolysis products are as follows:

a)Temperature: when dealing with two stage reactor, according to previous works with catalytic cracking of bio-oil upgrading (Miskolczi et al., 2010) (Srinivas et al., 2000) (Pütün et al., 2009), testing the second reactor temperature in the range of 400-600 °C seems reasonable.

b) Catalyst type: The best catalyst for catalytic cracking of bio-oil to obtain an upgraded product are zeolites, with the most promising one to be ZSM-5.

c) Catalyst amount: According to the work of Pan et al., (2010) by raising the amount of catalyst the liquid product, will decrease due to more cracking reactions. Char and gas yield increase instead. Considering the resulted gas composition, H_2 and CO reach a maximum at the ratio of 0.2:1 of

catalyst to biomass. Adding more catalyst causes a decline in the yield of these two gases and raise in CO_2. The CH_4 does not change significantly. Generally the range of 0.2:1 to 1:1 is worth to be examined.

2-3-2-Gasification of pyrolysis products

The desirable operational condition, when dealing with gasification of pyrolysis products in secondary reactor, can be clarified by the result of previous studies.

a) Type of oxidizing agent

Several previous researches are available for steam reforming of biomass in the catalytic process (Mahmood et al., 2013) (Wu et al., 2008) (Skoulou and Zabaniotou, 2012) (Wu et al., 2013). In some of the other researches air or oxygen was used in catalytic process as an oxidizing agent (Abdoulmoumine, et al. 2014) (Behainne and Martinez 2014) (Nordgreen, et al. 2006) (Wongsiriamnuay et al. 2013) (Pu et al. 2013). Both steam and oxygen and a mixture of both would be demanding. The use of steam is more attractive since it enhances water gas and steam reforming reactions and cause more H_2 production. Utilizing steam is also favorable for syngas production purposes and adjusting H_2/CO ratio. However, there are some drawback such as extra expenses and facilities needed for steam production. Besides, the lower temperature of steam in comparison to the gasification temperature would lower the overall temperature of the system.

Steam reforming is for sure more interesting process than partial oxidation with air or oxygen. In addition to the above advantage, the obtained biogas would have more heating value. However, more complicated facilities for steam production and feeding are necessary in steam reforming. The heating value of the produced gas is more with oxygen, rather than with air.

b) The amount of oxidizing agent

In the work of Abdoulmoumine et al., (2014) different ER ratio in the range of (0.15-0.35) were tested. More ER resulted to more conversion due to combustion and partial oxidation and therefore, lower char yield. Excess oxygen would also react with hydrogen and form water, which will result

more yield of liquid product. Excess oxygen favors complete combustion rather than partial oxidation. Hence, the biogas would contain more CO_2 rather than CO. H_2 would also decrease as a result of water formation reaction.

Considering different works investigated the effect of ER on products (Skoulou et al., 2008) (Sharma et al., 2014) (Nordgreen et al., 2006) (Wongsiriamnuay et al., 2013) (Pu et al., 2013), ER value of 0.2 looks favorable. Most of the researchers have studied the ER ratio of lower than 0.4 (Skoulou and Zabaniotou, 2012) (Skoulou et al., 2008) (Sharma et al., 2014) (Abdoulmoumine et al., 2014). So study of this range for ER is suggested, while the optimum value is expected to be around 0.2.

In the case of using steam as an oxidizing agent, the amount of steam added is another important operational parameter, which can affect the gasification product in steam reforming process. In the literature, it is sometimes reported as steam to carbon ratio (S/C). Most of experiments reported to be carried out with excess steam (6<S/C< 12). The S/C< 3 is not favorable. In the work done by Skoulou and Zabaniotou, (2012) the steam amount was indicated as steam to biomass ratio and the range of 0.86–6.03 was used. This work resulted that the favourable steam to biomass ratio is 3–6. At low Steam to biomass ratios, CO concentration increased and reached stable level, working at 1050 °C and 950 °C; thus, the H_2/CO ratio was maximized. This pattern may be due to the role of high temperature and steam availability in improvement of endothermic steam reforming reactions, but this condition is unfavourable for exothermic reactions. High amount of steam will lead to effective coke removal from the catalyst surface and also heat and mass transfer improvement, but it will increase the production costs (Bulushev and Ross, 2011) (Campanella and Harold, 2012) (Rennard et al., 2010). According to the work of Skoulou and Zabaniotou, (2012) in which the steam to biomass ratio in the range of 0.86–6.03 was used, working in the range of 2-7 can be interesting. The ratio of lower than 3 is not recommended. Wu et al., 2013 used 0.01 gr/min of steam for each gr of biomass available in the first reactor.

In the work of Wu et al., (2013) pyrolysis and gasification takes place in two stage fixed bed reactor, and the second reactor which is the location of the catalyst is fed by steam injection with the rate of

0.05 gr/min. The initial biomass they used in the first reactor was 0.5 gr. In that work, no improvement was observed as a result of steam addition. This may be as a result of very low amount of steam added. Addition of small amount of oxygen was also tested in this method. This small amount of oxygen, induces the exothermic oxidation reactions, and provides the required energy for the subsequent endothermic steam-reforming reaction. The added oxygen may also play a positive role in decrease of catalyst deactivation by burning some of the coke formed. However, the oxygen presence reduces hydrogen yield both experimentally and theoretically (Bulushev and Ross, 2011).

Asadullah et al., (2002) reported that by increasing the amount of steam, H_2 and CO_2 in the gaseous product would be enhanced.

Pu et al., (2013) reported that using low amount of steam (<15 g/hr) cause higher H_2 production as result of enhancing gas reaction and transformation reactions. While, addition of high amount of steam (>15 g/hr) will decrease the overall temperature of the system and yield lower hydrogen. High amount of steam will enhance the steam reforming reaction and increase of CO production.

c) Catalyst amount

Mahmood et al., (2013) performed pyrolysis and steam reforming of brewer spent grain in a two stage reactor system with Ni/Al_2O_3 catalyst using 1:10 ratio of catalyst to biomass.

Wu et al., (2013), used Ni-Mg-Al and Ni-Ca-Al catalyst in a two stage fixed bed reactor. The biomass was put in the first reactor and the gaseous products further gasified in the presence of catalyst and steam in the second reactor. The catalyst to biomass ratio of their work was 0.5.

Wongsiriamnuay et al., 2013 investigated gasification of bamboo in a fluidized bed in presence of steam and air. They have studied the effect of catalyst (dolomite) to biomass amount in three ratio (0:1, 1:1, 1.5:1); and low temperature range (400-600 °C). It was found that the content of H_2 and CO increased, while the content of CH_4 and CO_2 slightly decreased with increasing temperature and catalyst to biomass ratio. With increased catalyst to biomass ratio from 0 to 1.5, higher content of CO_2 was obtained due to the release of CO_2 from dolomite. With air-steam gasification, tar conversion was increased from 84 to 92% and 77 to 90% when catalyst to biomass ratio was increased from 1:1 to

1.5:1, respectively. In the previous work using dolomite as a catalyst in a fluidized bed three catalyst to biomass ratios (1:1 to 1.5:1) were studied (Wongsiriamnuay et al., 2013). Working with nickel as a catalyst the catalyst biomass ratio of 0.1:1 was used (Mahmood et al., 2013). As suggested by Wu et al., 2013, 0.5:1 ratio was satisfactory in a two stage fixed bed reactor system. Testing the ratio in the range of 0.2:1 to 1:1 would be preferable.

d) Type of catalyst

Working in a secondary reactor, both dolomite and nickel based seems promising. Alkali metals are not used in the secondary reactor. Nickel based catalyst are suitable for both tar and methane removal since they catalyze the steam reforming reactions, while dolomites are good only in tar removal. However when working with oxygen as oxidizing agent the non expensive dolomites can be used, as it was performed in previous works which were concerning gasification with air or oxygen (Taufiq-Yap et al., 2014) (Wongsiriamnuay et al., 2013).

Considering the catalyst use in the secondary reactor, both dolomite and nickel based seems promising. Alkali metals are not used in the secondary reactor. Nickel based catalyst are suitable for both tar and methane removal since they catalyze the steam reforming reactions, while dolomites are good only in tar removal. However when working with oxygen as oxidizing agent the non expensive dolomites can be used, as it was performed in previous works which were concerning gasification with air or oxygen (Taufiq-Yap et al., 2014) (Wongsiriamnuay et al., 2013).

In some researches, use of dolomite as a guard for nickel based catalyst was suggested (Sutton et al., 2001) (Wu et al., 2008). The optimum choice would be nickel based catalyst with dolomite as support. This way coke formation and catalyst deactivation would affect mostly the cheap dolomite catalyst.

e) Second reactor temperature

The normal gasification temperature range is 800-1200 °C. When the catalyst is used, this high temperature is not needed. According to previous researches on catalytic gasification, (Skoulou and Zabaniotou, 2012) (van Rossum et al., 2007) (Abdoulmoumine et al., 2014) (Wu et al., 2013) (Xie et al., 2012), generally, the temperature range of 700- 1000 °C worth testing.

3- Materials and methods

3-1- Materials

3-1-1- Biomass

The biomass used in this study is chicken manure supplied by "Centro Interdipartimentale di Ricerca in Scienze Ambientali". The biomass is pelletized in small cylinders with an average diameter and length of 5.4 and 12.5 mm respectively. Figure 3- 1 shows the biomass used in this study. The Proximate analysis of the material is obtained by thermogravimetric analysis in a Thermal Analysis Instrument TGA-Q500. The result of this analysis is shown in Table 3- 1 according to ASTM E1755, EN 15148, and ISO 17246 limitedly to the definition of fixed carbon.

The details of the calculations are reported in the Appendix (APP1.). The data evidence the high percentage of ash present in this kind of biomass and the high nitrogen content. By comparison, typical ash content of corncob is about 2.4% (Zhang et al., 2009) and ash of forestry residue is in the range of 0.4-1.2 % (Amutio et al., 2013). As for nitrogen, this is around 1% in typical lignocellulosic biomasses (e.g. forestry residue (Amutio et al., 2013)), while only algal biomasses show similar values (e.g. 5.8 wt% on DAF basis was reported for *Lyngbia* by (Maddi et al. 2011)).

Table 3- 1-Proximate and ultimate analysis performed on chicken manure investigated in the present Study

Biomass	Proximate analysis (wt%)			
	Moisture	**Ash**	**Volatile**	**Fixed carbon**
Chicken manure (fresh basis)	5	24	64	7
Chicken manure (dry basis)	------	25	67	8

Biomass	Ultimate analysis (wt%)				
	C	**H**	**N**	**S**	**O**
Chicken manure (dry basis)	34.0	5.9	4.5	0.9	29.7
Chicken manure (DAF basis)	45.3	7.8	6.0	1.1	39.7

Ultimate analysis data reported here were obtained by elemental analysis on dry chicken manure. Elemental analysis and drying procedure are explained further in the experimental techniques and procedure part (section 3-2 and 3-3).

Figure 3- 1- Chicken manure used as biomass

3-1-2- Catalyst

The catalyst used is T-4480 1/16" ZSM-5 (MFI) Extrudate from Clariant company. This is the most well-known catalyst for catalytic cracking of bio-oil for obtaining upgraded bio-oil product. This catalyst is not used for gasification and syngas production purposes, but for catalytic upgrading of bio-oil. Some of the properties of the catalyst are mentioned in Table 3- 2. ZSM-5 catalyst needs to be activated before use at high temperature for some hours (Pan et al., 2010). In this work, the catalyst was put in a furnace at 550 °C for 4 hours to be activated.

Table 3-2- Characteristic of ZSM-5 catalyst

SiO_2/Al_2O_3 Molar ration	38
Pore volume	>0.25 ml/gr
Specific surface area	>250 m^2/gr
Crushing strength	>98 N/cm^2
Attrition	<1 wt%

3-2- Experimental techniques

3-2-1- Thermogravimetric analysis

A Thermogravimetric (TG) Analyzer is a device in which the sample weight loss is detected while undergoing a user-defined temperature-time program. The main components of the instrument are a scale for weight measurement, a sample holder platform used for loading and unloading samples, a furnace for controlling the temperature and various auxiliary electronic and mechanical components such as heat exchanger for cooling, controllers, and inlet for supplying purge gas. The schematic diagram of the devise is depicted in Figure 3- 2.

In this study TA Instrument-Water (USA) TG-Q500 devise was used. The characteristics of the instrument are mentioned in Table 3- 3. During the test, the atmosphere around the sample is continuously purged by a gas flow (the gas may be an inert gas or a reactive gas). The inlet flow of the gas is constant over time.
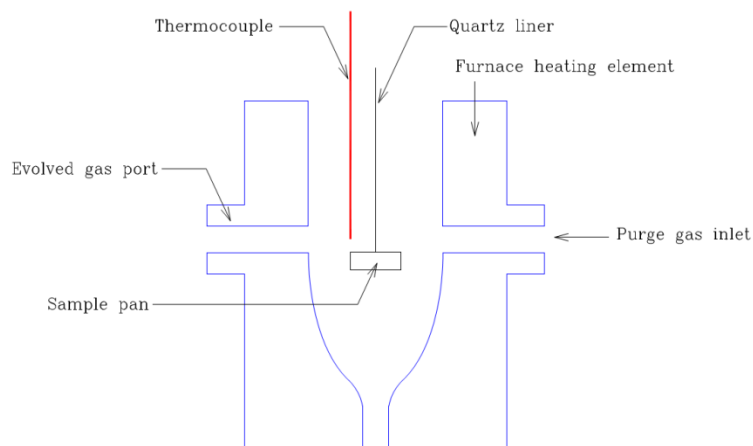
Figure 3- 2- Schematic of TG-Q500

Table 3- 3- Main characteristic of TG-Q500

	Depth 55.9 cm
Dimension	Width 47 cm
	Height 52.1
Room operating Temperature	15 °C to 35°C (non-condensing)
Temperature Control range	Ambient +5°C to 1000°C
Thermocouple	Platinel II
Controlled heating rate	0.1 to 100°C/min
Gas purge	Nitrogen or air (60 ml/min)
Sample pans	Platinum 50, 100 μl
Max sample weight	1 gr
Weighting precision	+/- 0.01 %
Sensitivity	0.1 μg
Furnace cooling (forced air/N$_2$)	1000-50 °C<12min

3-2-2- Differential scanning calorimetry (DSC) techniques

Differential scanning calorimetry (DSC) is a technique by which the difference in the amount of heat required to increase the temperature of a sample and a reference is measured as a function of temperature. This instrument can be used also for calculating heat of reaction. In this work the data were obtained using a DSC-Q2000 under atmospheric pressure. This device was supplied by TA Instruments (USA). The schematic diagram of the devise is depicted in Figure 3- 3. In the DSC-Q2000, typical sample weights around 7 mg and aluminum crucibles (d= 5.1 mm) were used. The sample cell was conditioned by a constant nitrogen purge flow (50 ml/min) at atmospheric pressure. Baseline calibration of the DSC signal was obtained by constant heating rate runs on the empty cell and on two 95 mg sapphire samples to determine the thermal resistance and heat capacity of

thereference and sample sensor. Heat flow and temperature calibration were obtained by constant heating rate runs carried out on known standards (indium and lead).
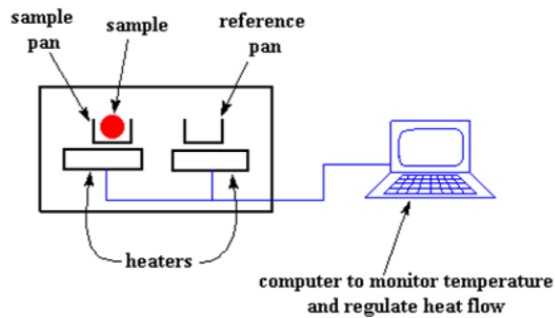
Figure 3- 3- DSC schematic diagram ("Differential Scanning Calorimetry," n.d.)

3-2-3- Material preparation instrument

a) Oven for sample drying

 Sample preparation for FBR tests included a drying procedure. This was carried out with a ventilated oven by Binder Company. This device is equipped with an electronic PID controller with digital display. The oven is heated electronically. Some characteristics of the oven are mentioned in Table 3-4. During this process the biomass was put in the oven for 4 hr at 105 °C in order to be dried.

Table 3-4- Characteristic of the oven

Nominal power	1.60 kW
Nominal current	7.0 Amp
Heating rate	To 70°C 6°C/min
	To 150°C 24 °C/min
	To 250 °C 45°C/min
Temperature range	From 5°C above ambient to 300°C

b) Furnace for activation of catalyst

Zeolite catalysts are molecular sieves and adsorb humidity quite fast in their pores. This catalyst must be activated before use in order to loss high amount of adsorbed water. This was done in a Carbolite

laboratory furnace (ELF 11/6), with W301 controller and was used for heating the reactor. The furnace is powered by voltage of 220 V single-phase and has a maximum temperature of 1100 °C. The heating zone is made of ceramic and is ventilated.

3-2-4- Fixed bed reactor techniques

A fixed bed reactor apparatus was built for investigating the pyrolysis of chicken manure in large scale. The setup of the apparatus is shown in Figure 3- 4. The main components of the apparatus are:

- Flow meter

- Tubular reactor

- Furnace

- Cooling traps

- FTIR
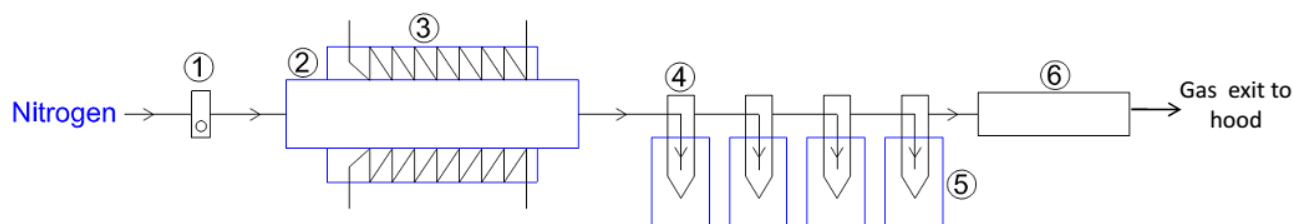
1. Flow meter
2. Reactor
3. Furnace
4. Traps
5. Ice bath
6. FTIR

Figure 3- 4- Schematic FBR set up

The main part of the system and other analytical instruments used are described in the following.

3-2-4-1- Flow meter

The flow of the carrier gas was fixed by the control flow meter (EL-FLOW F-201CV) mass flow controller, by Bronkhorst (The Netherlands) were used for pressure and gas flow control.

3-2-4-2- Reactor

The tubular reactor and its dimensions are depicted in Figure 3- 5. The reactor used is tubular, made of stainless steel. The sample is located in a spoon-shaped holder, which can be moved along the reactor in order to locate the sample inside or outside the heated part of the reactor pipe. Figure 3-5 shows the schematic view and dimension of reactor parts and sample holder.
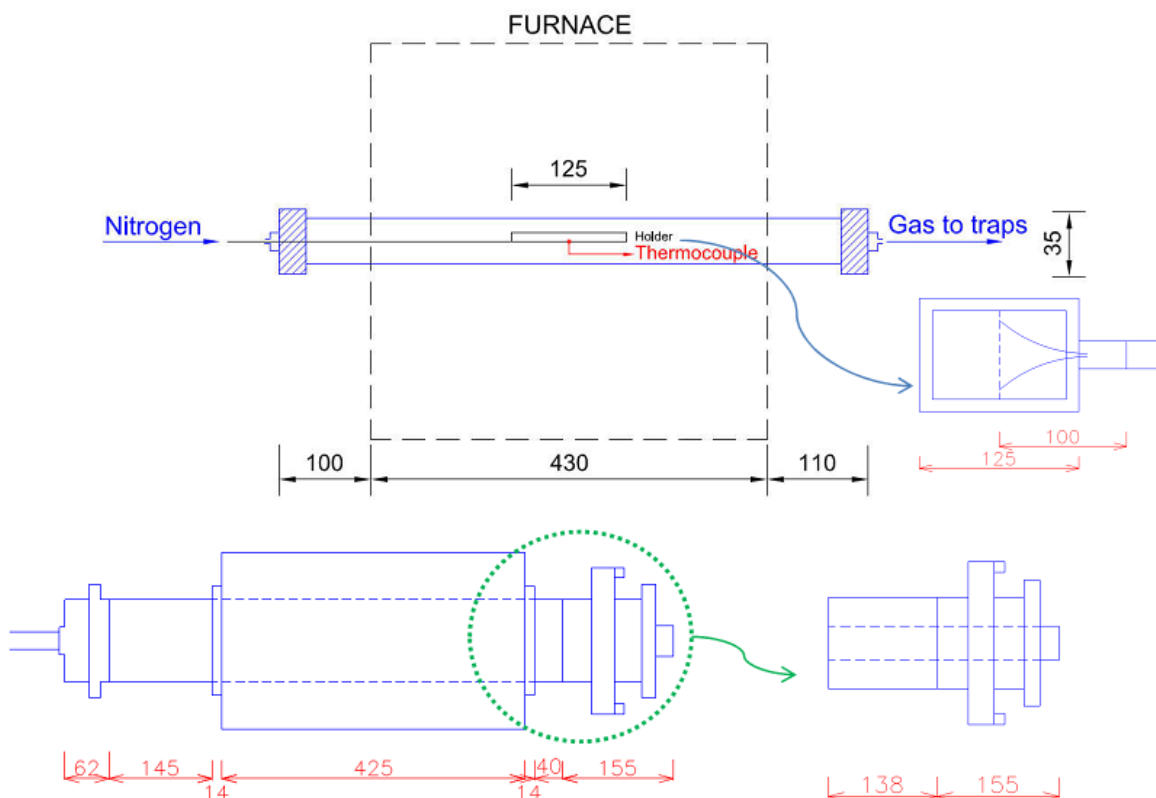
Figure 3- 5- Details and dimensions of the of the reactor parts

3-2-4-3-Furnace

The Carbolite horizontal single zone split tube furnace (HST 12/600), with W301 controller was used for heating the reactor. The furnace is powered by voltage of 220 V single-phase and has a maximum temperature of 1200 °C. This furnace can work with tubes with outer diameters of 20 to 110 mm.

3-2-4-4- Thermocouple and data logger

The temperature of the biomass sample is measured by a K type thermocouple located in the holder (under the biomass) connected to a data logger (Agilent model 34907A) for recording the sample temperature every 5 seconds. The Agilent benchlink data logger is connected to a PC for saving and analysing the measurements. The specifications of the instrument are mentioned in Table 3- 5.

Table 3-5- Agilent characterization

	Digital Input/output	Totalize Input		Analog Voltage (DAC) output	
Port 1,2	8 bit, input or output, non-isolated	Maximum count	2^{26}-1	DAC 1,2	±12 V, non-isolated
V_{in} (L)	<0.8 V (TTL)	Totalize input	100 kHz (max)	Resolution	1 mV
V_{in}(H)	>2.0 V(TTL)	signal level	1 Vp-p (min)	l_{out}	10 mA max
V_{out}(L)	<0.8 V @ l_{out}= -400 mA	Threshold	42 Vpk (max)	Setting time	1 ms to 0.01% of output
V_{out}(H)	>0.8 V @ l_{out}= -400 mA	Gate input	0 V or TTL, jumper selectable	Accuracy 1 year ± 5°C	±(% of output +mV)
V_{in}(H) Max	<42 V with external open drain pull-up	Count reset	Manual or read + reset	Temperature coefficient	0.25%+ 20 MV
Alarming	Maskable pattern match or state change	Read speed	85/s		±(0.015%+1 mV)/ °C
speed	4 ms (max) alarm sampling				
Latency	5 ms				
Read/Write speed	95/s				

3-2-4-5- Traps

The output gas from the reactor passes through four traps in series which are kept in an ice and salt mixture at -4 °C (measured by thermocouple), so that the condensable fraction of the gas would condense to form a liquid bio-oil. The dimensions of the trap are shown in Figure 3- 6. The first two traps are empty. Almost 80 gr of glass beads (diameter = 2 mm) were put in the third and the forth traps to help the precipitation of mists. On the way of outlet flow of these two traps, around 1.2 gr of glass wool filter was used to prevent the entrance of organic condensations in the FTIR. Figure 3- 6 shows the traps details and dimensions.
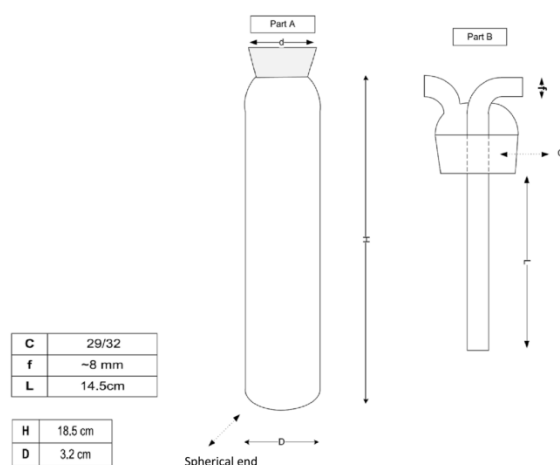
Figure 3- 6- Size of cold traps

3-2-4-6- Residence time in the different parts of fixed bed reactor system

According to the calculations the residence time of the vapours in the reactor was in the range of 0.3-0.6 minutes at different test temperatures. The residence time of the off gases was 3.4 minutes in traps. Table 3- 6 summarizes the residence time in different parts. The calculation details are reported inAPP 2. It must be mentioned that these values were reported considering the pure nitrogen to flow through the reactor. However, it is obvious that during the runs by production of volatile compounds the gas flow increasesand as a consequence the residence time changes and get less.

Table 3-6- Residence time in set up

Region	Residence time (min)
Hot zone of reactor	0.3-0.6
Trap trains	3.4
Overall	3.7-4.0

Figure 3- 7 is the picture of the whole FBR setup.

Figure 3- 7- Fixed bed reactor setup

3-2-5- Fourier transform infrared spectroscopy (FTIR)

Fourier-Transform Infrared (FTIR) spectroscopy characterization of non-condensable gas was carried out online during the FBR experimental runs using a Bruker Tensor 27 spectrometer, equipped with a mercury cadmium telluride (MCT) detector and a low-volume gas cell (8.7 mL, 123mm path length). The cell was maintained at a constant temperature of 200°C. A resolution of 4 cm^{-1} was used for collecting spectra, co-adding 16 scans per spectrum. This resulted in a temporal resolution of 9.5s. The spectra were recorded and elaborated using the Bruker OPUS/IR software.

A plastic pipe (250 cm length and 4.5 mm inner diameter) was used to connect the traps to the FTIR, which was in the laboratory environment without any isolation. The residence time in the pipe and the gas cell was calculated to be 0.31 min, considering the flow of pure nitrogen (seeAPP 2.). However, it is obvious that during the runs by production of volatile compounds the gas flow and as a consequence the residence time changes.

3-2-6- Elemental analysis

Elemental composition (HCNS) was determined by combustion using a Thermo Scientific Flash 2000 series analyser. The analysis gave the values of C, H, N and S. The oxygen amount then calculated by difference.

3-2-7- GC-MS

Bio-oil analysis was performed with a 6850 Agilent HP gas chromatograph connected to a 5975 Agilent HP quadruple mass spectrometer. Analytes were separated by a HP-5 fused-silica capillary column (stationary phase poly [5% diphenyl/95% dimethyl] siloxane, 30 m, 0.25mm i.d., 0.25 mm film thickness) using helium as carrier gas (at constant pressure, 33 cm s^{-1} linear velocity at 200 °C). Mass spectra were recorded under electron ionization (70 eV) at a frequency of 1 scan s^{-1} within the 45–450 m/z range.

3-3- Experimental procedure

3-3-1- TGA procedure

TGA analysis of the biomass was conducted with different procedure according to different purposes, but some features are common in all of them:

- The use of (60 ml/min) nitrogen as a purge flow to prevent sample oxidation and remove gaseous pyrolysis products

- A drying step at the beginning of each test at 105°C for 10 minutes

- Raising the temperature to 800° C then switching the purge gas to air (since the sample may be not homogenous in all experiment) in order to determine the ash content

- Using platinum plates to hold the sample

The main types of experiments are described in the following, while the temperature programs used for each experiment are reported in the appendix (APP 3.).

a) Biomass characterization

In these experiments, the purge gas used was an inert (nitrogen) or an oxidizing (air) agent. The experiment was performed with heating up the sample (2-25 mg) up to 800° C by a ramp of 10 °C/min, to observe the degrading behaviour of chicken manure in both conditions, and investigate the main pyrolysis stages. The use of nitrogen prevents the presence of air and at the same time sweeps gaseous products away and the secondary reactions are minimized. The same test was done by using oxidizing agent (air) as the carrier gas, for comparison. In addition, the consistency of the results with different sample weight was tested in this part.

b) Isothermal

Isothermal TGA curves were obtained by inserting samples (1-2 mg) in TGA furnace and heating it by a jump to desired temperature (400-800 °C) after drying for 10 min at 105 °C, and keeping the sample for 1 hour at that temperature.

c) Constant heating rate

In constant heating rate analyses, different heating rates (5, 10, 20, 45, 75 and 100 °C/min) were used to heat up the sample up to 800 °C, (after drying). TGA and DTG curves were obtained. Typical mass of the sample was 3-5 mg in these experiments.

e) Simulation of FBR condition

The biomass sample temperature was recorded by data logger in FRB tests and was investigated and the similar pattern was used in TGA as temperature program to compare the FBR and TGA char yields. The obtained curve and the applied programs are mentioned in detailsinAPP 3. For each experiment 1-2 mg of chicken manure was put in the holder.

f) Char characterisation

A sample of char obtained from each FBR experiment was analysed in TG. The temperature program similar to which was done for biomass characterization tests (constant heating rate of 10 °C/min up to 800°C) was applied. These tests were aimed at the identification of the amount of convertibles

remained in the char and study the consistency of results. Initial weight of char used in experiment was 4-6 mg.

3-3-2- DSC procedure

During the DSC run, a sample of around 7 mg was used. Samples used in DSC runs were previously dried at 105°C under a nitrogen flux of 100 mL/min for 10 min (conditioning). DSC runs started at 40°C. A constant heating rate of 10°C/min, was used, up to the final temperature, set at 600°C. At the end of each run, the furnace was cooled down to 40°C under nitrogen purge gas flow (50 mL/min) and a second run was performed on the char sample using the same temperature–time program. In order to eliminate from the results the contribution of heat radiation phenomena in the sample cell (Rath et al, 2002), the heat flux of the sample and of the char were subtracted at each temperature.

3-3-3- Fixed bed reactor procedure

3-3-3-1- Non-catalytic FBR procedure

At the beginning of each FBR run, 15 gr of biomass, which was dried in the oven for four hours at 105 °C, was inserted in the sample holder. The traps were weighted and put in the ice bath and were connected to the outlet of reactor. The last trap was connected to the FTIR by a plastic pipe in order to identify the evolved gas. The reactor was located in the furnace, having care that the sample holder is in the initial cold zone of the reactor, while the furnace is heating up with the rate of 100 °C/min, to the desired temperature of each experiment (400-800°C). In this period, the holder was left in nitrogen atmosphere, so that all the air would be sweep out and preventing oxidation. Nitrogen with 8.5 NL/hr flow was used for this purpose. When the furnace reached the desired temperature, the sample holder was pushed forward to the hot region of the tubular reactor (Figure 3- 8). At the same time, the chromatography started with FTIR. The background signal of FTIR was checked right before pushing the holder in hot zone. During all the experiment, a nitrogen flow rate (8.5 NL/hr) was used to sweep the gases to the traps and then FTIR. The condensable fraction of evolved gas condensed in the traps and formed bio-oil, while the non-condensable fractions go through the FTIR. Reactor bed

temperature was recorded by use of a K-type thermocouple connected to a data logger during all experiment. The process continued 30 min. This time was observed by TGA experiments to be enough for conversion (see section 4-1).
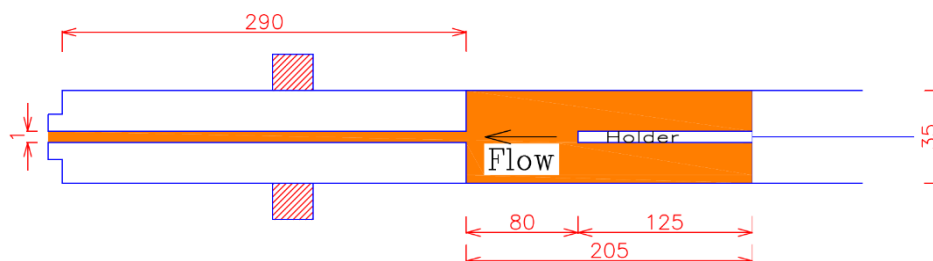
Figure 3- 8- Hot region where the spoon is located during the experiment

During the process the outlet flow rate of the gases coming out of FTIR was measured by bubble flow meter several times, to assure that the flow passes well through the system and the reactor compartments are not clogged by tar.

After 30 minutes, the nitrogen valve was closed, FTIR chromatography was stopped and the furnace was turned off. The bed was brought to the initial colder zone of reactor and let to be cool down. The trap train was separated from the reactor and their weight was measured again to understand bio-oil yield which is calculated by the traps weight difference before and after experiments. The reactor outlet was clamped to prevent oxygen entrance and char combustion occurrence. The bio-oil obtained in the traps was poured in a vial, while the heavy fraction of that condensed on traps wall and was inseparable. By putting the traps in the oven at the medium temperature (50 °C) these fractions liquefied and was added to the vials. The vial was kept in the fridge for further elemental analysis and GC-MS of bio-oil. Bio-oil is composed of two phases including organic and aqueous. Before analysis of bio-oil, two phases were separated using centrifuge at 3000 rpm for 15 minutes. The low viscose water phase was then separated by Pasteur pipette.

Another obtained product defined as char (the solid present in the sample holder at the end of the run). The yield of this product was obtained by measuring the weight of biomass residue in holder. The char was kept in a desiccator to be analysed in future both with TG and elemental analysis.

Biogas (the volatiles which were not able to be condensed in traps and were analysed by FTIR) is another product of the process. The yield of this product is calculated by difference (subtracting bio-oil and char yields from the initial biomass).

When reactor reached the ambient temperature, it was disassembled and weighted again. While in theory the accumulation of condensable products in the reactor could have been estimated by this approach, the experimental errors in the weight measure were such that inconsistent results were obtained: therefore this accumulation was considered negligible in the calculations.

Traps and reactor were also washed with solvent and the tubes were replaced at the end of each experiment.

3-3-3-2- Catalytic FBR procedure

The procedure for catalytic process is almost the same as non-catalytic, except that at the beginning of the process, a proper amount of primary activated catalyst (in a furnace at 550 °C for 4 hours to be activated) was mixed with biomass and was put in the sample holder. The proper amount of catalyst tested in this work varied in the range of 0.25 to 1.25 of catalyst to biomass ratio.

At the end of the catalytic process, the coke formed on the surface of the catalyst was measured using thermogravimetic analysis with the method suggested by Aho et al., (2010). A small sample of coked catalyst was put in TGA-Q500 thermogravimetric analyzer (TA Instruments-Water (USA)) and was exposed to the following thermal program: 10 °C/min from 25 °C to 795 °C with an isothermal at 100 °C for 15 minutes under flow of air at 100 ml/min.

Phase separation of bio-oil, elemental analysis and GC-MS were not done for catalytic product.

3-3-4- FTIR procedure

The resolution of 4 cm^{-1} was used for collecting spectra with co-adding 16 scan per spectrum. This resulted in temporal resolution of 9.5 s. The concentration of gaseous compounds and spectral absorbance at a given wavenumber can be related linearly with Lambert-Beer law, which is usually used in integral form over a characteristic wavenumber interval.

$$I = \int_{v1}^{v2} A\,(v)dv = \int_{v_1}^{v_2} \in (v)l.c.\,dv = KC \qquad\qquad \text{Equation 3-1}$$

In Equation 3-1, I is the integral value, A is measured absorbance, $\in$ is the extinction coefficient of the gaseous compound, l is the optical length used in the measurement, C is the concentration, and (v_1, v_2) is the wavenumber interval selected for the measurement. K is the constant and if the deviation from Lambert-Beer law can be neglected, is independent. The compound considered, the wavenumber interval, gas temperature, path length and resolution are the factors affecting the K. Therefore, calibration must be done to obtain reliable K value. The calibration procedure described by Bak et al. 1995was applied. By quantification of the result of the FTIR over time, the overall products can be calculated.

3-3-4-1- Calibration

In order to quantify the compounds identified by FTIR, there is a need to obtain the K value of Lambert-Beer law. Therefore, the calibration of instrument is necessary for each separate compound, before quantification. The obtained integral value of each peak can then be related to the compound concentration by use of calibration coefficient. The method used for integration of each peak is mentioned in the Table 3- 7.

All the compounds except CO_2, CO and CH_4 were considered negligible and quantification was done only for these three major compounds. Hence, also the calibration was done only for them.

Table 3- 7- Integration methods used for compounds calibration
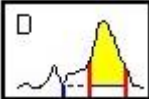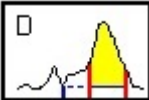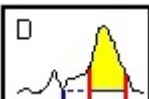
Desired component	Domain of integration (cm^{-1})	Integration method
CO_2	3775-3657	**Baseline:** 3790 cm^{-1}
CO	2205.6-2096.6	**Baseline:** 2500 cm^{-1}
CH_4	3025.84-3001.28	**Baseline:** 3400 cm^{-1}

Figure 3- 9 to Figure 3- 11 show the obtained calibration line for CO_2, CO and CH_4 respectively.
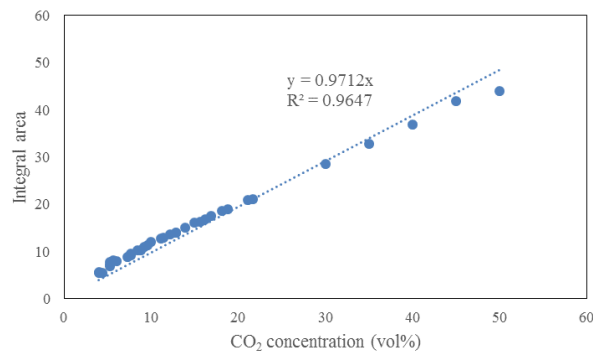
Figure 3- 9-CO_2 calibration line for FTIR measurement
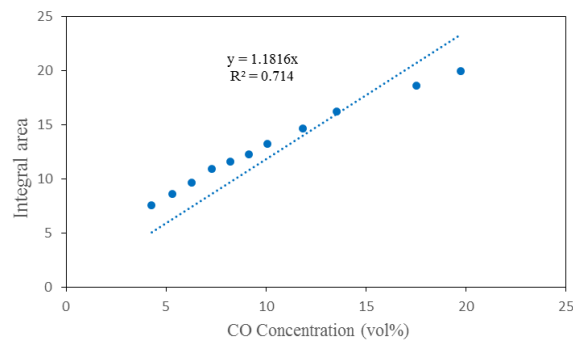
Figure 3- 10- CO calibration line for FTIR measurement
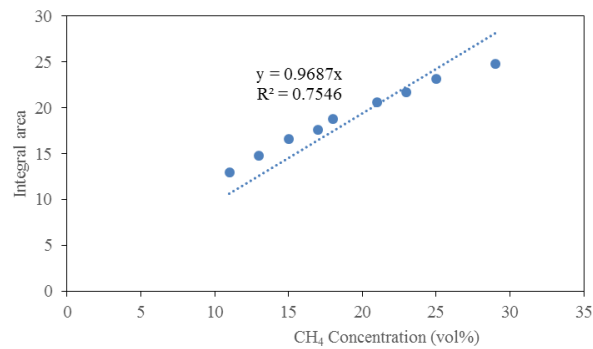
Figure 3- 11- CH_4 calibration line for FTIR measurement

According to the calibration, lines the calibration coefficient used for quantification of each component were obtained and are mentioned in Table 3- 8:

Compound	Calibration coefficient
CO_2	0.9712
CO	1.1816
CH_4	0.9687

Since there is a lack of fit for the linear curve of CO and CH_4 calibration, polynomial calibration curve was also allocated by assigning second order curve to the points, to enhance the precision of the calculations. No significant change was observed in the final results, while the complexity of the calculation increases quite a lot. Therefore, the allocation of linear calibration curve was considered enough for the calculations. An example of second order calibration and the result can be seen in App 7.

3-3-4-2- Quantification

By knowing the calibration coefficients, change of concentrations with time and temperature were obtained and are shown in results sections. In concentration curves, the time was modified considering the delay time which is the summation of the residence time in the reactor, traps and FTIR. For residence time calculation, the flow rate at each time interval was considered by knowing the concentration of all three components.

3-3-5- Elemental analysis procedure

The samples (biomass, char and bio-oil, about 2-4 mg) are placed in a crucible of tin and mixed with about 10 mg of vanadium pentoxide (catalyst to obtain a better identification of the sulfur) and burned at a temperature of 900 °C under nitrogen flow.

The ash content was determined as the mass percent of the residue remaining after dry oxidation at 575°C for 5h in a muffle oven (ASTM E1755:2015). The oxygen content was calculated by Equation 3-2:

$$O\% = 100 - (C\% + N\% + H\% + S + A\%)$$

Equation 3- 2

3-3-6- GC-MS procedure

Mass spectra were recorded under electron ionization (70 eV) at a frequency of 1 scan s^{-1} within the 45–450 m/z range. The organic phase of the condensables was analysed after silylation using the following thermal program: 100°C with a hold for 5 min, then ramping up with a heating rate of 5°C min^{-1} until 310°C.

A sample of the organic condensable was dissolved in cyclohexane-acetone solution (1:1 v/v) to a 1% w/v concentration. As silylation procedure, an aliquot of the solution (100 μl) was combined with internal standard (sorbitol 10 mg/L in ACN), silylated with BSTFA/TMCS/pyridine for 2 h at 60 °C, and analysed by GC–MS.

The area of each peak in the chromatogram obtained in the TIC (total ion current) and the quantification was done using external standard of ethyl benzoate, according to the Equation 3-3:

$$Q_c = (A_c \times Q_{ix} \times F)/A_{ix}$$ Equation 3-3

In which:

A_{ix} = Peak area external standardized

Q_{ix} = External standard quantity

Q_c = analyte quantity

F = Response factor

For the quantification of all compounds response factor (F) has been considered as unitary.

3-4-Modelling Techniques

3-4-1- Design of experiment techniques (DOEs)

Design of experiment techniques (DOEs) decrease the cost of expensive analysis methods, since the final modelling and result prediction for the whole desired range of factors, is based on the results of limited number of experiment and statistical evaluation of those results. This way, time and expense saving can be achieved using a proper DOE (Montgomery, 2001). Full factorial, Taguchi, Placket

Bergman and RSM are among famous DOEs, while RSM is a well known and the most common DOE technique, when process optimisation is considered.

3-4-1-1- Response surface methodology

When it comes to process optimisation, response surface methodology (RSM) is the best available DOE method. RSM is a collection of mathematical and statistical techniques to design experiments, develop models, evaluate factors, and finally optimize conditions. By this method, the role of each single parameter on the outcome of the process can be studied as well. RSM makes it possible to design different projections and helps in visual interpretation of the functional relations between the response and experimental variables by providing graphic illustrations (Baniasadi et al. 2014). RSM provides models and easily converts them to response contour plot and response surface plots. A proper RSM design gives rise to a model with small prediction error and ability to evaluate the adequacy of this model. In other words, proper design contains replicated experiments, which makes performance of lack of fit possible. Another characteristic of good design is the encoding fewest possible number of experiments (Montgomery, 2001). There are several classical RSM design families including Central Composite and Box Benken.

RSM starts the modelling with a suitable approximation for functional relationship between the responses and set of independent factors. In the range of independent variables, RSM models the responses usually by a low-ordered polynomial. If the functionality of the responses to the factors is linear, the approximation function is first order model (Equation 3-4): (Montgomery, 2001)

$$y = \beta_0 + \sum_{i=1}^{k} \beta_i x_i + \epsilon \qquad \qquad \text{Equation 3- 4}$$

where y is the response, β_0 is the constant coefficient, x_i are variables and β_is are the linear interaction coefficients. In the above equation, k is the number of factors in experiment.

In the case of presence of curvature in the system, first order model is not adequate anymore and a polynomial of higher degree must be used to describe the functionally of the responses to the factors. Equation 3-5 is an example of a second order model: (Montgomery, 2001)

$$y = \beta_0 + \sum_{i=1}^{k} \beta_i x_i + \sum_{i=1}^{k} \beta_{ii} x_i^2 + \sum \sum_{i<j} \beta_{ij} x_i x_j + \epsilon \qquad \text{Equation 3-5}$$

In the above equation, the definition of β_0, x_i and β_is are the same as Equation 3-4, while β_{ii}s are

quadratic interaction coefficients and β_{ij}s are second-order interaction coefficients, and ε is the

residual for each experiment.

The above mentioned models (first and second order models), are enough in almost all of the RSM

problems. Polynomial model works well when small region of variables is considered. To estimate the

parameters of polynomial the least square method is used.

Montgomery (2001) described well the procedure of RSM as a sequential procedure and analogized it

to "climbing a hill" in the case of maximization and "descending into valley" in the case of

minimization. Usually the procedure starts at a point, which is remote from the optimum. This point is

illustrated in the Figure 3- 12 as current operating condition. At this point, there is little curvature in

the system and the first order model would be enough. RSM goes a long path of improvement to the

region of the optimum. In that region a more elaborated model, such as second order model may be

employed and the analysis to locate the optimum is performed.
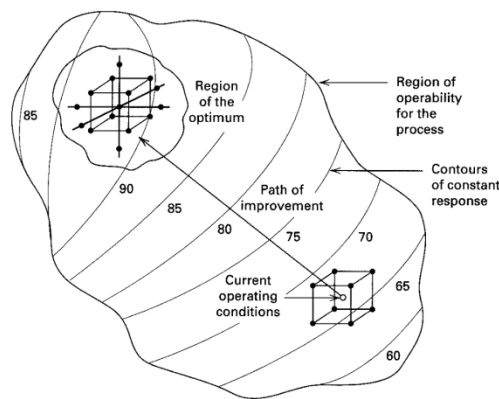
*Figure 3- 12- **RSM sequential procedure (Montgomery 2001)***

3-4-1-2- Analysis of variance (ANOVA)

Analysis of variance is a method widely used to explore the correlation and further confirm the adaptability of the model. ANOVA is based on comparison of variation between groups and variation among groups. In other words, ANOVA by calculating the ratio of signal to noise evaluate if the model and the result of experiment set are significant.

The lack of fit of model is usually correlated to coefficient of determination (R^2 value). However, high R^2 value does not imply the significance of the model. F-test must be carried out in order to study the ratio of mean squares for regression and the errors. Mean squares are determined based on the degree of freedom and sum of square based on regression model. Degree of freedom is related to the number of estimated parameters and number of observations. ANOVA table provides F-statistic (F-ratio). This value can then be compared with critical F-value and the probability is calculated based on degree of freedom and confidence interval error. Confidence interval error can be 90% or 95 %, which means that p-value of <0.1 or <0.05 is acceptable as a significance of the model (Brown, 2009).

3-5-Modelling procedure

3-5-1- Design of experiment (DOEs)

Use of RSM for optimization of catalytic pyrolysis has been done before by several researchers(Mante et al. 2013) (Ren et al, 2013) (Brown, 2009).

In the work of Mante et al. (2013),RSM was used to optimize the catalytic pyrolysis process of hybrid poplar wood in a bubbling fluidized bed. The catalyst used was Y zeolite based FCC. Box-Behnken was used as RSM and gave 15 numbers of runs to study the effect of three factors, which were temperature, weight hourly space velocity, and vapor residence time. Minitab software was used to perform design, modelling and optimization. Final goal of the study was improving yield and characteristic such as viscosity, carbon content … of bio-oil. The presence of combustible (CO, CH_4 and H_2) in gas was optimized as well. Another aim of the design was reducing the coke formation.

In the study on fast pyrolysis of bark as biomass, done by Ren et al, 2013, central composite rotatable design (CCRD) was used. Design Expert was used as software. The effect of three factors (temperature, gas flow rate and particle size) was studied. The aim of study was producing phenol-rich bio-oil.

Another fast pyrolysis study in which Central Composite method was used for optimization of process, used red oak as biomass (Brown 2009). Auger reactor was used in this study and the factors studied were heat carrier temperature, heat carrier mass feed rate, rotational speed of reactor and volumetric flowrate of carrier gas. The aim of study was improving the yield and characteristic of bio-oil and improving the fraction of combustibles (CO, H_2) in gas.

No study was found on optimization of slow pyrolysis process. However, in all the above mentioned fast pyrolysis process, temperature was reported to be one of the most important factors affecting the pyrolysis products.

In this work, design of experiment techniques was used only for catalytic process. When dealing with catalytic pyrolysis of chicken manure in fixed bed reactor, two variables can influence the results mainly, which are pyrolysis temperature and catalyst to biomass ratio. For experiment design, analysis of response, modelling and optimization, Design-Expert® Software Version 9 Free Trial was used ("Design-Expert® Software Version 9 Free Trial - Software," n.d.). Dealing with two factors with aim of optimization of process, RSM is the best technique to be used. Central composite is the most conventional RSM, but this method usually divide the variables range in predefined intervals, therefore suggests to work in non round values of temperature. Since the round values were interested, the user-defined method was used. This method is based on D-optimal method. In this method a model must be selected which is quadratic in this case and therefore five level of each factor was considered. Some candidate points are selected. In this method the vertices, center of edges, axial check points, interior points and overall centroid are assigned as candidate points. To check the repeatability three center points were also added. Therefore, in total 20 runs were designed. Temperature was studied in the range of 400-800 °C. The catalyst to biomass ratio was studied in the

range of 0.25 to 1.25. This range was selected after comprehensive literature review (section2-3-1). All the candidate points are shown in Figure 3- 13.

Responses were considered in a way to evaluate the process from energy point of view. Therefore, two responses were considered for the process, which are the amount of energy transferred to gas and the energy consumption of the process. This way the process can be optimized with the aim of energy valorization of the process in order to minimize the energy consumption of the process and maximize the energy transferred in the gas. All these (design of the process, results evaluation, and optimization of the process) were performed by Design-Expert® Software Version 9 Free Trial ("Design-Expert® Software Version 9 Free Trial - Software," n.d.).
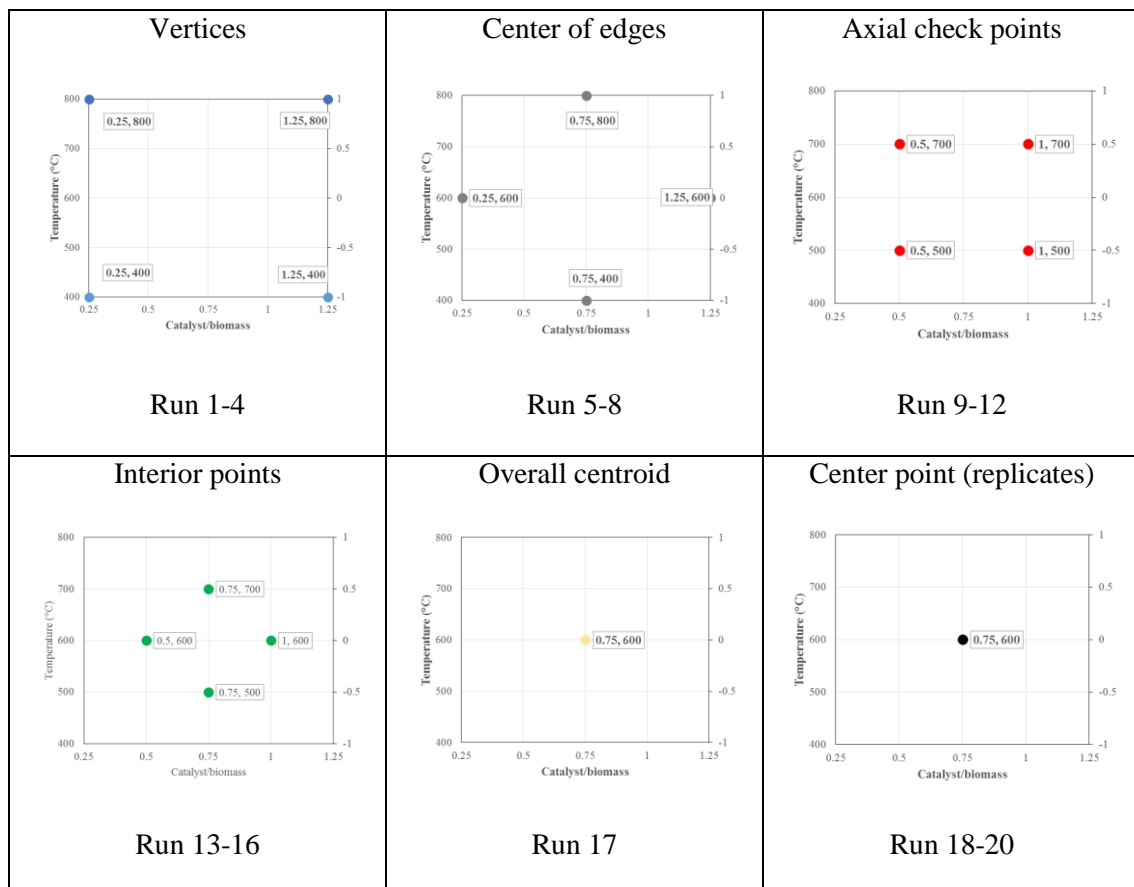
Figure 3- 13-Candidate points selected for DOE

3-5-2-Optimization

When the process produces multiple responses, regions where the requirements simultaneously meet critical properties must be determined. This way a set of operating conditions that can optimize all responses or at least keep them all in the desired range is obtained (Montgomery, 2001).

When working with few process variables, overlay of the contour plots for each response can be a straightforward approach.

To obtain the desirable region numerically, use of desirability function is common. First, the desirability (d_i) is defined as a function of y_i for each separate response in the range of 0-1. When the response is at the target, the desirability value is equal to 1 and when the response is out of the acceptable range, the desirability is equal to 0.

The individual desirability function is different according to the target and can be obtained by Equation 3-6. The importance of each target to be achieved can be also weighted.

$$
\begin{array}{cc}
\text{Maximizing} & \text{Minimizing} \\
\end{array}
$$

$$
d_i = \begin{cases} 0 & y_i < L_i \\ (\dfrac{y_i - L_i}{T_i - L_i})^s & L_i \leq y_i \leq T_i \\ 1 & y_i > T_i \end{cases} \qquad d_i = \begin{cases} 1 & y_i < T_i \\ (\dfrac{y_i - U_i}{T_i - U_i})^s & T_i \leq y_i \leq U_i \\ 0 & y_i > U_i \end{cases} \qquad \text{Equation 3-6}
$$

In the Equation 3-6 L_i is the lowest response U_i is the highest response and s is the weight of each target. For the aim of maximizing and minimizing T_i which is the target value, is equal to highest and the lowest response respectively. It must be mentioned that y_i is the value of modelled response (Montgomery, 2001).

The overall desirability is then calculated by Equation 3-7:

$$D = (d_1 \times d_2 \times ... \times d_m)^{1/m}$$
<div align="right">Equation 3-7</div>

In which, m is the number of responses.

In this work for non-catalytic process the optimization was performed using Equation 3-7. For catalytic process, the Design Expert software was used for optimization. However, the software does the calculation with the same principles according to Equation 3-7.

4- Results and discussion

4-1- TGA results

4-1-1- Biomass characterization

TG and DTG curves, at constant heating rate (10 °C/min) were obtained for chicken manure and are depicted in Figure 4- 1. The curves shown in the figure were obtained as the mean of at least three experimental runs. The test was done for four different values of initial biomass, to study the effect of sample size as well.

The results evidence the presence of the three main steps in the biomass degradation process: a first step at temperatures between 150°C and 320°C, a second at temperatures between 320°C and 480°C, and a third one among 650°C and 750°C.

The first weight loss step is mainly caused by the start of the thermal degradation phenomena (e.g. hemicellulose in fibers, proteins in manure, etc.), combined with the evaporation of oligomers and low molecular weight components present in the poultry litter (Giuntoli et al., 2009) (Koufopanos, 1989) (Sanchez-Silva et al., 2012).

The second pyrolysis step takes place between 320°C and 480°C and can be attributed to the overlapping of degradation phenomena for different components present in the poultry litter. Cellulose and lignin, the main components of the fibers in the litter, are known to show a main decomposition step with the heating rates used in the present study at temperatures between 280°C and 400°C (see e.g. Basile et al., 2014, Antal et al, 1995, Heikkinen et al. 2004, Yang et al. 2007). Proteins and lipids were reported to show decomposition steps in the range from 140°C to 540°C (Sanchez-Silva et al., 2012), (Marcilla et al., 2009). The slow weight loss present at higher temperatures (above 480°C) can be attributed to the thermal annealing of char (Koufopanos, 1989) (senneca et al., 1998) (Fu et al., 2009). The last weight loss step, between 650°C and 750°C, is likely related to the degradation of $CaCO_3$, as suggested by Giuntoli et al., (2009) since this material is used as a food additive to strengthen the chicken egg shells. According to the thermodynamic equilibria (Blamey et al., 2010),

the degradation of $CaCO_3$ is possible in this range of temperatures at atmospheric pressure as long as the concentration of CO_2 in the gas phase is kept below a few percent (e.g. 3.5% at 700°C), which is a condition compatible with the TGA experiments using nitrogen sweep gas. The TG-FTIR results of Zhang et al., (2011) confirmed this hypothesis, showing no CO_2 evolution at 700°C for acid washed poultry litter samples.
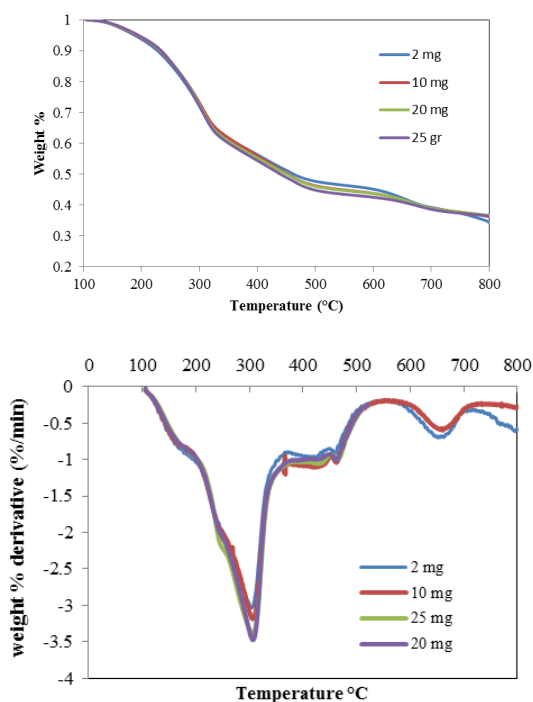
Figure 4- 1- TG and DTG curves obtained from chicken manure with nitrogen and ramp of 10 °C/min with different sample weight (dry basis)

However, Zhang et al., 2011divided the hen compost decomposition in to two stages: primary decomposition of biomass into primary products and gas (H_2, CH_4) and char which is related to fracture of chemical bands of biomass structure and secondary decomposition stage, cracking of products into gas and carbon. Metals, especially calcium have catalytic effect on second stage.

The fact that most important weight loss happens in the range of 200-370 °C, with a maximum at 300°C, shows that the most composition of chicken manure is cellulose. The total weight loss of the sample is 67%. This value is 86% on a dry ash free (DAF) basis. These results are more or less

identical to result of some prior studies (Giuntoli et al., 2009) (Zhang et al. 2009) (Ro et al. 2010) (Dejong et al., 2007).

To investigate the effect of oxidizing agent on thermal degradation of sample, TGA at constant heating rate was performed both with nitrogen and air as flue gas. The results were reported in DAF basis in order to be comparable and are shown in Figure 4-2. Up to 200 °C the degradation behaviour are almost the same, then the degradation due to combustion become rapid (ignition process). At around 450 °C there is great weight change due to the combustion. The same ignition phenomena was observed in the previous work by Joseph at al. (2012).
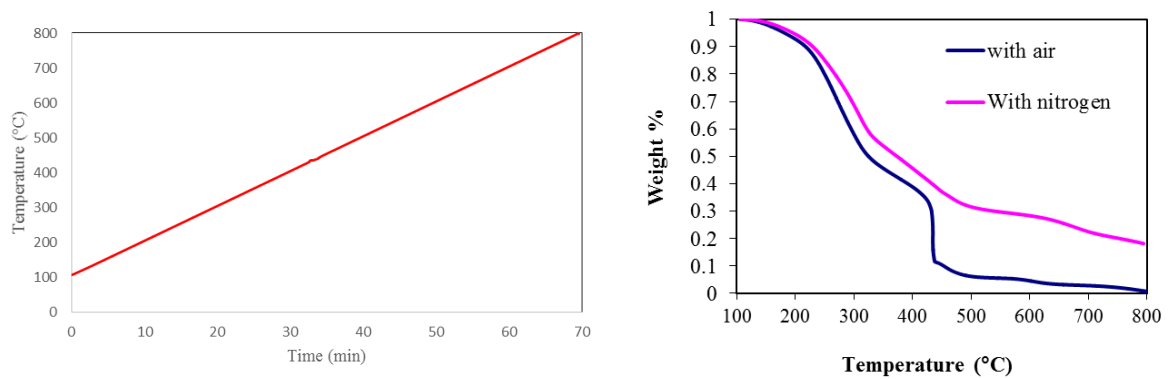
Figure 4-2- Comparison of result of TG runs carried on chicken manure in inert and oxidizing atmosphere with constant heating rate of 10°C/min (DAF basis)

4-1-2- Isothermal runs

The curves depicted in Figure 4-3, are obtained at isothermal condition with chicken manure in nitrogen at different temperatures. Obviously, the solid residue will decrease by raising temperature as a result of more volatile arousing from the biomass and temperature has a significant effect on the solid residue yield. It also can be seen in Figure 4- 3 that after 30 minutes the conversion is completed and the remaining char does not change, therefore 30 minutes was selected as duration of the test to perform the FBR experiments. By raising temperature from 600 °C to 700 °C the solid residue yield changes drastically since at around 700 °C there is peak in weight loss which may be due to decomposition of limestone as it is observable in Figure 4- 2 (Zhang et al., 2011). The DAF graph is also depicted in APP 4.
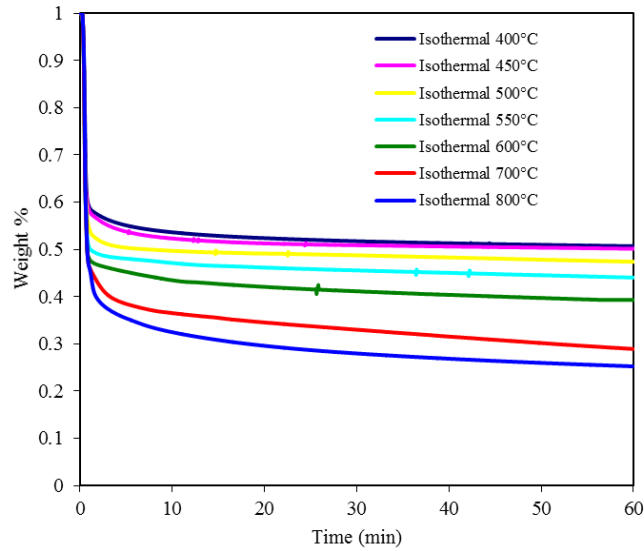
Figure 4-3- Isothermal weight loss TG curve of chicken manure in N_2 at various temperatures (dry basis)

4-1-3- Constant heating rate runs

Results of TGA and DTG at different ramps are shown in Figure 4- 4. With higher heating rate, the peak of conversion is shifted to higher temperature and decomposition takes place at wider temperature range. The different behaviour of sample exposing to high heating rate (heating rate >45 °C) and low heating rate (heating rate <45 °C) is observable in Figure 4-4. The char yield obtained from high heating rate pyrolysis is less than what obtained from low heating rate pyrolysis. As it is observable at high heating rate (more than 75 °C/min) there is a decomposition peak at above 700 °C. As it was mentioned in the introduction part (section 1-7-3) the lower heating rate, favours the production of char.
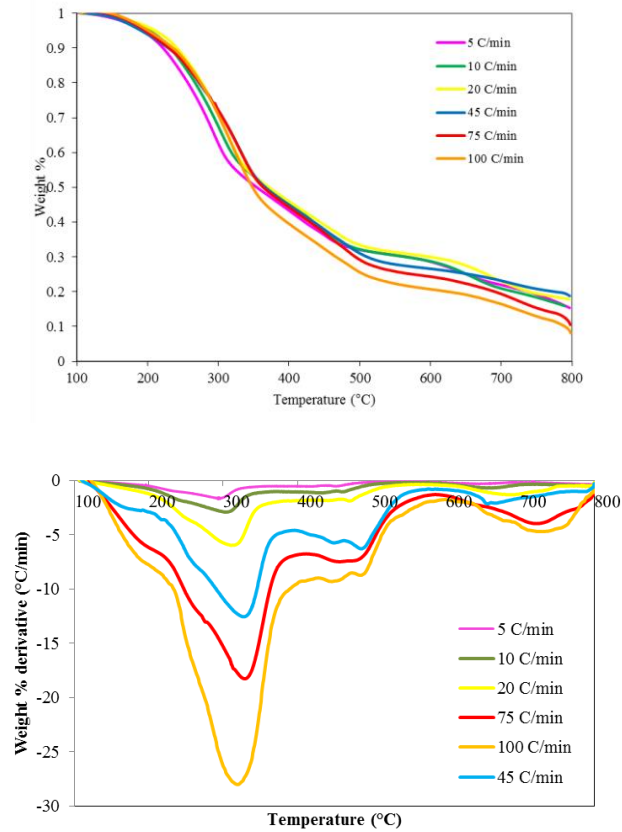
Figure 4-4-TGA and DTG results on chicken manure in N_2 with different ramp (DAF basis)

4-1-4- Runs with condition identical to FBR

The curves obtained by TG for simulating FBR thermal conditions at different temperatures are shown in Figure 4-5. Thermal conditions of the biomass inside the reactor was monitored and recorded during the test by k-type thermocouple and agilent data logger (see section 3-2-4-2). The amounts of char obtained by these experiments are mentioned in Table 4- 1. It is again observable here that after 30 minutes the conversion is complete. The drastic change between the yield of solid residue at 600 and 700 °C is took place also here. These results were used further for calculating the sensible heat of biomass heating to pyrolysis temperature (Section 4-3-5-2). The DAF curve of this TGA test are mentioned in APP 4.
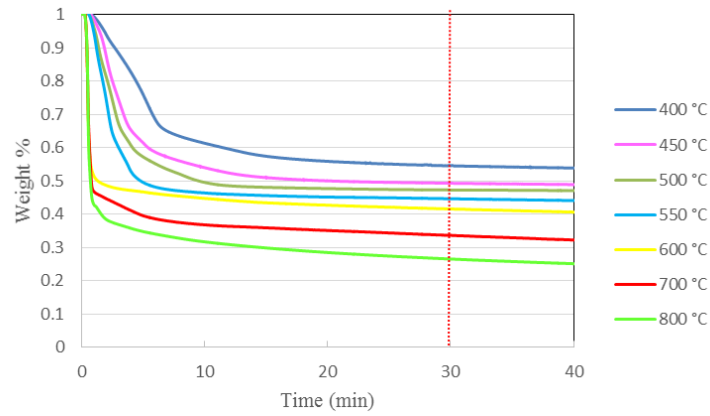
Figure 4-5- TG curves obtained at different temperature in N₂ with chicken manure at FBR thermal conditions (dry basis)

Table 4- 1- Char yield obtained by TG at thermal condition similar to FBR (dry basis)

Temperature (°C)	Char from TG after 30 min (wt%) (dry basis)
400	54
450	49
500	47
550	44
600	41
700	32
800	25

4-1-5- Char characterisation with TGA

As mentioned before (section 3-3-1), the char obtained from FBR was analysed by TG. The conversion happens during these analyses are shown in Figure 4-6 .
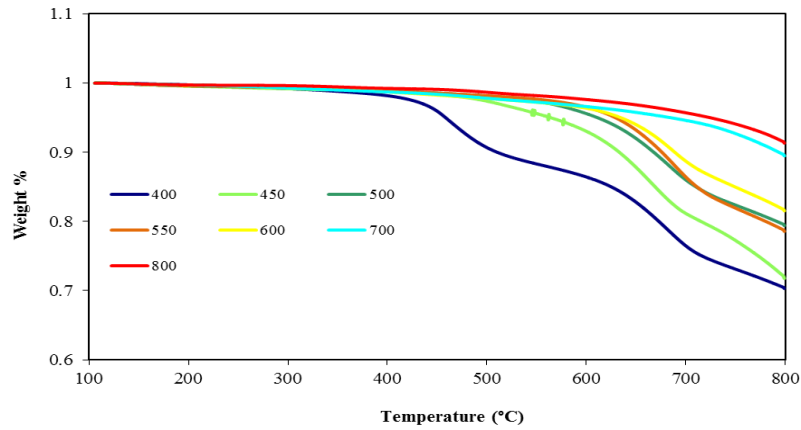
Figure 4-6- TGA analysis of char in N₂ with constant heating rate 10 °C/min (dry basis)

Discussion of consistency of these results with the results of FBR is mentioned in FBR results section (Section 4-3-1).

4-2- DSC results

Figure 4-7 reports the results of the DSC runs; the heat flux curve was obtained as the mean of three experimental runs, with differences in heat flux smaller than 2%. This curve was obtained by subtracting the DSC curve of biomass and char, which can be observed in APP 5. The heat flux curve shows a main endothermic peak to occur between 105°C and 290°C, immediately followed by a small exothermic peak. This roughly coincides with the first degradation phase identified in TGA and was interpreted to be the combined effect of degradation and evaporative phenomena. Above 290°C the thermal effects are much less pronounced, though a couple of exothermic peaks are recognised at 450°C and 475°C. The overall pyrolysis heat demand of 136J/g (endothermic, dry basis.) was estimated in the range 105°C and 600°C by integrating the main peaks of the DSC heat flux curve.

The presence of a first endothermic phase, followed by exothermic phenomena, has been previously evidenced for lignocellulosic biomasses, and is generally attributed to the interplay of primary pyrolysis endothermic reactions in the char and secondary exothermic reactions between the forming char and the evolved vapours (Rath et al., 2002) (Basile et al., 2014) (Guathier et al., 2013). This data, though appropriate for a preliminary estimation, should be used with due caution as the DSC set-up can not measure the thermal effects from possible gas-phase reactions.
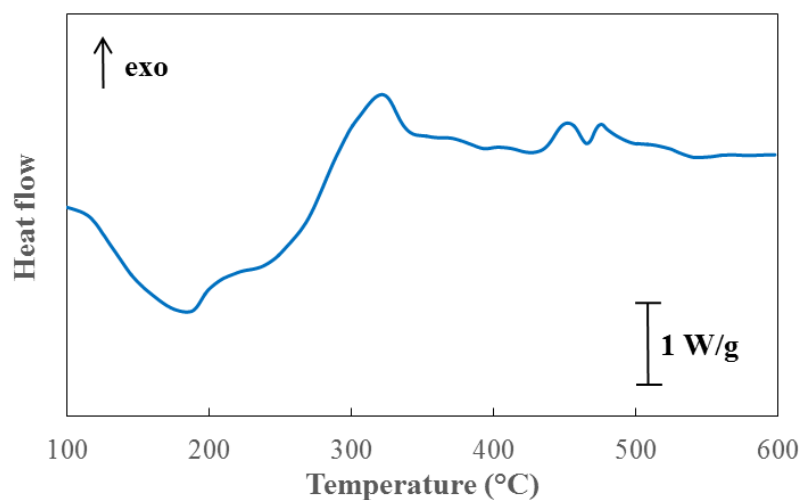
Figure 4-7- DSC curve at constant heating rate of 10°C/min in nitrogen atmosphere (50 mL/min), dry basis

4-3- Non-catalytic results

By non-catalytic FBR experiments the yields of each product and their characterisation was investigated. The results are reported in the followings.

4-3-1- FBR results

In FBR experiments, the reactor was heated up to various temperatures, which is called "test temperature" in this text. The yields of different products were measured after pyrolysis and are mentioned in Table 4- 2.

Temperature (°C)	Product yields			Standard deviation		Standard error	
	Bio-oil (wt%)	Char (wt%)	Biogas (wt%)	Bio-oil	Char	Bio-oil	Char
400	26.1	53.6	20.3	0.025	0.009	0.018	0.004
450	33.6	47.9	18.5	0.031	0.012	0.022	0.006
500	34.2	46.5	19.3	0.005	0.009	0.004	0.005
550	35.3	45.0	19.7	0.055	0.009	0.027	0.003
600	29.1	43.4	27.5	0.047	0.013	0.023	0.005
700	28.7	38.6	32.7	0.010	0.004	0.007	0.002
800	25.4	36.7	37.9	0.040	0.004	0.023	0.002

Table 4-2 are estimation coming from result of different repeats (For all repeats and statistical evaluation of the results seeAPP 6.) It can be seen that the consistency of char results is quite well and the results are consistent with the results of TG simulation (Table 4- 1). There are no completely comparable works to check the result. However, Mante and Agblevor (2010) obtained 0.43, 0.43 and 0.14 as yield for liquid, char and gas product respectively with fast pyrolysis of chicken litter in bench scale bubbling fluidized bed at 450 °C. Maximum yield of 0.23 was obtained for bio-oil from chicken litter in work of Kim et al. (2009) at 500 °C in fluidized bed and also 0.63 from fast pyrolysis of chicken manure at 350 °C in work of Monreal and Schnitzer (2011).

Figure 4-8 and Figure 4-9 show the photo of the produced bio-oil and char respectively. The presence of two phase (organic and water phase) is evident for bio-oil. This two phases were separated before the analysis using centrifuge at 3000 rpm for 15 minutes. For phase separation of bio-oil, two repeats were performed at each test temperature. The results of each phase separation are mentioned in Table 4-3.

Figure 4-8- Picture of the produced bio-oil

Figure 4-9- Picture of produced char

Table 4-3- The results of phase separation of the bio-oil

Temperature	Water bio-oil percentage			Organic bio-oil percentage			Standard	Standard
(°C)	Rep 1	Rep 2	Average	Rep 1	Rep 2	Average	deviation	error
400	0.46	0.45	0.46	0.54	0.55	0.54	0.005	0.004
450	0.23	0.27	0.25	0.77	0.73	0.74	0.027	0.019
500	0.28	0.19	0.23	0.72	0.81	0.77	0.062	0.044
550	0.30	0.29	0.29	0.70	0.71	0.71	0.008	0.006
600	0.31	0.38	0.34	0.69	0.63	0.66	0.048	0.033
700	0.41	0.36	0.39	0.59	0.64	0.61	0.035	0.025
800	0.41	0.45	0.43	0.59	0.55	0.57	0.029	0.021

Figure 4- 10 shows the yield of four different products of the slow pyrolysis process obtained at each test temperature. The error bar for char shows the standard deviation of the char results obtained by several repeats, while the error bar of bio-oil phases is the combination of the error of total bio-oil measurment and the error of the phase separation and was calculated by the equations below:

$$\frac{STD_{water}}{Yield_{water}} = \frac{STD_{Total}}{Yield_{Total}} + \frac{STD_{Centrifuge}}{Water\ fraction}$$

Equation 4-1

$$\frac{STD_{Organic}}{Yield_{Organic}} = \frac{STD_{Total}}{Yield_{Total}} + \frac{STD_{Centrifuge}}{Organic\ fraction}$$

Equation 4-2
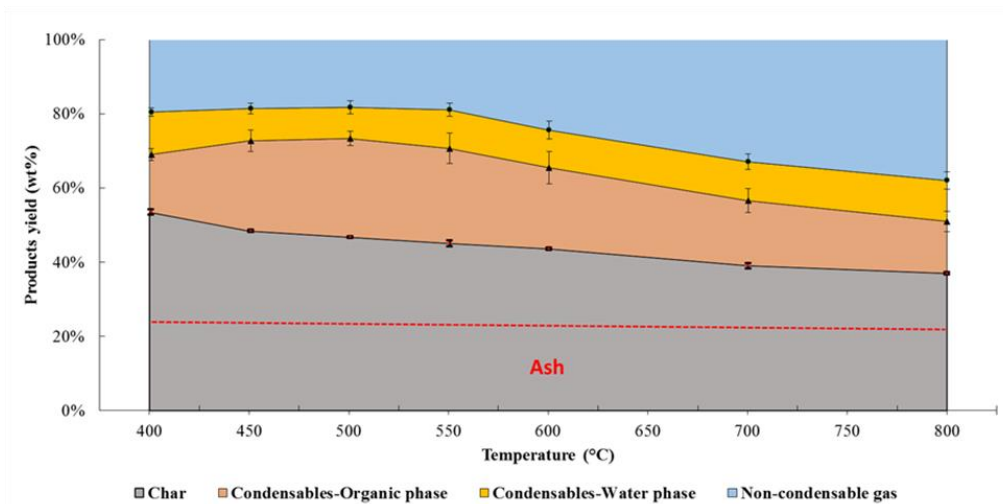
Figure 4-10- Products yields with temperatures on dry basis

The differences in yield with respect to the temperature in different runs were less than 5%. It is evident from the figure that the char yield decreases with the increase of the test temperature. The yield of the water phase remains almost constant over all the explored test temperature range, suggesting that most of the water formation and release occurs below 400°C. The yield of the organic condensable phase increases with test temperatures up to 550°C, but for tests at higher temperatures it progressively reduces, presumably due to gas-phase secondary cracking reactions: these promote the formation of lower molecular weight components, which are non-condensable compounds. The non-condensable gas yield, which is more or less constant for test temperatures lower than 550°C and increasings for higher test temperatures, confirms this interpretation.

A similar trend in the yields of the liquid fraction was shown in other studies on slow pyrolysis: for example, Pan et al., (2010) report a maximum in the liquid product yield at 400°C for algae *Nannochloropsis* in a fixed bed reactor. They suggested that, this fact may be due to formation of volatiles at higher temperatures which may undergo various reactions such as thermal cracking and

dehydration. S.-Y. Zhang et al., 2009 suggested that this behavior is a result of the secondary cracking of vapors, which increases gas yield and decreases liquid yield at the higher temperatures.

A method used for verification of conversion in FBR and its consistency with TGA is mentioned in the following. With this method, two facts can be checked: consistency of the weight loss between the FBR and TGA and also equal degradation behavior of the sample at temperatures higher than that achieved. Figure 4- 11 used for this verification.
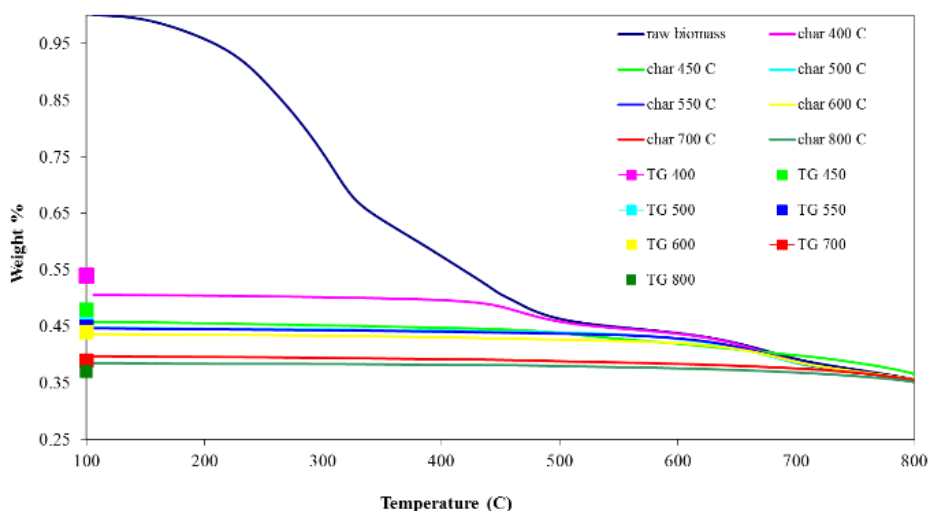
Figure 4-11- TGA curves performed on samples of char obtained from FBR at different test temperatures in N_2 (dry basis)

The TGA values were normalized with respect to the final weight value expected. It is assumed that all the TG up to 800 °C, produce a residue of 0.33 (weight %) of initial biomass at 800 °C (see section 4-1-1). For this purpose all the values were rescaled by Equation 4-3.

$$R = \frac{w_x \times 0.33}{w_f}$$
Equation 4-3

In which w_x is the obtained weight loss at each moments and w_f is the final weight of sample. In this case, all the samples will end up at 0.33 weight% at 800 °C. At the same time, the points plotted at the left part of graph are the char yield obtained by FBR. The similarity between these points and the start of TGA curves is the confirmation of results consistency. All these lead to conclude the consistency of the result of tubular reactor and TGA.

4-3-2- FTIR results

4-3-2-1- Identification

The main components of gas phase were determined by FTIR and were CO, CH_4 and CO_2. This is in accordance with the result of some previous studies (Zhang et al., 2011) (Ro et al., 2010) (Sheth and Bagchi, 2005) (Giuntoli et al., 2009). Figure 4-12 shows the spectrum obtained from chicken manure pyrolysis at 550 °C in FBR. This spectrum is extracted when the maximum absorbance intensity during the process was observed. All the identified elements are mentioned in Table 4-4.
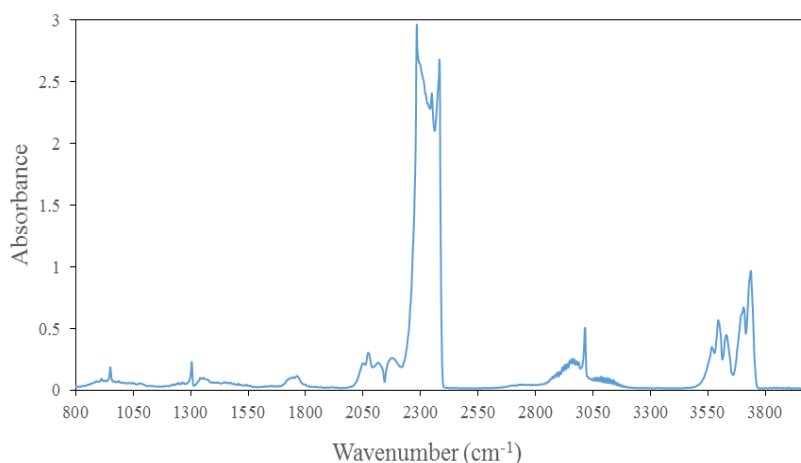
Figure 4-12- An example of FTIR spectrum obtained from chicken manure pyrolysis at 550 °C

Table 4-4- The identified compounds from chicken manure pyrolysis at 550 °C

Compound	Peak0 (cm^{-1})
CO_2	3737, 2383, 670
CH_4	3016, 1304
Acetaldehyde	2733
CO	2167
N=C=S group	2072
Carbonyl group	1761
Ethylene	950

By knowing the calibration coefficients (section 3-3-4-1), change of concentrations with time and temperature were obtained and are shown in Figure 4- 13. In these curves, the time was modified

considering the delay time which is the summation of the residence time in the reactor, traps and FTIR. For residence time calculation, the flow rate at each time interval was considered by knowing the concentration of all three components.
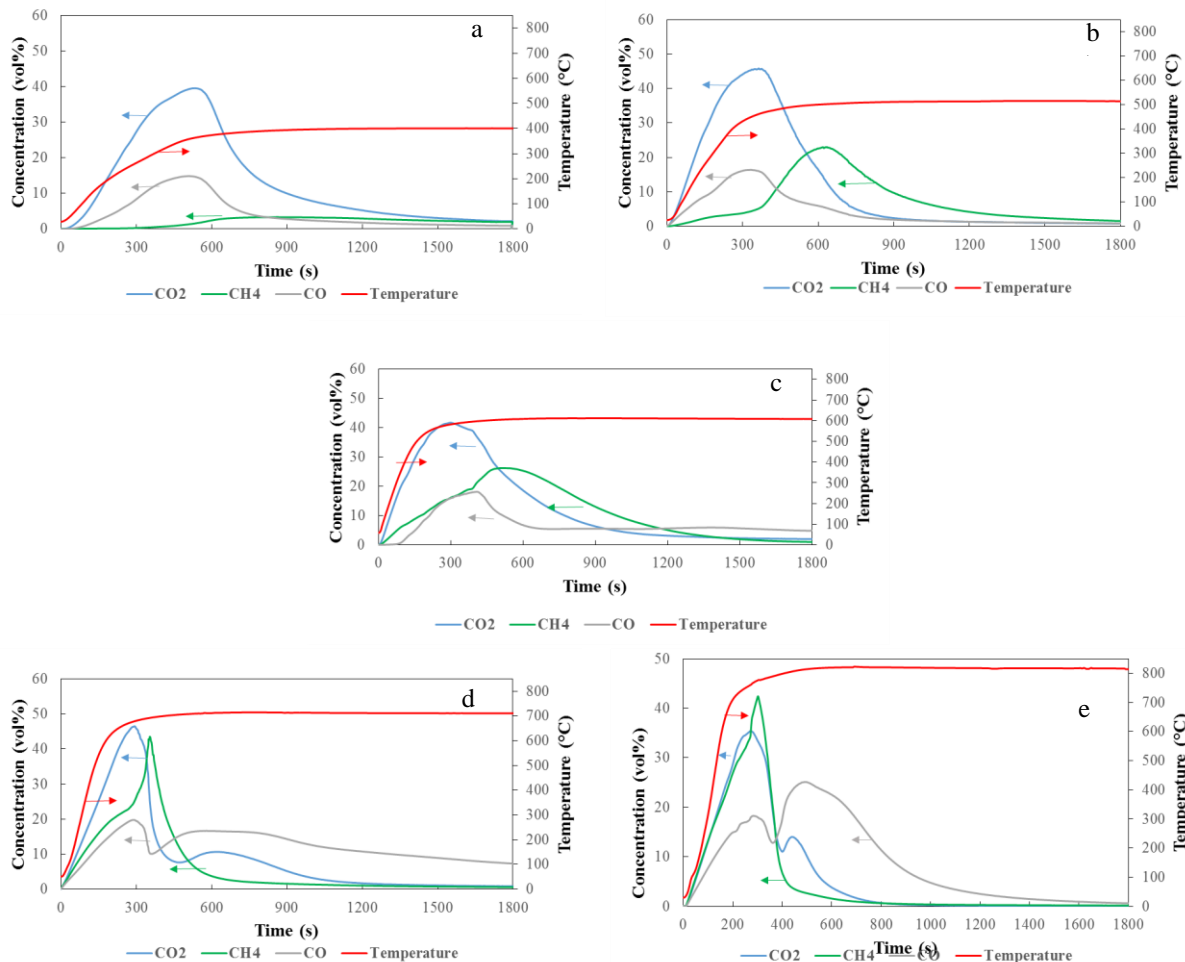
Figure 4-13-Concentration and temperature over time for a) 400 °C b) 500 °C and c) 600 °C d) 700 °C e) 800 °C

Figure 4- 14 shows the effect of temperature on the concentration of CO_2 during the test. It can be seen that by raising the temperature, the peaks are higher and takes place sooner in the process. The temperature has the same effects on the concentration of CO and CH_4, which are not shown here for brevity.
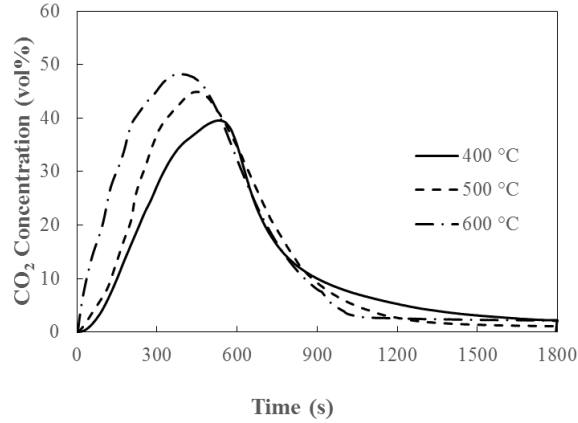
Figure 4-14- The effect of temperature on the concentration curve of CO_2

As it is evident in Figure 4- 13, the dominant compound is CO_2, which start to be produced at the beginning of the process and reaches the maximum at 350 °C. CO production is much lower but more or less has the same trend with temperature. Higher than 700 °C a new CO_2 production peak is observable which as mentioned before is the result of $CaCo_3$ degradation to CaO and CO_2.

Methane production takes place at high temperature and reaches a maximum at 500 °C. The same trend was observed in the work of Giuntoli et al. (2009). There is almost no methane production at temperatures lower than 400 °C.

In the experiments with higher temperatures, the curves are narrower than in the experiments with lower temperatures and the maximum occur sooner in the process.

Flow rate calculations of each compound were done by assuming that all compounds except CO_2, CH_4 and CO were negligible. Knowing the concentration of these three compounds and using the above assumption the concentration of inert nitrogen can then be calculated. Since the nitrogen flow rate is fixed (8.5 Nl/hr) during the process, the total flow rate of produced gas can be obtained. The flow rate of each component can then be easily calculated with multiplying the total flow rate by the concentration of that component. Equation 4-4 toEquation 4-6 are the formulas used for quantification.

$Nitrogen\ concentration = 100 - \sum Three\ components\ concentartions$ Equation 4-4

$Total\ flow\ rate = Measured\ nitrogen\ flow\ rate\ \left(\frac{l}{s}\right) / Nitrogen\ concentration$ Equation 4-5

116

$$Component\ flow\ rate\ \left(\frac{l}{s}\right) = Total\ flow\ rate\ \left(\frac{l}{s}\right) \times compnent\ concentration \qquad Equation4\text{-}6$$

Figure 4- 15a) to Figure 4- 15c) show how the flow rate of CO_2, CH_4 and CO, respectively change with time at each run. It can be seen that by raising the temperature, the maximum flow rate increases and takes place sooner and the flow rate-time curve is compressed.
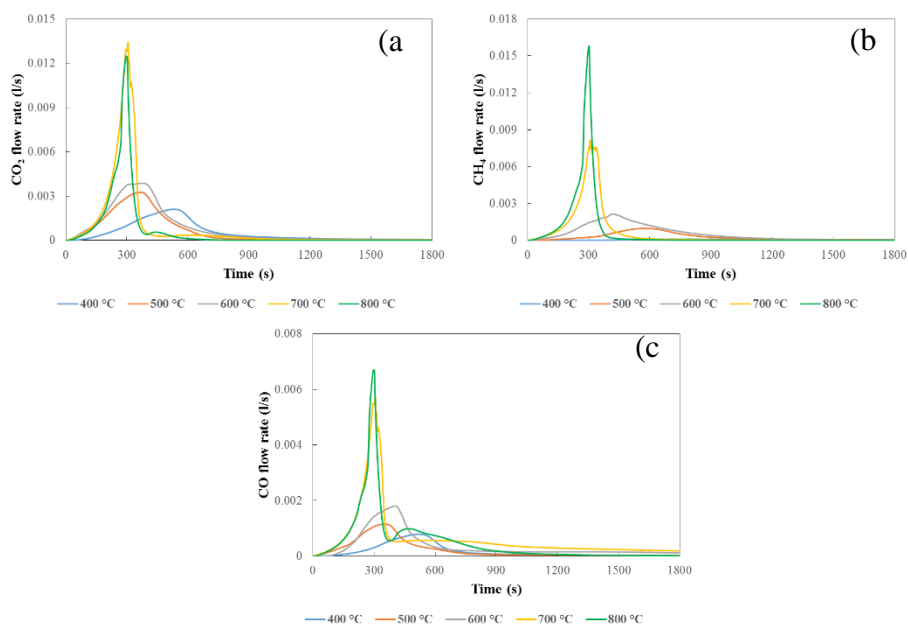
Figure 4-15- Flow rate with time for a) CO_2 b) CO and c) CH_4

As mentioned before in the section 3-3-3, the outlet flow of the FTIR was measured by a bubble flow meter periodically during the process to check the well passing of the flow through the system. The results are mentioned in the appendix part APP 8.

By integrating the flow rate over time (using Equation 4-7) the total volumetric amount of each produced compound would be calculated. The following formula was used for integration:

$$Integral = \sum(t_2 - t_1)(\frac{f_2 + f_1}{2}) \qquad Equation\ 4\text{-}7$$

Here, the resulted integration is the total production of each compound (liter) and f_1 and f_2 refer to flow rate (l/s) at each time interval and t_1 and t_2 are the time at which the measurment is done.

The above calculation was performed for all the temperatures and for all the three compounds. Each experiment was repeated several times and at least two consistant results were obtained for each temperature. Table 4- 5 shows the yields of different gaseous compounds. This results were obtained

after evaluating the consistency of the summation of the yields of gaseous products with the gas yield of FBR mentioned in Table 4- 2 (section 4-3-1). For all the repeats and the consistancy check of the resuls with FBR results see APP 9.

Table 4-5- Yields of gaseous compounds (dry basis)

Temperature (°C)	CO_2 gr/gr dry biomass	CH_4 gr/gr dry biomass	CO gr/gr dry biomass	Total gr/gr dry biomass	Biogas yield of FBR Run yield General yield
400	0.12	0.01	0.03	0.16	0.203
450	0.13	0.02	0.03	0.17	0.185
500	0.14	0.03	0.03	0.20	0.193
550	0.19	0.04	0.05	0.28	0.197
600	0.18	0.05	0.06	0.28	0.275
700	0.18	0.05	0.09	0.33	0.327
800	0.17	0.06	0.15	0.38	0.379

The effect of temperature on the yield of each gaseous compound is shown in Figure 4- 16 in dry basis. Methane shows an almost constant increase up to 600°C, while at higher test temperatures the yield is almost constant. This is in accordance with the TG results that show that the main sample primary pyrolysis is completed at temperatures lower than 600°C. Carbon dioxide is the product showing the higher yield, though the increase of CO_2 yield is negligible at test temperatures above 550°C. Carbon monoxide yield, instead, seems to constantly increase over all the range of test temperatures, almost equaling CO_2 yield at 800°C.
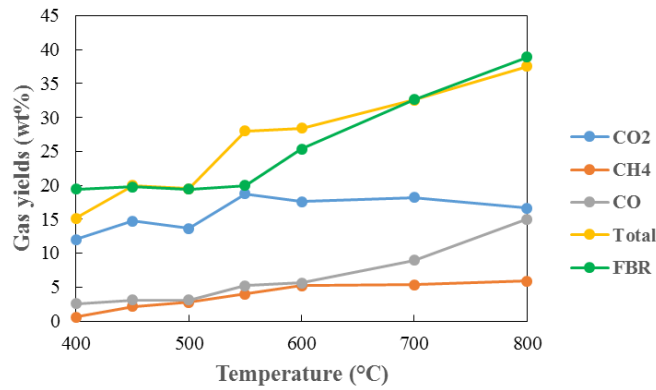
Figure 4-16- Gas production over temperature (dry basis)

The dry basis yields can be converted to DAF result by Equation 4-8. The ash of dry biomass considered to be equal to the ash obtained by proximate analysis 25%.

$$Gas\ produced\left(\frac{gr}{gr_{daf\ biomass}}\right) = \frac{Gas\ prouced\left(\frac{gr}{gr_{dry\ biomass}}\right)}{1-\left(\frac{ash\%\ biomass}{100}\right)}$$
Equation 4-8

Table 4- 6 shows the DAF results obtained.

Table 4- 6-Gaseous compounds yields (DAS basis)

Temperature (°C)	CO₂ (gr%/gr d.a.f biomass)	CH₄ (gr%/gr d.a.f biomass)	CO (gr%/gr d.a.f biomass)	Total gas (gr%/gr d.a.f biomass)
400	15.9	0.8	3.3	27.2
450	19.4	2.8	4.1	24.6
500	17.9	3.6	4.1	25.8
550	24.7	5.3	6.9	26.4
600	23.1	6.8	7.4	36.7
700	23.9	7.1	11.8	43.7
800	21.9	7.7	19.8	50.5

Figure 4- 17 shows the volumetric composition of obtained gas from pyrolysis. It must be considered that in this figure other gaseous compounds except CO_2, CO and CH_4 were neglected. It can be seen that by raising the temperature the fraction of combustible compounds (CO and CH_4) raises, which is

119

the evidence of the production of a gas with HHV. This fact will be described later in details in section 4-3-5-1.
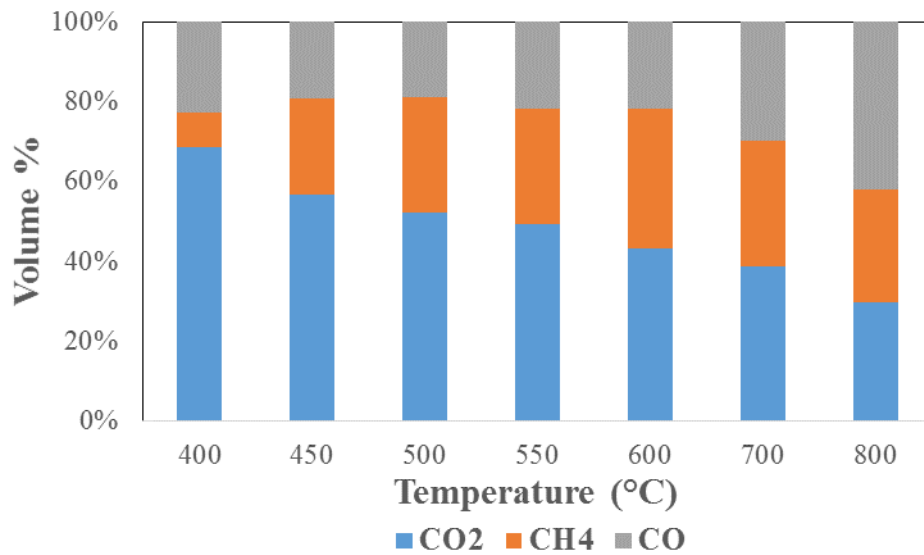
Figure 4-17- Biogas volumetric composition

There is no completely similar research to compare the obtained FTIR results. However, the results of some relevant works on gas product obtained from pyrolysis analysis were compared.

The results of Ro et al., (2010) which is a research on chicken manure slow pyrolysis in the skied mounted reactor at 620 °C are shown in Table 4- 7.

Lima et al., 2009, conducted fast pyrolysis of broiler litter at 700, 800 and 900 °C in a pyroprob/gas chromatography system and obtained total 10 wt% of gas yield. The yields (wt%) dry of each compound obtained in that work are mentioned in Table 4- 8. However, it must be considered that the condition of fast pyrolysis will yield to different reaction mechanism and as a result of different products.

Table 4-7- Comparison of biogas composition (mol%) of current work with (Ro et al., 2010) work

Reference results at 620 °C		Current work result at 600 °C	
Compound	mol %	Compound	mol%
CO_2	27.5	CO_2	43.3
CO	16.1	CO	22.8
CH_4	10.9	CH_4	34.9
H_2	17.2		
N_2	18		
C_{2+}	6 to 10		

Table 4-8- Comparison of gas analysis results (gas yields wt %) of current work with Lima et al., 2009 work (dry basis)

Reference result						
Temperature (°C)	CO_2 (wt%)	CO (wt%)	CH_4 (wt%)	C_2H_4 (wt%)	C_3H_6 (wt%)	H_2 (wt%)
700	5.2	2.8	0.5	0.4	0.2	<0.1
800	6.1	2.5	0.7	0.4	0.2	<0.1
900	8.9	2.5	1	0.4	0.2	<0.1
Current work results						
Temperature (°C)	CO_2 (wt%)		CO (wt%)		CH_4 (wt%)	
700	18.19		8.97		5.37	
800	16.64		15.02		5.87	

4-3-3- Elemental analysis results

4-3-3-1- Characterisation of bio-oil with elemental analysis

Elemental analysis was performed on both phases of bio-oil. The result of elemental analysis performed on both water and organic phases are shown in Figure 4- 18.
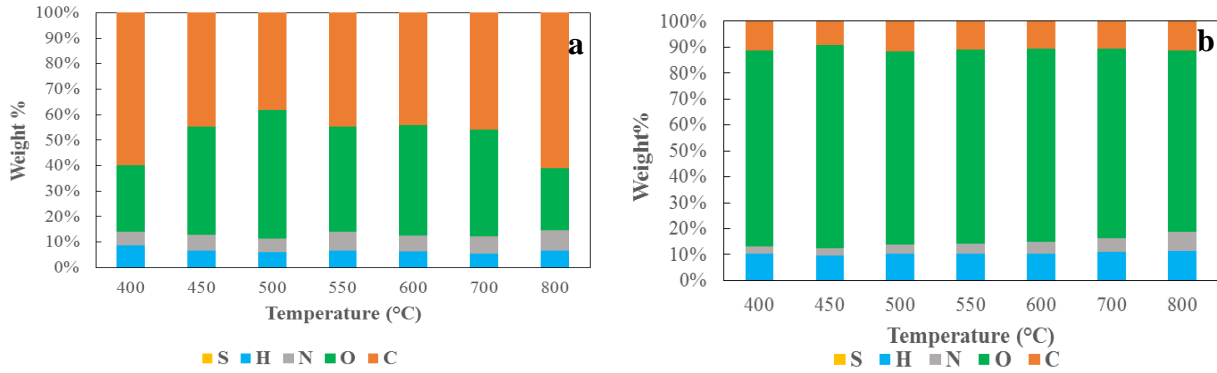
Figure 4-18- Bio-oil elemental analysis a) organic phase b) water phase

The results clearly evidence that the amount of sulphur in condensable fractions is very low (below 0.2%). It is also evident that the water fraction contains some soluble carbon and nitrogen compounds. At higher temperatures, the oxygen in bio-oil decreases

No research was found on the elemental analysis of bio-oil obtained from fast pyrolysis of chicken manure. However, Kim et al., (2009), conducted fast pyrolysis of chicken litter in fluidized bed at 500 °C and obtained elemental composition of bio-oil. In that study, the H/C of biomass was 1.53 and for bio-oil was almost the same (1.55), while the O/C ratio of biomass was 0.64 in that work which yield to the bio-oil with O/C of 0.27.

4-3-3-2- Char characterisation with elemental analysis

Elemental analysis was performed on the remained char as well. The results are shown in Figure 4-19. The DAF calculation was done using the Equation 4-9. The value of ash $_{char}$ is thevalue obtained by elemental analysis as it is shown in Figure 4- 19a.

$$\text{DAF elemental composition of char} = \frac{\text{wt\% of elemets}}{100 - \text{wt\% of ash }_{char}} \qquad \text{Equation 4-9}$$

122
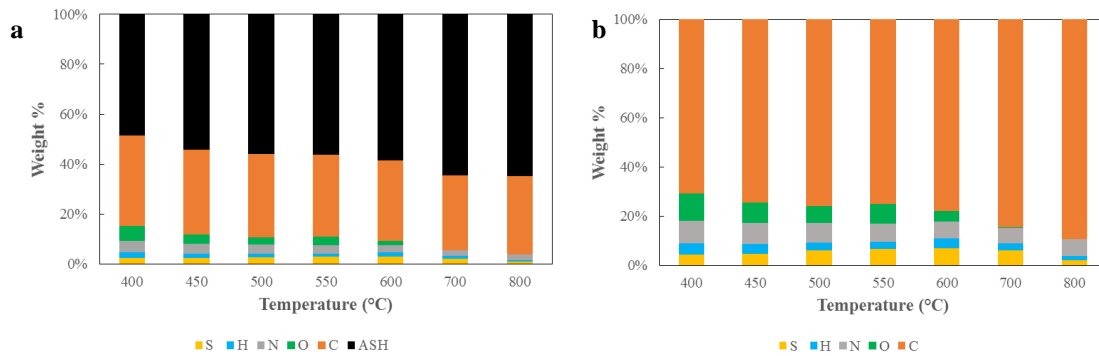
Figure 4-19- Char elemental analysis a) dry basis b) DAF basis

The fraction of carbon in the char increases with the final temperature of the test, passing from 71% DAF at 400°C to 89% DAF at 800°C as it can be seen in Figure 4- 20. Most of the sulphur contained in the original biomass remains in the char during the pyrolysis process. High amount of ash, carbon, and nitrogen which are proved by the elemental analysis, give char the potential to be used for soil amendment purposes.
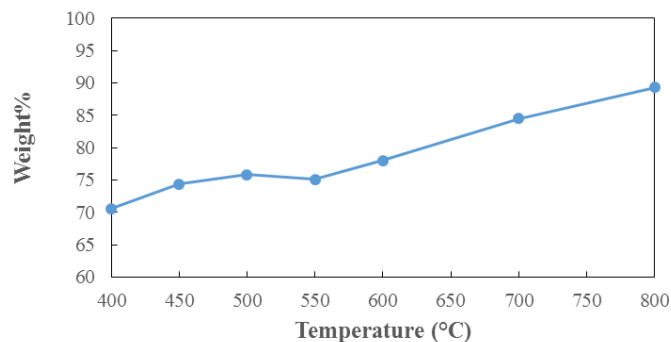
Figure 4-20- Carbon weight% in char over temperature

Figure 4- 21a) and Figure 4- 21b) compare the O/C and H/C atomic ratio respectively among the char at different FBR test temperatures and the original biomass. Both O/C and H/C ratios show a decrease with pyrolysis temperature. The H/C and O/C values obtained in the present study are more than four times smaller than the corresponding values for the raw biomass, further evidencing the effect of pyrolysis in increasing the carbon content of the char in comparison to original biomass. This composition candidates the char for potential soil amendment application (Güngör et al., 2012)

(Prayogo et al., 2014), while use as a fuel has to take into account the issues related to the sulphur content.
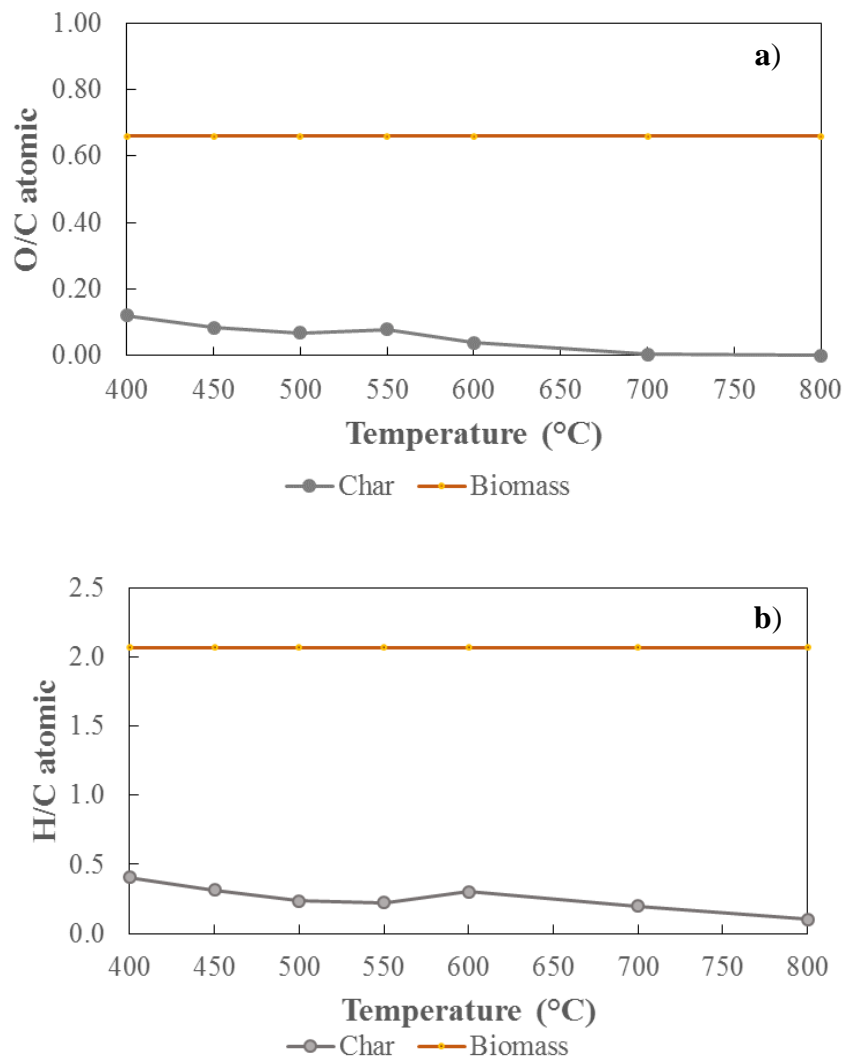
Figure 4-21- The effect of final temperature of pyrolysis tests on O/C ratio (panel a) and H/C ratio (panel b) of the char

Van Kravelen diagram, which plot H/C vs. O/C, is shown in Figure 4- 22. This graph shows how the H/C and O/C ratio changes from biomass to char and bio-oil product obtained from slow pyrolysis at 800 °C. It can be observed that both H/C and O/C are lower in the solid and liquid product, in comparison to the original biomass.
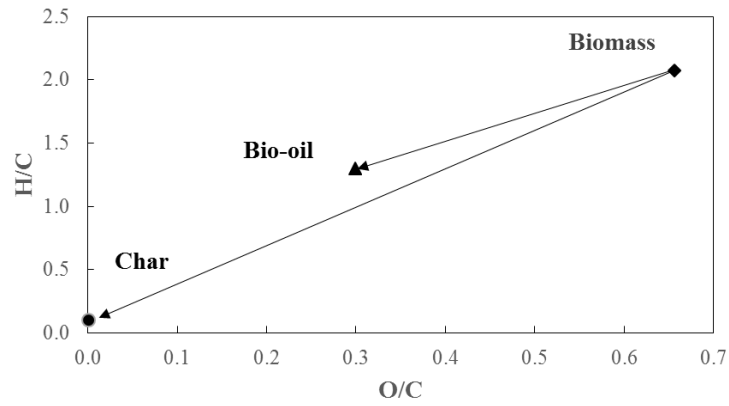
Figure 4-22- Van Kravelen diagram of chicken manure slow pyrolysis products at 800 °C

4-3-3-3- Estimation of gas elemental composition

Knowing the yields and elemental composition of each phase the composition of biogas can be estimated by mass balance. Elemental composition of feedstock (chicken manure) was reported earlier as ultimate analysis in Table 3- 1. The mass balance calculations were done by converting all the data to DAF basis

The DAF yields of the different products are mentioned in Table 4- 9, while the dry basis yields were mentioned before in Figure 4- 10. For converting the dry yields to DAF basis yields, Equation 4-10 to 4-14 were used:

Table 4-9- Pyrolysis products yields in DAF basis

Temperature (°C)	Water bio-oil	Organic bio-oil	Char	Biogas
400	17.3	20.4	39.6	22.7
450	10.7	32.0	33.7	23.6
500	9.1	35.0	29.4	26.5
550	13.3	32.4	29.2	25.4
600	13.7	28.8	26.9	30.6
700	14.4	23.0	21.1	41.4
800	13.8	18.5	19.9	47.8

$$Bio-oil_{DAF} \ yield = \frac{W_{Bio-oil}}{W_{OB,daf}} \times 100 \qquad \text{Equation 4-10}$$

$$Char_{DAF} \ yield = \frac{W_{Char.daf}}{W_{OB,daf}} \times 100 \qquad \text{Equation 4-11}$$

$$W_{Char.daf} = W_{Char}(1 - ash_{Char}\%) \qquad \text{Equation 4-12}$$

$$W_{OB,daf} = W_{OB}(1 - ash_{OB}\%) \qquad \text{Equation 4-13}$$

$$Biogas_{DAF} \ yield = 100 - Bio-oil_{DAF} \ yield - Char_{DAF} \ yield \qquad \text{Equation 4-14}$$

$Ash_{OB}\%$ is the ash% reported in proximate analysis Table 3- 1which was obtained by TGA and is equal to 25% on dry basis.

While $ash_{char}\%$ is obtained by elemental analysis on char samples and was shown in Figure 4- 19a. The obtained values for ash and comparison with theoretical ash are mentioned Table 4- 10 for making a comparison with theoretical ash which is calculated by Equation 4-15:

$$Theoretical \ ash\% = ash_{OB} \%/char \ dry \ yield \qquad \text{Equation 4-15}$$

Table 4- 10-Ash % in char

Temperature (°C)	Ash% in char by TG	Theoretical ash
400	43.4	45.2
450	48.0	48.7
500	51.6	52.1
550	50.4	53.6
600	51.5	56.4
700	58.3	62.3
800	58.2	66.5

The biogas elemental composition was calculated using Equation 4-16 and is reported in Table 4- 11 and Figure 4- 23.

$$wt\%_{in \ biogas} = wt\%_{in \ biomass(DAF)} - wt\%_{in \ char \ (DAF)} \times y_{char(DAF)} - wt\%_{in \ organic \ bio-oil} \times$$
$$y_{organic \ bio-oil \ (DAF)} - wt\%_{in \ aqueous \ bio-oil} \times y_{aqueous \ bio-oil \ (DAF)}$$
Equation 4-16

Table 4-11- Yield of each element in biogas phase

Temperature (°C)	N (gr%/gr DAF biomass)	C (gr%/gr DAF biomass)	H (gr%/gr DAF biomass)	S (gr%/gr DAF biomass)	O (gr%/gr DAF biomass)
400	0.9	3.2	2.4	0.0	16.2
450	0.9	5.0	3.4	0.0	14.4
500	1.4	9.0	4.0	0.0	12.5
550	1.0	7.4	3.5	0.0	13.3
600	1.8	10.2	3.6	0.0	15.1
700	2.3	15.4	4.4	0.0	19.2
800	2.1	14.8	4.7	0.0	25.3
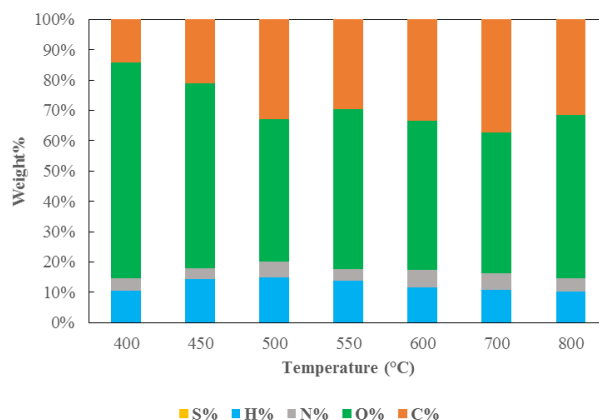
Figure 4-23- Estimated elemental composition of biogas

Having the elemental composition of the all four pyrolysis products, the H/C and O/C atomic ratio of the products can be obtained and compared with those ratios of biomass. Figure 4- 24a) and Figure 4-24b) show these two values in the biomass and in the products as function of temperature. The atomic values were obtained by dividing the mass values by molecular weight.

The consistency of the results of FTIR with elemental analysis was also investigated and mentioned in APP 10.
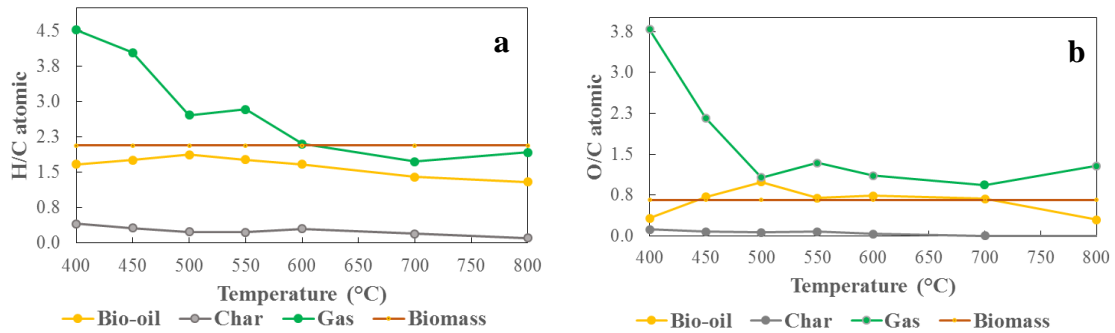
Figure 4-24- a) H/C and b) O/C atomic ratio of the biomass and pyrolysis products over temperature

It can be seen that H/C and O/C atomic ratio of biogas and char decreases by temperature.

4-3-3-4- Fate of elements during pyrolysis process

By rearranging the data, it can be revealed how each single element distributes among four phases. It would be very helpful to understand the fate of nitrogen and sulphur for environmental issues. Figure 4- 25 show the distribution of each element in the four product phases.

By increasing the pyrolysis temperature, the fraction of nitrogen and carbon that is present in the gaseous phase increases. More moderate is the effect of the test temperature on the content of these elements in the liquid phase. Hydrogen follows a similar trend, but temperature has a less evident effect. The oxygenated compounds, which are usually associated with a low quality of the pyrolysis bio-oil (Güngör et al., 2012) are transferred mostly to the gas only at higher temperatures. As already evidenced, most of the sulphur present in the original sample is found in the char after pyrolysis.
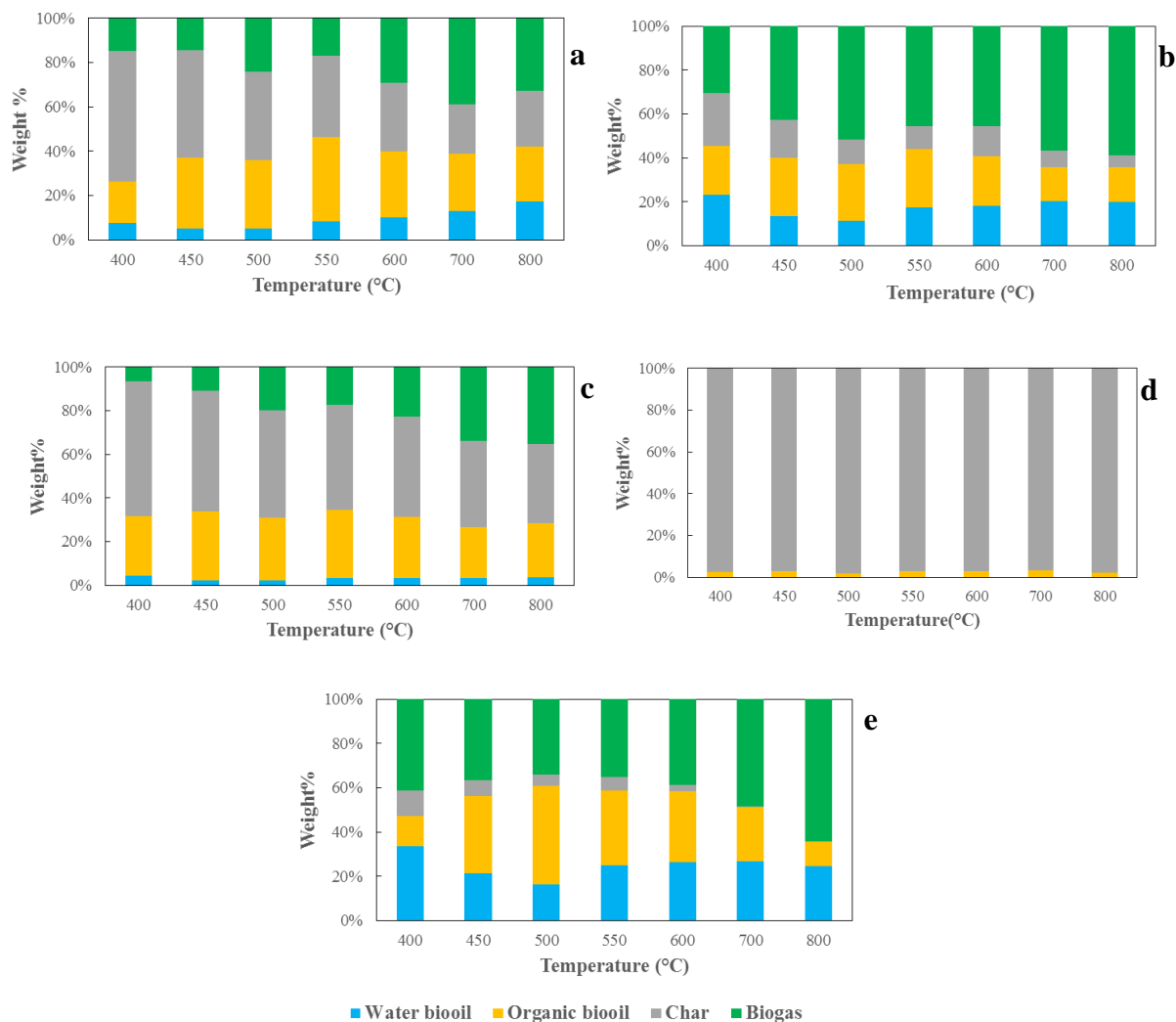
Figure 4-25- Distribution of the biomass elements among different phases a) Nitrogen b) Hydrogen c) Carbon d) Sulphor

e) Oxygen

4-3-4- GC-MS results of bio-oil

GC-MS was done on the organic phase of bio-oil to reveal the chemical groups available in that phase. The results of GC-MS showed the compounds available in the organic bio-oil. The GC-MS analysis of the organic fraction of condensables identified a set of 33 compounds present in this product fraction, which are listed in Table 4- 12. The identified compounds are categorized in five main groups: phenols, fatty acid, sterols, N-compounds and others.

Phenols	Fatty acids	Sterols	N-compounds	Others
2-methylphenol	Hexanoic acid	Sitosterol	Hydroxypyridine	2-hydroxymethylfurane
4-methylphenol	Pentanoic acid	Stigmasterol	Methylhydroxypyridine	1,2-dihydroxybenzene
Dimethylphenol	Palmitic acid	Ergostene ether	Methylphenylpyridine	1,4-dihydroxybenzene
Propenylguaiacol	Octadecenoic acid	Cholesterol	N-phenylacetamide	1methyl3,5hydroxybenzene
	Stearic acid	Stigmastan-3,5-diene	Indole	1,3,5-hydroxybenzene
	Linoleic acid	Cholesteryl valerate	Cyclo (-Ala-Ala)	
	Arachidic acid			
	Docosanoic acis			
	Octanoic acid			
	Methyl palmitate			
	Monopalmitin			
	Monostearin			

The identified groups available in bio-oil were quantified. Figure 4- 26 shows the quantitative composition of bio-oil obtained from chicken manure slow pyrolysis at 550 °C. It can be seen that fatty acids comprise the major part of the organic bio-oil. Bio-oil obtained from pyrolysis at other temperatures was also quantified. The changes in quantities with temperature are shown in Figure 4-27.
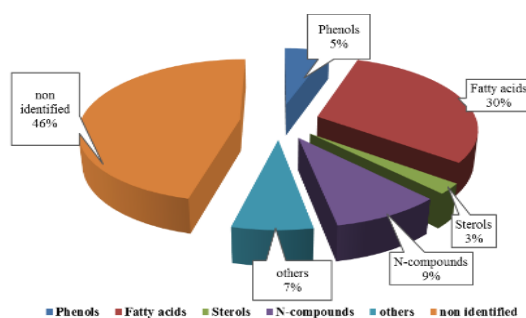
Figure 4- 26- Quantitative composition of bio-oil obtained from chicken manure pyrolysis at 550 °C
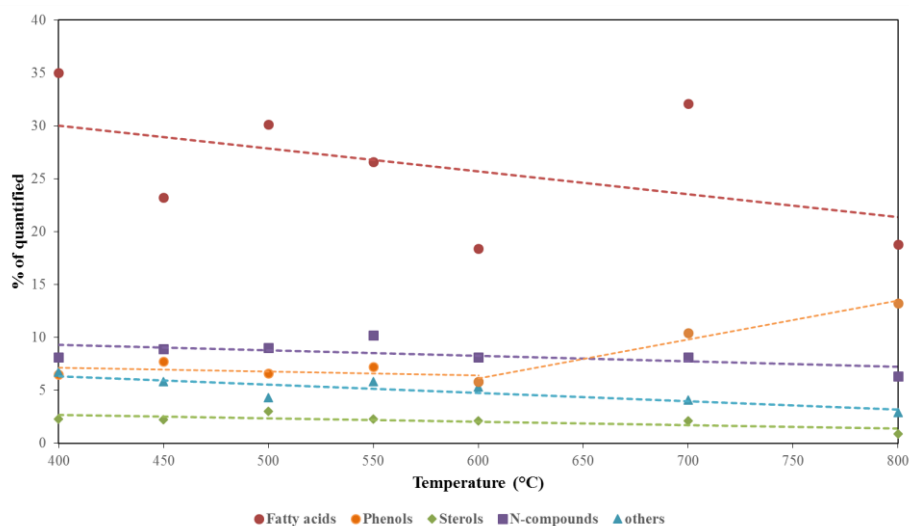
Figure 4- 27- Bio-oil composition obtained from biomass slowpyrolysis over test temperature

The main group of identified compounds at all the test temperatures was fatty acids (18.8-35.0 %), with palmitic acid and oleic acid as the most abundant products, in good accordance with the results of Ma et al., (2014). N-containing compounds represent the second abundant group with values ranging between 6.3 and 10.2%. In addition, phenols showed values ranging between 5.8 and 13.2%. Finally, sterols represent the less abundant group with values between 0.9 and 2.3%.

However, it should be noted that the absolute amount of compounds quantifiable by GC-MS analysis was low (10-20% of the analysed sample), as also evidenced by similar studies in the literature (Ma et al., 2014). Indeed, the organic condensable contains a high amount of compounds barely identifiable and quantifiable by GC-MS, and not all the condensable components are amenable to GC-MS analysis (e.g. lignin oligomers). Nevertheless, the composition of the organic condensable phase suggests that it can be used as biofuel only after an appropriate upgrading. Furthermore, the organic condensable phase can be a possible source of N-compounds (especially heterocyclic) which are of potential interest for different applications in the pharmaceutical, chemical and food industries, though economic aspects have limited so far the effective separations of single chemicals from pyrolysis oils (Czernik and Bridgwater, 2004).

The effect of the final pyrolysis temperature on the overall quantity of compounds belonging to the five main groups is also shown in Figure 4- 27. For all of the quantified compounds (except phenols)

the general composition of the organic condensable was comparable at different temperatures, with a slight decrease as the temperature is increased. On the other hand, phenols concentration becomes more than double as the FBR test temperature increased from 600°C to 800°C. This phenomena can be due to the thermal release of a portion of phenols moieties, which bears the char residual oxygen and are retained in the char at lower temperature (<600°C) (Conti et al., 2014). With respect to this aspect, the GC-MS analysis is in good agreement with the elemental analysis, which shows a sudden change in the oxygen content of char between 600°C and 700°C of the FBR tests (Figure 4- 19).

The direct use of the organic phase of the condensable for fuel purposes has to take into account a number of practical issues, typical of any pyrolysis oil, and related to the high content of heavy and light oxygenated compounds: high viscosity, acidity, blending limitations and aging effects (Czernik and Bridgwater, 2004) (Tzanetakis et al., 2010) (San Miguel, 2012). Also the high nitrogen content of the organic phase of the condensable should be carefully considered, since fuel NO_x seems to be the dominant formation mechanism in the combustion of pyrolysis oils (Moloodi et al., 2012).

The processes available for bio-oil upgrading were discussed earlier in section 1-9.

The high nitrogen content of the organic fraction of the condensate also suggests the possible use as a component for waste-derived fertilizers: pyrolysis oils were previously applied successfully to fertilization, but nitrogen had to be added from other sources (Bridgewater, 2000) (Radlein et al., 1997).

4-3-5-Energy balance

For energy balance, there is a need to calculate the HHV of all the products stream and the feed. The energy consumption of the system must be known as well.

4-3-5-1- HHV calculations

The HHV of the gas can be calculated by knowing the gas volumetric composition (Figure 4- 17) and HHV of the combustible compounds which are 39.82 MJ/Nm^3 for methane and 12.63 MJ/Nm^3 for CO

obtained from the reference (Basu, 2013). Equation 4-17 was used for this calculation and the results are mentioned in Figure 4- 28.

$$HHV = HHV_{CH4} \times fraction\ (v\%)_{CH4} + HHV_{CO} \times fraction\ (v\%)_{CO} \qquad \text{Equation 4- 17}$$
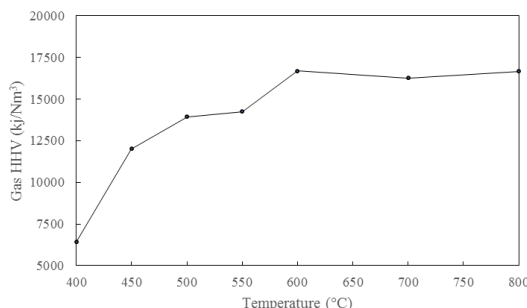
Figure 4-28- Gas HHV vs pyrolysis test temperature

The HHV for biomass, two phases of liquid products and char was calculated by Channiwala and Parikh (2002) equation: (Equation 4-18)

$$HHV\ = 349.1C + 1178.3H + 100.5S - 103.4O - 15.1N - 21.1Ash \qquad \text{Equation 4-18}$$

The HHV for water phase of bio-oil was calculated after subtracting the water content, evaluated under the hypothesis that all of the oxygen was part of water molecules.

The HHV of all the products and the feed are mentioned in Table 4- 13.

Energy transferred to each phase can be calculated by Equation 4-19.

$$E_i\ = HHV_i \cdot Y_i \qquad \text{Equation 4-19}$$

where E_i is the potential combustion energy in product i per mass of biomass, HHV_i is the higher heating value of product i and Y_i is the mass yield of product i. Figure 4- 29 shows the amount of potential combustion energy in the feedstock transferred to each pyrolysis product. It can be observed that by raising pyrolysis test temperatures the amount of energy transferred to the gas phase increases sharply, while the amount of energy transferred to the organic condensable slightly decreases. From the graph is also evident that, by raising the temperature, the energy content that remains in the char decreases. At 550°C, where the yield of the organic condensable phase is the highest, about 31% of

the potential combustion energy in the feedstock is transferred to this product, while about 34% is left in the char.

Table 4-13- Estimated higher heating value (HHV) of raw biomass and main pyrolysis products (kJ/kg dry basis)

Temperature of the pyrolysis test (°C)	Poultry litter	Char	Organic condensable	Non-condensable gas
-	15 200	-	-	-
400	-	14 100	28 000	4 180
450	-	12 600	18 800	8 080
500	-	11 900	15 000	10 000
550	-	11 600	19 100	10 600
600	-	12 000	18 100	12 300
700	-	10 700	18 000	13 200
800	-	10 300	26 400	13 200
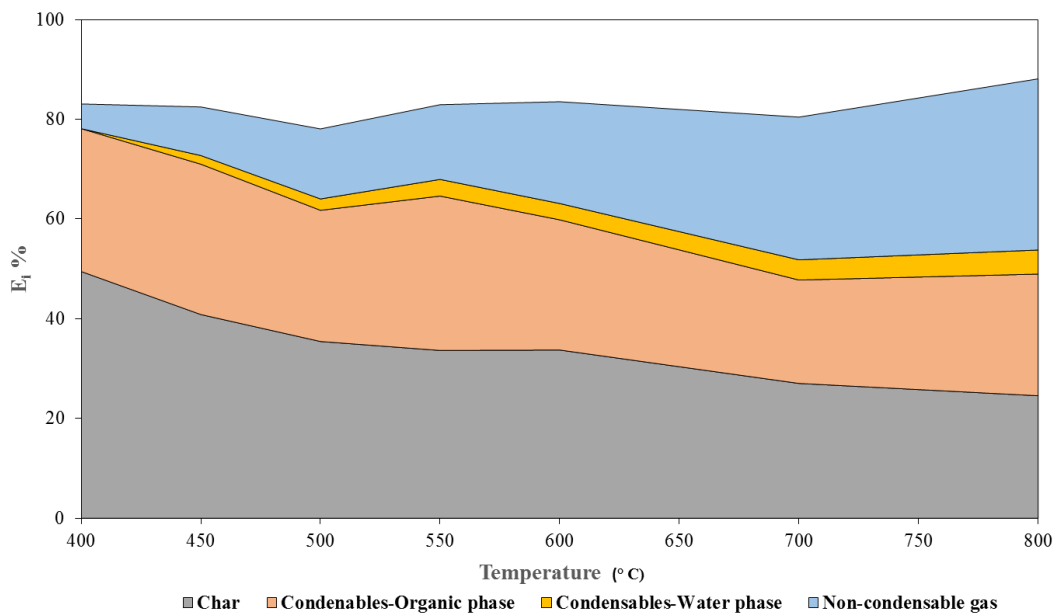
Figure 4-29- Energy transferred to the products as a function of test temperature

The share of energy content of the char, organic phase condensables and non-condensable gas is compatible with a possible use of these streams as fuel; as discussed above this application has to take into account the oxygen, sulphur and nitrogen content and may require upgrading processes. The low

heating value makes the water phase of the condensables unsuitable for combustion processes. Possible routes for the valorization of this stream include bio-gas production by fermentative processes (Torri and Fabbri, 2014) or pre-treatment of the biomass to improve pyrolysis yields (Dalluge et al., 2014) (Oudenhoven et al, 2013).

4-3-5-2- Calculating heat demand of the process

Heat demand of the system is a combination of biomass heating to the pyrolysis temperature (400-800 °C), pyrolysis heat and the heat necessary to warm up the nitrogen carrier gas. Heat of pyrolysis is obtained as discussed earlier by DSC (section 4-2) and is equal to 136 kj/kg. The heat necessary to warm the biomass to the pyrolysis temperature is obtained by the method of Basile et al., (2014), (Equation 4-20) since during the biomass heat up, also the conversion takes place, and as a result the sample is the combination of char and biomass at every moment of the experiment with different fractions. These fractions can be obtained by the simulation of reactor thermal condition in FBR (which was recorded by Agilent) by TGA, the result of which is mentioned in section 4-1-4:

$$Q_{sensible\ heat} = \left(1 - x(T)\right).m_0 C_{p,biomass}\frac{dT}{dt} + x(T).m_{char}C_{p,char}\frac{dT}{dt} \qquad \text{Equation 4-20}$$

InEquation 4-20, $C_{p,biomass}$was considered to be 1.4 J/g °C, which was reported by Ahn et al., (2009) for turkey litter. For $C_{p,char}$ the value used in the work of Koufopanos, (1991) was used which is $C_{p,char} = 1003.2 + 2.09T$ (J/kg k).

The conversion (x(T)) was obtained by rearranging the TGA results according to Equation 4-21:

$$x(T) = \frac{m_0 - m_T}{m_0 - m_{char}} \qquad \text{Equation 4-21}$$

In Equation 4-21, m_0 is the initial biomass sample (dry), m_T is the weight of sample at each temperature condition in TGA, and m_{char} is thefinal weight recorded at the moment in which, the test temperature is achieved.

There is also the need for heating the carrier gas (nitrogen) which is feeding to the system continuously with the rate of (8.5 Nl/hr). The sensible heat to warm up nitrogen from the ambient

temperature (22 °C) to the test temperature was calculated by considering the total mass of nitrogen fed during 30 minutes of the process and heat capacity of the nitrogen, which is $C_{p,charN2} = 6.50 + 0.001T$ (cal/K mol) according to Perry et al., (1997).

The results of the FBR heat demand are mentioned in Table 4- 14.

Table 4- 14– Heat demand of the system (kj/kg dry)

Temperature (°C)	400	450	500	550	600	700	800
Pyrolysis reaction heat (kj/kg)				136			
Biomass heat to pyrolysis temperature (kj/kg)	387	435	472	538	594	670	733
Nitrogen heating (kj/kg)	149	170	178	211	216	257	295
Total heat demand(kj/kg)	672	741	786	885	947	1063	1164

However, the energy necessary for nitrogen heating can not be generalized for all the reactor scales, since the necessary amount of the nitrogen needed must be studied and optimised again at the condition and scale of the work.

The above calculations are in the dry basis, and the drying heat was not considered. However, the biomass contains 5% moisture as mentioned in Table 3- 1 for proximate analysis. Therefore, the energy necessary for biomass dying is calculated to be 241 kj/kg for the biomass as received using the latent heat of water and heat capacity of water (Perry et al., (1997)), and heat capacity of turkey litter (Ahn et al., 2009).

To compare the heat demand results with the energy recovery of the gas obtained by Equation 4-19, it can be seen that the ratio (see Table 4- 15) is lower than 1. This means, even accounting for any reasonable efficiency factor of the actual heating technology, the produced gases (at higher 450 °C) are therefore suitable for sustaining a self-sufficient pyrolysis process. It must be considered that, for a slightly higher moisture content of the biomass, this self-sufficiency may not be achieved.

Table 4-15- Investigation of self-sufficiency of the system (basis: as received biomass)

Temperature (°C)	400	450	500	550	600	700	800
Energy recover in gas (kj/kg)	792	1494	1789	1991	3436	4019	4957
Heat demand of process (kj/kg)	737	783	818	881	934	1007	1066
Drying				241			
Pyrolysis heat				129			
Heating to test temperature	368	413	449	511	565	637	696
Ratio	0.93	0.52	0.44	0.44	0.27	0.25	0.22

Sankey diagram of process at 400 °C and 800 °C are shown in Figure 4- 30. It can be seen that at high temperature (800 °C), much lower amount of biomass energy remains in the char, which give a sharp increase to the amount of energy transferred to non-condensable gases.
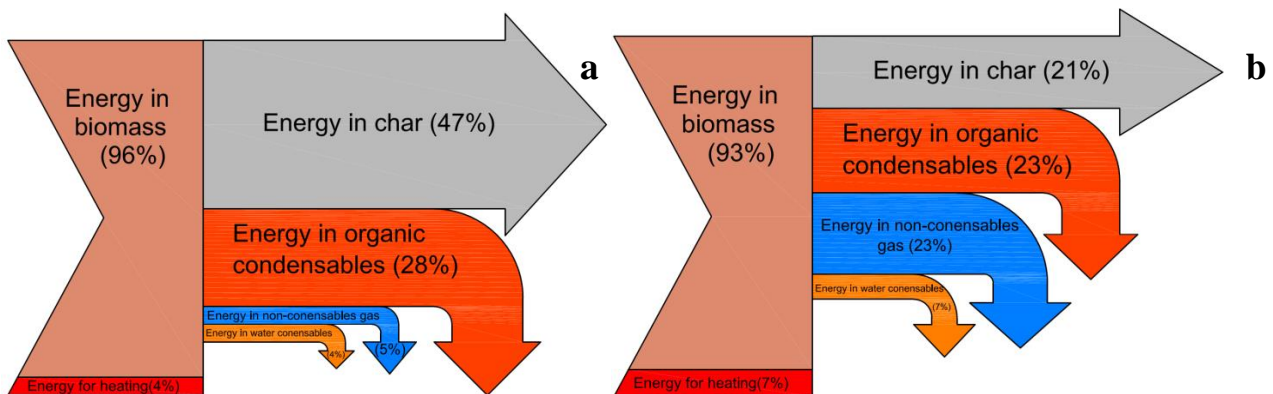
Figure 4-30- Sankey diagram of the slow pyrolysis process at a) 400 °C and b) 800 °C

4-3-6- Optimisation of non-catalytic process

For optimisation of the process, three responses were considered, which were the amount of energy transferred to gas and organic phase bio-oil obtained by Equation 4-19, while the third response is considered to be the heat demand of the process, which was calculated by the method mentioned in section 4-3-5-2 and the results are mentioned in Table 4- 14.

Equal weights (s=1) was considered for all the responses and the optimization was performed with the aim of maximizing the amount of energy transferred in bio-oil and gas and minimizing the heat demand of the system. Figure 4- 31 shows the change of the three responses as a function of temperature. The desirability was calculated for each single response and the combination of responses, with the method mentioned in section 3-5-2. Figure 4- 32 shows the calculated desirability of the responses and the general process. It can be observed that the most desirable responses were obtained at 490 °C. The details of the optimal condition are mentioned in Table 4- 16.
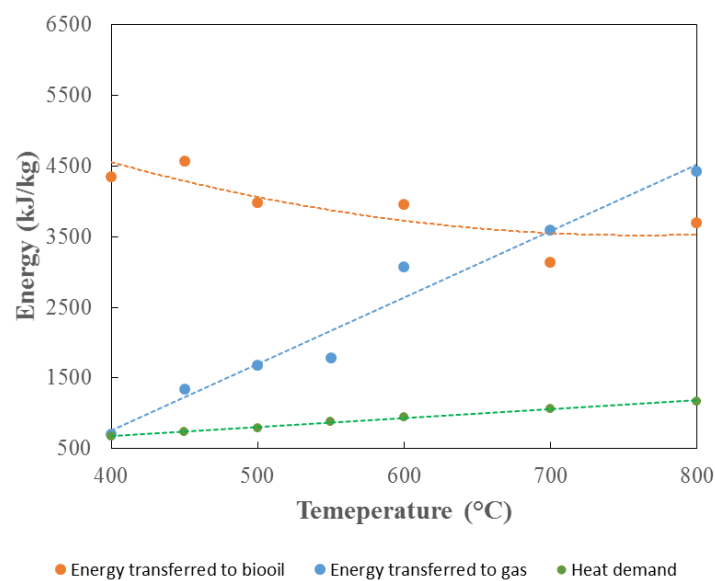
Figure 4-31- Non-catalytic responses vs. temperature
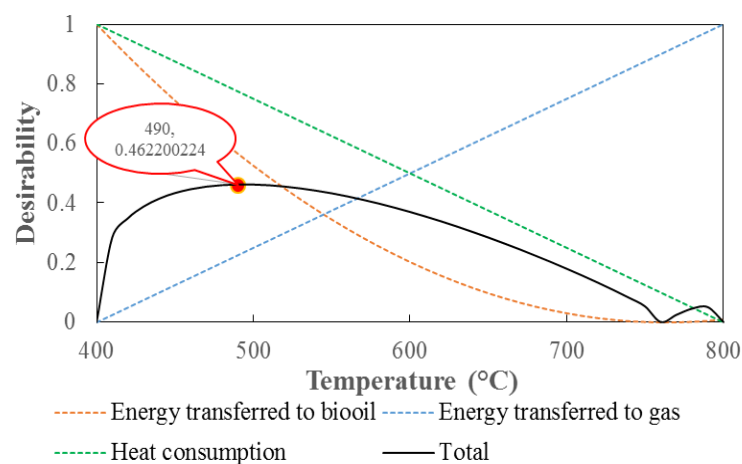
Figure 4-32- Desirablity of the non-catalytic responses

Table 4-16- Optimal condition for non-catalytic slow pyrolysis of chicken manure

	Non-catalytic process
Optimal parameter	
Temperature (°C)	490
Results	
Energy transferred to bio-oil	4100
Energy transferred to gas	1607
Energy demand	792
Desirability score	0.4622

4-4- Catalytic results

As mentioned earlier in section 3-5, for the catalytic process the experiment design techniques were used, in order to investigate the effect of two factors, which are temperature and the amount of catalyst in the range from 400-800 °C and 0.25-1.25 of catalyst to biomass ratio. The values (-1 to +1) are called the coded value and are the indication of the position of the value of the factor in the selected range, since the factors range were divided in five intervals (see Figure 3- 13).

Table 4-17- *List of the experimental factors obtained by design experiment techniques*

Std	Run	Factor 1 Temperature (°C) [A]	Factor 2 Catalyst/biomass [B]
10	1	500 *(-0.5)*	1.00 *(+0.5)*
6	2	600 *(0)*	0.25 *(-1)*
8	3	800 *(+1)*	0.75 *(0)*
1	4	400 *(-1)*	0.25 *(-1)*
9	5	500 *(-0.5)*	0.50 *(-0.5)*
15	6	600 *(0)*	1.00 *(+0.5)*
7	7	600 *(0)*	1.25 *(+1)*
5	8	400 *(-1)*	0.75 *(0)*
20	9	600 *(0)*	0.75 *(0)*
19	10	600 *(0)*	0.75 *(0)*
14	11	600 *(0)*	0.50 *(-0.5)*
2	12	400 *(-1)*	1.25 *(+1)*
4	13	800 *(+1)*	1.25 *(+1)*
13	14	500 *(-0.5)*	0.75 *(0)*
18	15	600 *(0)*	0.75 *(0)*
12	16	700 *(+0.5)*	1.00 *(+0.5)*
17	17	600 *(0)*	0.75 *(0)*
11	18	800 *(+1)*	0.25 *(-1)*
3	19	700 *(+0.5)*	0.50 *(+1)*
16	20	700 *(+0.5)*	0.75 *(0)*

Table 4- 17 shows the list of experiments. These 20 runs were performed and the FBR results and FTIR results were obtained for all these conditions, and were elaborated from energy point of view. According to the results of these 20 runs, using statistical analysis and evaluations, the repeatability of the results and the significance of the error were checked.

4-4-1- FBR catalytic results

The product yields obtained from catalytic FBR of different runs are shown in Table 4- 18. The bio-oil yield mentioned in this table is the yield of two phase liquid product, since the phase separation was not done. The new product of the catalytic process is coke, which is formed on the catalyst surface as a result of catalytic cracking of the product during the process. Figure 4- 33 shows the difference between the fresh and used catalyst. The deposition of coke on the surface of the catalyst is observable.

Figure 4-33- Fresh and coked ZSM-5 catalyst pellets

The coke yield was obtained using the method suggested by Aho et al., (2010) et al., with TGA-Q500 thermogravimetric analyzer from TA Instruments-Water (USA) using the following thermal program:10 °C/min from 25 °C to 795 °C with an isothermal at 100 °C for 15 minutes under flow of air at 100 ml/min. Campanella and Harold, (2012) mentioned Equation 4-22 for the relative amount of coke which is shown in Figure 4- 34:

$$x_{coke} = (m_{100} - m_{795})/m_{795} \qquad \text{Equation 4-22}$$

Table 4-18- *Product yields of the slow pyrolysis catalytic process*

| Std	Run	Factor 1 Temperature (°C)	Factor 2 Catalyst/biomass	Bio-oil yield (wt%) dry	Char yield (wt%) dry	Gas yield (wt%) dry	Coke yield (wt%) dry
10	1	500	1	29.0	46.0	18.4	6.6
6	2	600	0.25	31.8	42.7	24.4	1.1
8	3	800	0.75	28.0	34.5	36.4	1.1
1	4	400	0.25	31.8	52.8	13.4	2.0
9	5	500	0.5	25.9	46.7	24.1	3.3
15	6	600	1	30.7	43.7	21.2	4.5
7	7	600	1.25	32.5	43.9	18.0	5.6
5	8	400	0.75	20.2	53.3	20.6	5.9
20	9	600	0.75	28.8	43.2	24.7	3.3
19	10	600	0.75	33.8	42.2	20.7	3.3
14	11	600	0.5	32.0	43.5	22.3	2.2
2	12	400	1.25	27.5	53.8	8.8	9.9
4	13	800	1.25	25.8	34.2	38.1	1.9
13	14	500	0.75	30.0	46.7	18.3	5.0
18	15	600	0.75	24.4	42.5	29.8	3.3
12	16	700	1	34.0	38.7	25.2	2.1
17	17	600	0.75	30.4	43.3	23.0	3.3
11	18	800	0.25	29.0	36.2	34.4	0.4
3	19	700	0.5	32.0	38.8	28.1	1.1
16	20	700	0.75	27.9	38.1	32.4	1.6
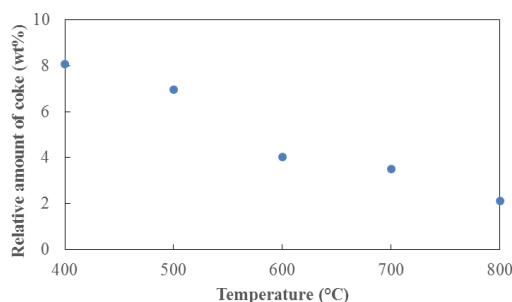
Figure 4-34- Relative amount of coke formed on the catalyst surface vs. temperature

Pan et al., (2010) obtained the same trend regarding to the amount of coke formed as a function of temperature and suggested that coke on catalyst surface could be easily formed at relatively low temperature, and partly decomposed at higher temperature over 400°C.

Figure 4- 35 shows the effect of temperature and the amount of catalyst on the yield of the produced bio-oil. The fitted surface to the experimental method is shown in a 3D graph in this graph. It can be seen, that the effect of catalyst on the amount of organic bio-oil yield is much less than the effect of temperature. Up to the ratio of 0.75, the increase of catalyst amount leads to lower yield of bio-oil.At higher catalyst/biomass ratios, the bio-oil seems to increase as the amount of catalyst increases. Below 0.75, the catalyst causes cracking of organic bio-oil to gaseous compound and therefore lower amount of total bio-oil is obtained. The increase in total bio-oil yield (this includes aqueous and organic fraction of the bio-oil) for higher catalyst/biomass ratios was explained as an increase in theformation of the aqueous fraction of the bio-oil, as a result of the catalytic cracking reactions. The same trend of bio-oil with catalyst amount was observed in the work of Pan et al. (2010).

In the work of Wang et al., (2010), the slow pyrolysis of herb residue was studied in the fixed bed reactor. More catalyst to biomass ratio in that work improved the yield of char and water condensables, and decreased the yield of organic condensables and gas. It was suggested that condensable product of catalytic cracking process contains higher amounts of water, in comparison to non-catalytic process. This water is the product of deoxygenation from the biomass pyrolysis gas

catalyzed by Y-zeolite and activated alumina. Further degradation of light and heavy compounds in condensables leads to more gas production (Wang et al., 2010).
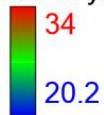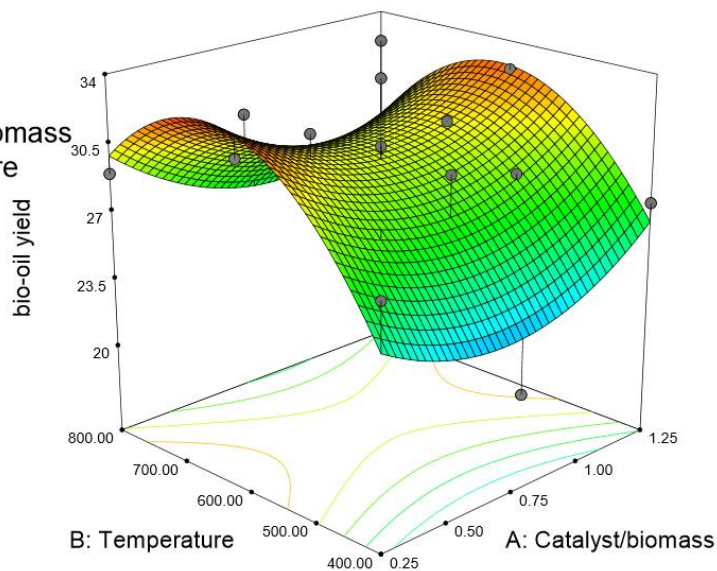
Figure 4-35- The yield of condensable products from slow pyrolysis of biomass (wt% dry) as a function of temperature and catalyst amount

4-4-2- FTIR catalytic results

The same on-line FTIR analysis was performed during the catalytic FBR experiments. The calibration and identification of the products were same as non-catalytic process. The quantification procedure and calculation were based on the same methods and equation of the non-catalytic process.

Table 4- 19 shows the yields of the gaseous products obtained by catalytic slow pyrolysis of biomass.

Table 4-19- Gaseous compounds production (gr%/gr biomass dry)of catalytic FBR run

Std	Run	Factor 1 Temperature (°C)	Factor 2 Catalyst/biomass	CO_2 yield (gr%/gr$_{biomass,dry}$)	CH_4 yield (gr%/gr$_{biomass\ dry}$)	CO yield (gr%/gr$_{biomass,dry}$)
10	1	500	1.00	15.9	3.8	4.5
6	2	600	0.25	17.4	4.0	5.4
8	3	800	0.75	20.4	7.7	12.8
1	4	400	0.25	12.5	1.0	2.9
9	5	500	0.50	16.3	3.6	4.0
15	6	600	1.00	21.4	5.7	6.8
7	7	600	1.25	17.5	4.5	6.6
5	8	400	0.75	12.7	1.4	3.1
20	9	600	0.75	17.5	3.9	6.4
19	10	600	0.75	19.1	5.0	7.1
14	11	600	0.50	16.9	3.9	5.7
2	12	400	1.25	12.8	0.9	3.1
4	13	800	1.25	21.2	8.9	16.3
13	14	500	0.75	15.9	4.7	4.2
18	15	600	0.75	18.8	6.1	7.6
12	16	700	1.00	30.8	8.2	14.7
17	17	600	0.75	31.2	7.7	10.2
11	18	800	0.25	17.5	7.3	12.6
3	19	700	0.50	17.2	4.5	6.1
16	20	700	0.75	28.3	8.7	9.8

Figure 4- 36, shows the gaseous compound yield obtained as a function of temperature and catalyst to

biomass ratio which are the best fitted plots surface to the experimental results of catalytic process. It

can be seen in the figure that by raising the temperature and the catalyst to biomass ratio, the gaseous

compounds production increases. The effect of temperature is much more significant than the effect of catalyst to biomass ratio in the range of study. The most gaseous production improvement by increasing catalyst amount was observed for methane. This can be related to the breakdown of long chain hydrocarbons to smaller one (such as methane) which takes place in the presence of catalyst.

Pan et al., (2010) studied the effect of catalyst to biomass ratio in the range of 0.2-1 for slow pyrolysis of algal biomass, and reported that the yield of CO_2 and methane increase while the yield of CO decreases.

Figure 4- 37 shows the gaseous compounds production as a function of catalyst amount, which is obtained at 600 °C. It can be seen in this figure that the CO_2 is the major component produced; CO and CH_4 are much less. CO production is more than CH_4.
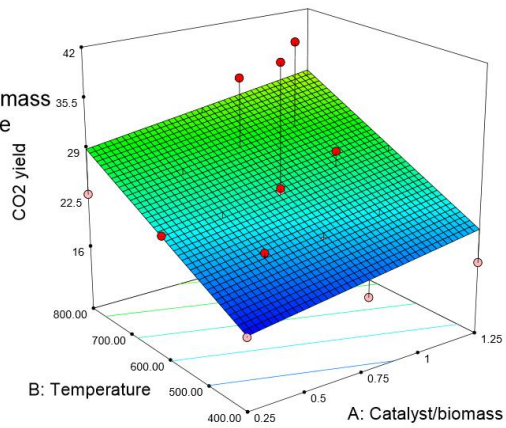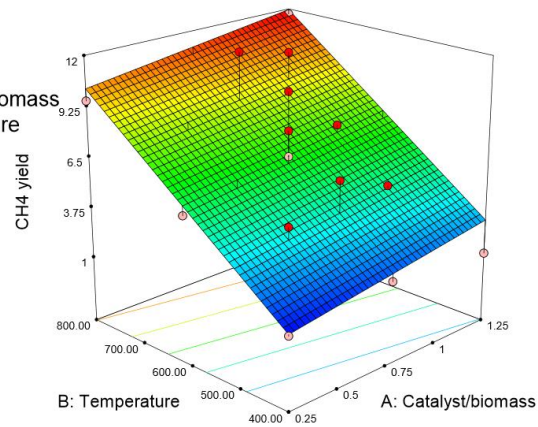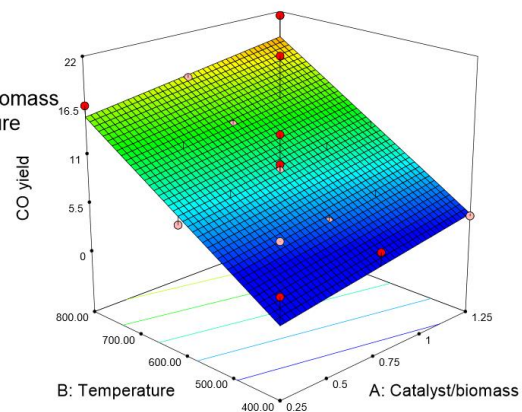
Figure 4-36- The effect of temperature and catalyst/biomass on non-condensable gas compounds obtained from catalytic

FBR a)CO₂, b) CH₄ c) CO
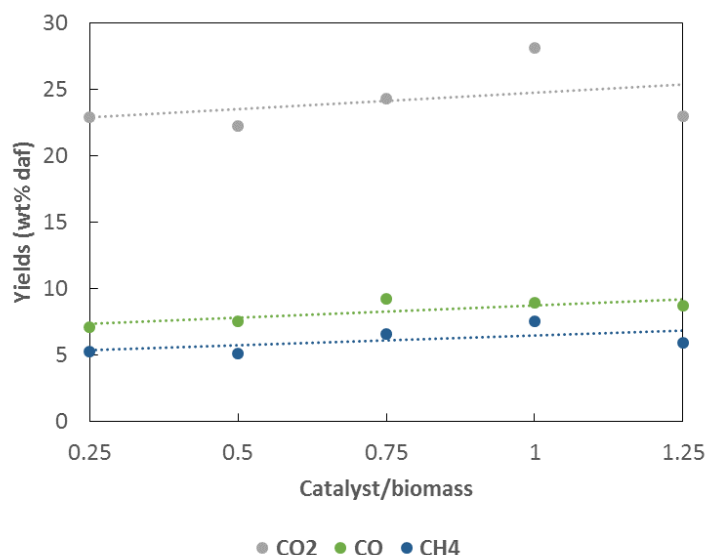
Figure 4-37- Effect of catalyst/biomass ratio on the yield of gaseous components (slow pyrolysis of poultry litter at 600

°C)

4-4-3- Statistical analysis of catalytic results

For investigating the repeatability and see, whether the results are significant or not, some statistical evaluations are needed. The statistical analyses were performed for bio-oil yields and the yields of different gaseous compounds. This was not done for char yield, since the results were obviously consistent, and for the gas yield, since it was not obtained experimentally but by the difference.

Normal plot of residuals and predicted vs. actual plot of all the experimental results of catalytic process are shown in Figure 4- 38. Normal plot of residuals is a tool to check if the error term is normally distributed. The linearity of the plot signifies that error terms are normally distributed. The vicinity of the experimental dots to the straight line in predicted vs. actual plot is an indication of well-fitting models to experimental results. It can be seen that the normal distribution of error is quite good for all the responses, while the lack of model fitting is observable for all of results except for CO.

Design-Expert® Software
bio-oil yield

Color points by value of
bio-oil yield:
34
20.2

Normal Plot of Residuals

a

Predicted vs. Actual
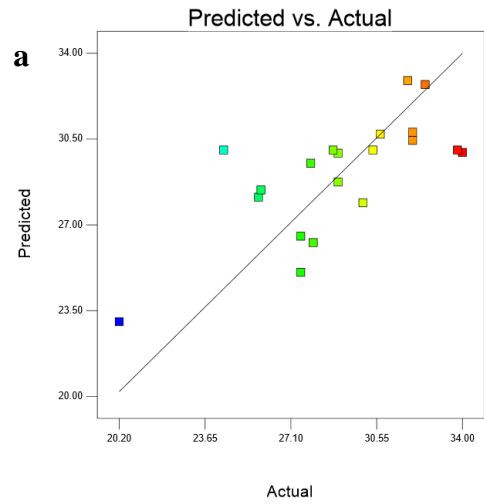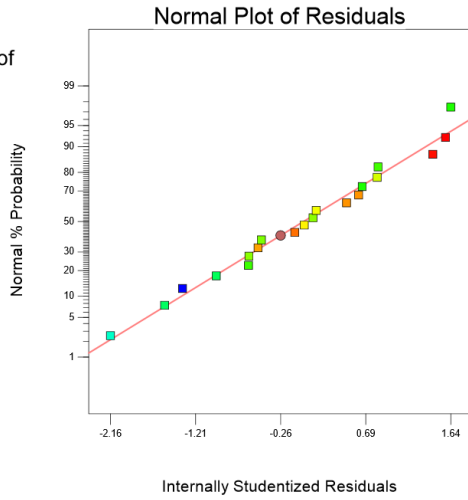
Design-Expert® Software
CO2 yield

Color points by value of
CO2 yield:
31.2
12.5

Normal Plot of Residuals

b

Predicted vs. Actual
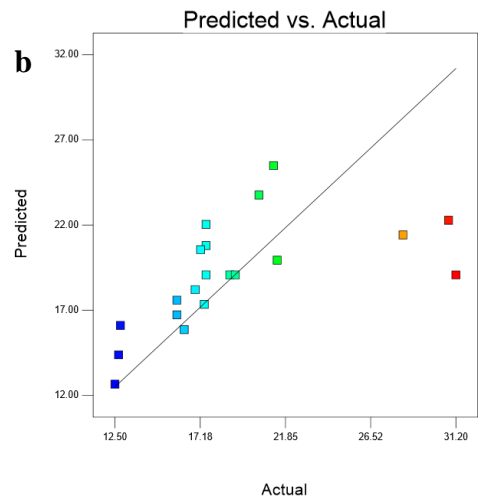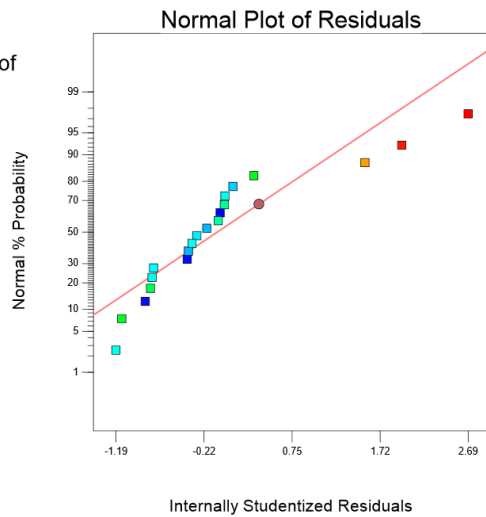
Design-Expert® Software
CH4 yield

Color points by value of
CH4 yield:
8.9
0.9
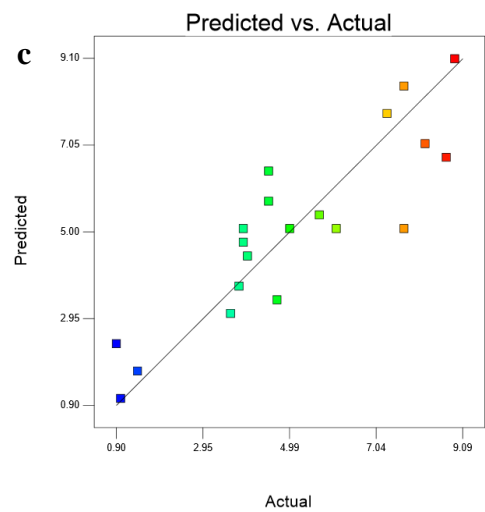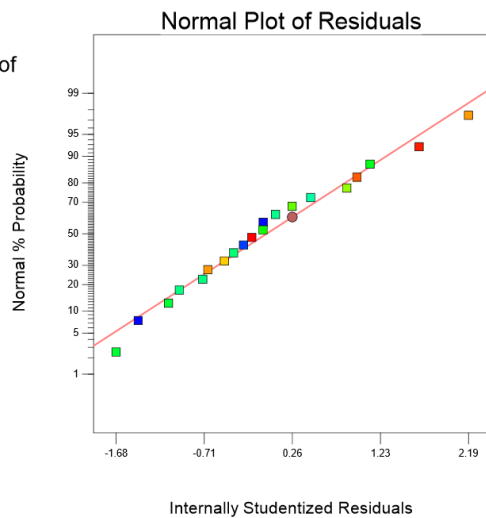
Normal Plot of Residuals

c

Predicted vs. Actual

149
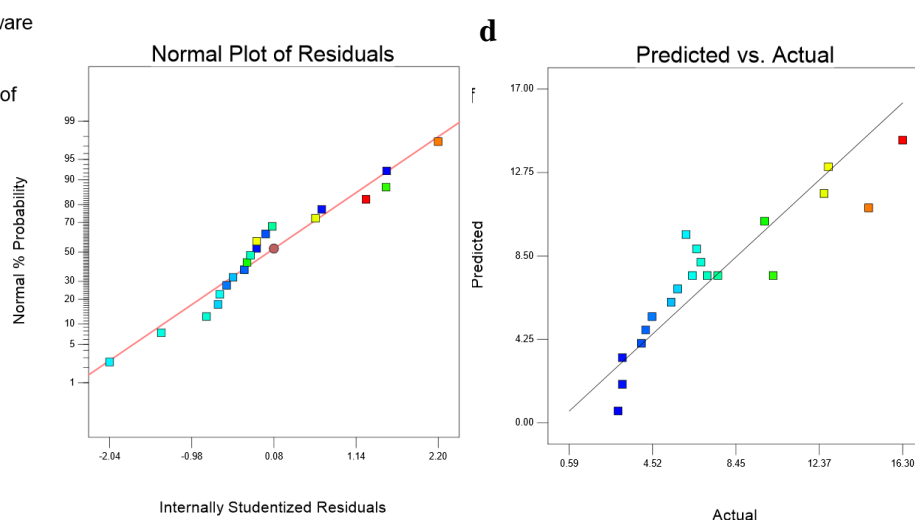
Figure 4-38- Normal plot of residuals and predicted vs. actual of the catalytic responses a) Bio-oil yield b) CO_2 yield c) CH_4 yield d) CO yield

4-4-3-1- Analysis of variance (ANOVA) of the catalytic experimental results

The ANOVA table of the four main experimental results (bio-oil, CO_2, CH_4 and CO yield) are mentioned in Table 4- 20 in which A is temperature and B the amount of catalyst/biomass. The best fitted model to the gaseous compounds was linear, while the one for bio-oil yield is quadratic. The low value of probability (<0.1) means that the results are significant. Probability value is much lower for CO and CH_4 yields, and is high but still significant for the bio-oil yield and CO_2 yield.

It can conclude from the ANOVA table that the most influencing factor on the amount of all of the results is temperature.

Table 4-20- ANOVA for response surface models applied to catalytic responses

Response	Model						
		ANOVA					
		Source	**Sum of square**	**DF**	**Mean square**	**F value**	**prob>F**
Bio-oil yield (wt% dry)	Quadratic	**Model**	**110.26**	**5**	**22.05**	**2.89**	**<0.0537**
		A^2	86.67	1	86.67	11.36	0.0046
		B^2	22.56	1	22.56	2.96	0.1076
		Residual	106.85	14	7.63		
		(R^2= 0.5078, R^2_{adj}=0.3321)					

Response	Model						
		ANOVA					
		Source	**Sum of square**	**DF**	**Mean square**	**F value**	**prob>F**
CO_2 yield (wt% dry)	Linear	**Model**	**187.57**	**2**	**93.78**	**4.39**	**0.0291**
		A	165.21	1	165.21	7.73	0.0128
		B(catalyst/bi	22.36	1	22.36	1.05	0.3207
		Residual	363.38	17	21.38		
		(R^2= 0.3404, R^2_{adj}=0.2628)					

Response	Model						
		ANOVA					
		Source	**Sum of square**	**DF**	**Mean square**	**F value**	**prob>F**
CH_4 yield (wt% dry)	Linear	**Model**	**88.14**	**2**	**44.07**	**29.23**	**<0.0001**
		A	85.01	1	85.01	56.38	<0.0001
		B(catalyst/bi	3.14	1	3.14	2.08	0.1674
		Residual	25.63	17	1.51		
		(R^2= 0.7747, R^2_{adj}=0.7482)					

Response	Model						
		ANOVA					
		Source	**Sum of square**	**DF**	**Mean square**	**F value**	**prob>F**
CO yield	Linear	**Model**	**244.06**	**2**	**122.03**	**36.91**	**<0.0001**
		A	230.19	1	230.19	69.62	<0.0001

(wt% dry)	B(catalyst/bi	13.87	1	13.87	4.20	0.0563
	Residual	56.21	17	3.31		
	(R^2= 0.8128, R^2_{adj}=0.7908)					

4-4-4-Energy evaluation of catalytic process

For energy evaluation of the process, the amount of energy transferred to the non-condensable gas phase and heat demand of the process was evaluated. The amount of energy transferred to the bio-oil in catalytic process could not be achieved as a consequence of lack of elemental analysis results on the bio-oil obtained from catalytic process. However, the following evaluation of the process from energy point of view was done.

4-4-4-1- HHV of the catalytic gas product

Knowing the volumetric composition of the produced gas, the HHV can be calculated by Equation 4-17.The obtained HHV of the gas product of each catalytic run is mentioned inTable 4- 21. Figure 4-39 is the best fitted surface to values reported for HHV in Table 4- 21. It can be seen that the amount of catalyst does not have any significant effect on the HHV of the non-condensable gas, while by raising temperature, more HHV is obtained in the gas phase. The amount of biomass energy transferred to gas was also calculated by Equation 4-19 and the results are mentioned in Table 4- 21. Figure 4- 40 show the effect of temperature and catalyst to biomass ratio on the amount of energy transferred to the gas.
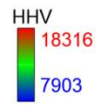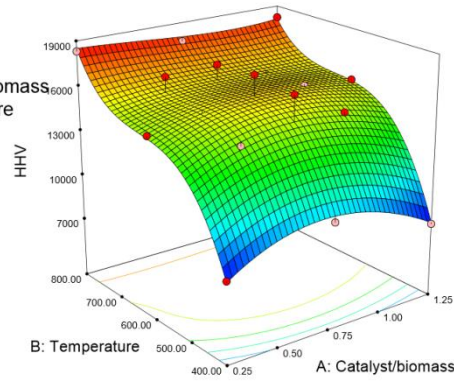
Figure 4-39- The effect of temperature and catalyst/biomass on higher heating value (HHV) of non-condensable gas
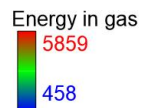
obtained from catalytic FBR
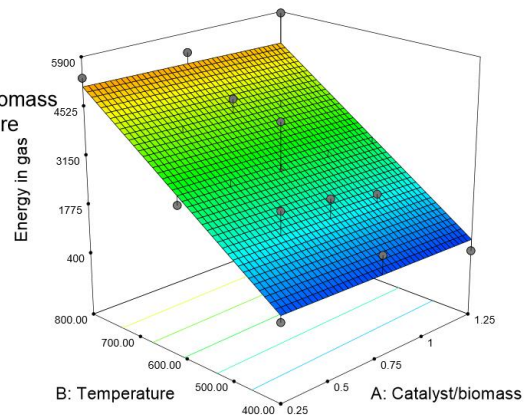
Figure 4- 40- The effect of temperature and catalyst/biomass on energy transferred to non-condensable gas obtained from

catalytic FBR

Table 4-21- HHV and energy transferred to non-condensable gas obtained in each FBR catalytic run

Std	Run	Factor 1	Factor 2	HHV	Energy
		Temperature (°C)	Catalyst/biomass	(Kj/Nm³)	transfer to gas (kj/kg)
10	1	500	1.00	15058	2099
6	2	600	0.25	14849	2753
8	3	800	0.75	17729	5341
1	4	400	0.25	8338	743
9	5	500	0.50	14476	2599
15	6	600	1.00	15833	2586
7	7	600	1.25	15543	2179
5	8	400	0.75	9967	14000
20	9	600	0.75	14501	2710
19	10	600	0.75	15649	2513
14	11	600	0.50	14729	2481
2	12	400	1.25	7903	458
4	13	800	1.25	18194	5859
13	14	500	0.75	16927	2450
18	15	600	0.75	17240	4136
12	16	700	1.00	15578	3075
17	17	600	0.75	15258	2681
11	18	800	0.25	18316	5326
3	19	700	0.50	16888	3065
16	20	700	0.75	17000	4377

4-4-4-2- Heat demand of catalytic process

There is no difference in the heat demand calculation for catalytic and non-catalytic process. Except that, the pyrolysis reaction heat is not the same in catalytic and non-catalytic processes, as a consequence of different degradation mechanism. However, since the reaction heat comprise low fraction of total heat demand (around 10%) the same value was used as an indication of heat consumption of catalytic process. This value was not considered as the exact value for energy balance purposes, but as an indication of heat consumption of the process, and used further in optimization part.

4-4-5- Optimisation of catalytic process

The optimization of the catalytic results was done with the aim of maximizing the energy transfer to the gas phase and minimizing the heat demand of the system. The optimization was done for catalytic process using Design-Expert® Software Version 9 Free Trial. However, the calculation is based on the statistical methods mentioned in section 3-5-2. For both two goals same weigh (s=1) was considered. Figure 4- 41 shows the desirability of the responses at different temperature and catalyst/biomass range. The optimal condition and the expected results are as mentioned in Table 4- 22.

Table 4-22- Optimal condition and expected responses for catalytic process

Optimal parameter	
Temperature (°C)	553
Catalyst/biomass	0.2
Results	
Energy transferred to gas	2518
Heat demand	1269
Desirability score	0.474

Design-Expert® Software

Desirability
1
0

X1 = A: Catalyst/biomass
X2 = B: Temperature
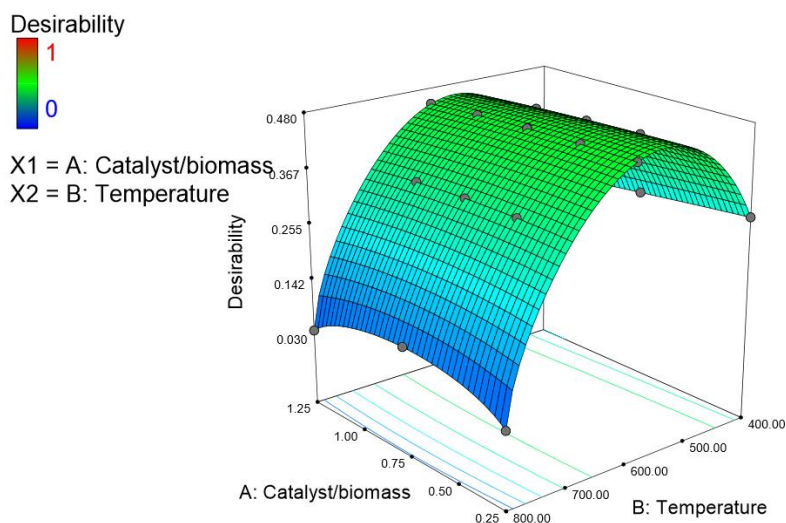
Figure 4-41- Desirability of the catalytic responses

4-4-6-Carbon elemental analysis

The only elemental analysis performed was obtaining the carbon in the bio-oil, which is the mixture of two phases. This result was used in combination with the carbon elemental composition of biomass and char, in order to estimate the carbon elemental composition of gas. This was done by considering the coke composition of one hundred percent carbon. By rearranging the data the distribution of elemental carbon of biomass among the products was investigated and is shown in Figure 4- 42.
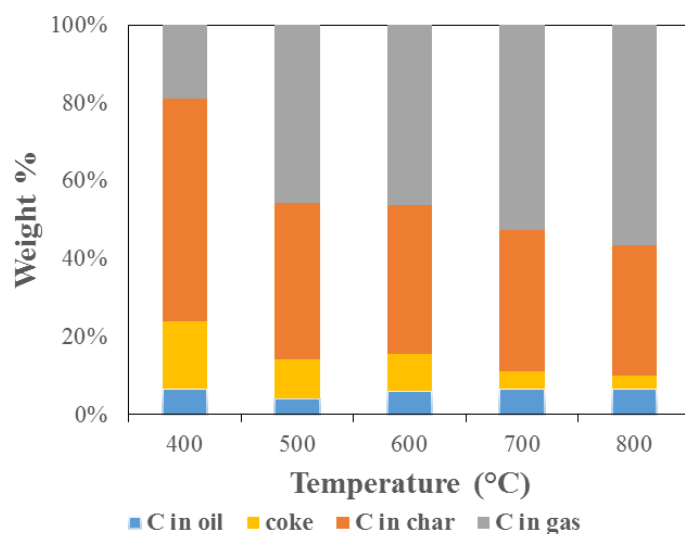
Figure 4-42- Distribution of carbon among the products of catalytic slow pyrolysis

4-4-7- Comparison of the catalytic and non-catalytic results

The yields of different product obtained from FBR are shown in Figure 4- 43 for both non-catalytic and catalytic process. The catalytic results reported in this graph are for the constant catalyst/biomass ratio of 0.75 which is the middle level in the range. All the products have a same trend that was observed for non-catalytic process by temperature increase. By comparing the non-catalytic and catalytic yields, it can be seen that, the presence of catalyst cause a little decrease in the char yield. While the condensable yield decreases by catalyst use, since the catalyst upgrade the bio-oil by cracking of high molecular weight alkanes and alkenes to low molecular weight one. Catalytic cracking therefore increase the yield of non-condensable gases by reducing the yield of condensable organic phase. In the work of H. Zhang et al., (2009), HZSM-5 catalyst was used for fast pyrolysis of corncob. Also in that work decrease of char and condensable organic phase yield was observed, while the yield of gas and condensable water phase increased in the presence of catalyst. Adam et al., (2006) in the slow pyrolysis of spruce wood in the in situ presence of MCM catalyst, observed a slight decrease in the yield of char, an increase of water bio-oil and gas products with the expense of organic bio-oil.

By comparing the concentration curve obtained from FTIR for different gaseous compounds it can be seen that, catalyst application definitely shift the concentration curve of all gaseous compounds higher. Figure 4- 44 and Figure 4- 45 are an example of the effect of catalyst amount on the obtained concentration curve, which are obtained at 700 °C and 800 °C. Therefore, the total yield (wt% dry) of the gaseous products is increased by adding the catalyst as it is shown in Figure 4- 46. The yield of CO did not change drastically, while the improvement of CO_2 and CH_4 yield occurred specially at high temperatures. It must be considered that the comparison was performed with the catalytic processes in which the catalyst/biomass ratio was at middle value of the range (equal to 0.75).
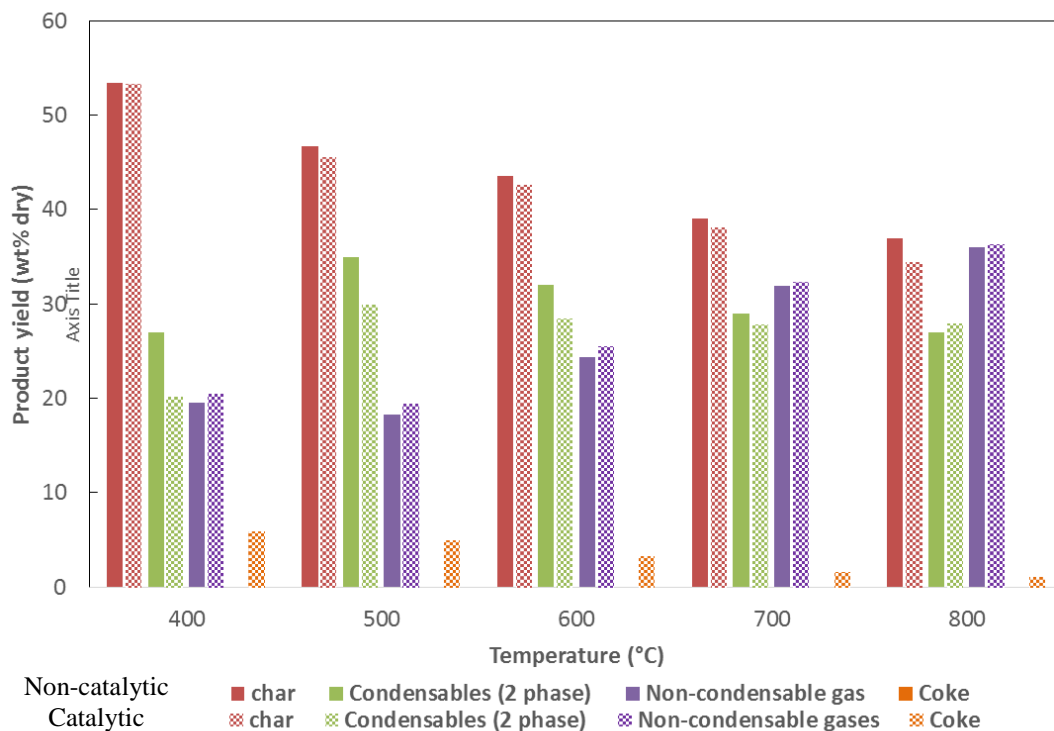
Figure 4-43- Compariosn of the slow pyrolysis of chicken manure product yields (wt% dry) in catalyticand non-catalytic

process
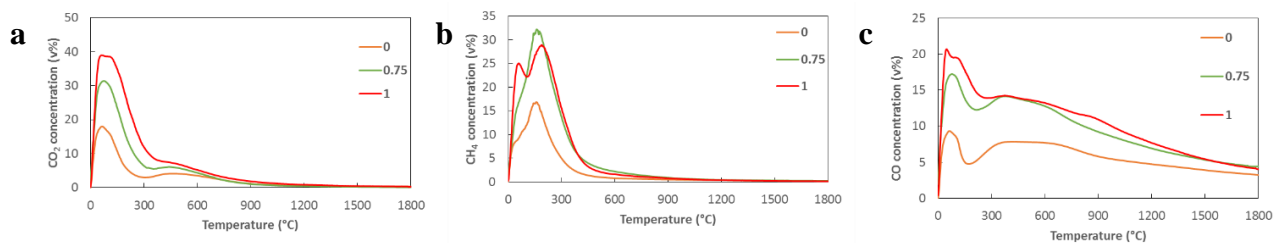
Figure 4-44- The effect of catalyst amount on the concentration curve of evolved gas from slow pyrolysis at 700 °C a) CO_2

b) CH_4 c) CO
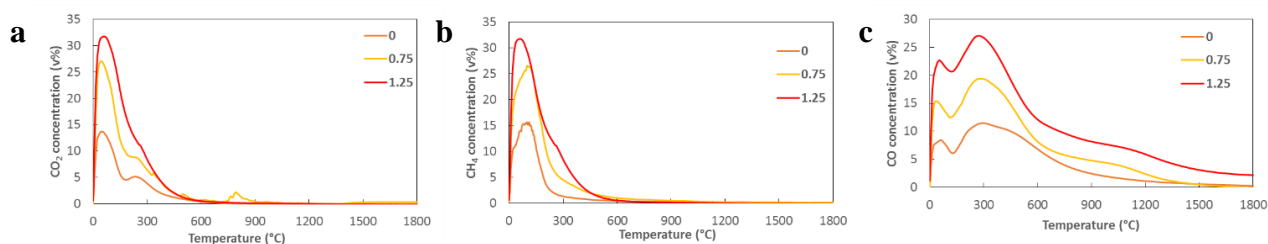
Figure 4-45- The effect of catalyst amount on the concentration curve of evolved gas from slow pyrolysis at 800 °C a) CO_2

b) CH_4 c)CO

158
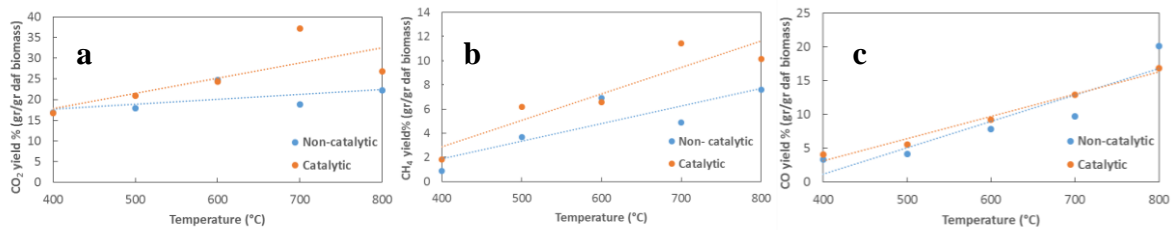
Figure 4-46- Comparison of the yields of gaseous compounds for catalytic (catalyst/biomass=0.75) and non-catalytic processes a) CO_2 b) CH_4 c) CO

In the work of H. Zhang et al. (2009) comparison of non-catalytic and catalytic was performed in a fluidized bed. The biomass used was corncob and the catalyst was HZSM-5. They have reported that, at 550 °C and catalyst/biomass=5, the yield of all evolved gases (CO_2, CO and CH_4) was increased. In the work of Adam et al., (2006) during the slow pyrolysis of spruce wood and presence of MCM catalyst, the yield of all three gases increased, in comparison to non-catalytic process. In the work of Güngör et al., (2012) slow pyrolysis of pine bark was performed in fixed bed reactor in 2 step. The catalyst to biomass ratio was very low in that work. The yield of CO and methane increased, while CO_2 yield decreased in comparison to non-catalytic process.

Figure 4- 47 compares the volumetric composition of the non-condensable gas phase obtained from non-catalytic and catalytic process. The mentioned results for catalytic process were obtained at catalyst/biomass equal to 0.75. It can be seen in the figure that, at lower temperature (<600 °C) the portion of combustibles in the gas improves, as a result of catalyst application. At higher temperature (> 600) this portion is equal in the presence and absence of the catalyst. However, the fraction of methane, which is the compound with great HHV is more in catalytic process at all temperature. Miskolczi et al. (2010) compared the catalytic and non-catalytic slow pyrolysis of refused derived fuels using ZSM-5 catalyst. They have reported the gaseous product of non-catalytic process contains more CO_2 and CO, while product of catalytic process contains mostly hydrocarbons.
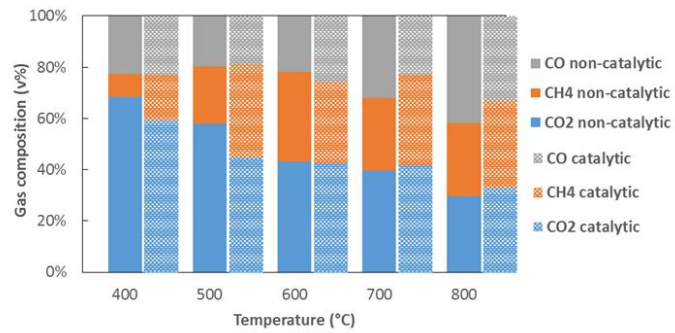
Figure 4-47- Comparison of volumetric composition of non-condensable gases in catalytic and non-catalytic process

Figure 4- 48 compares the amount of HHV of the non-condensable gases obtained in non-catalytic and catalytic process. The mentioned results for catalytic process were obtained at catalyst/biomass equal to 0.75. At lower temperatures (<600 °C) the HHV of the non-condensable gases is greater for catalytic process. The effect of catalyst on HHV becomes less at higher temperatures.
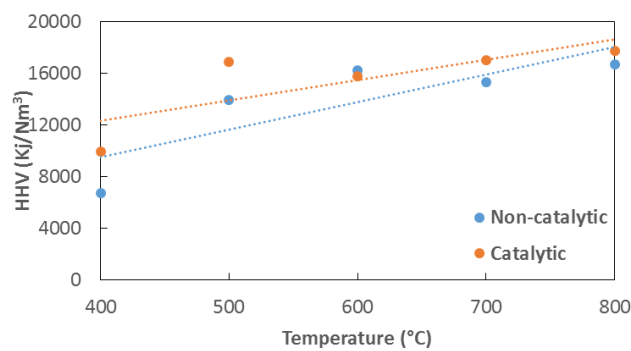
Figure 4-48- Comparison of the HHV of non-condensable gases for catalytic (catalyst/biomass=0.75) and non-catalytic
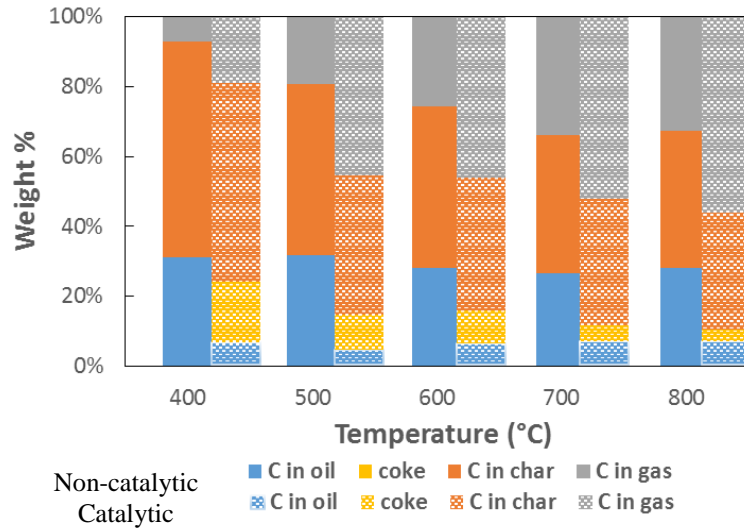
processes

Figure 4-49- Comparison of the carbon distribution among the pyrolysis products for catalytic and non-catalytic process

Figure 4- 49 compares carbon distribution among the slow pyrolysis products, for catalytic and non-catalytic process. It can be seen that, the amount of carbon transferred to biogas is much more for catalytic process, in comparison to non-catalytic process. Very low amount of carbon present in bio-oil is the result of low amount of organic bio-oil yield, since as mentioned before by addition of catalyst, the bio-oil cracks to coke and biogas and water bio-oil. Carbon distribution results can confirm the higher amount of CO_2, CH_4 and CO obtained by use of catalyst, as it was shown in Figure 4- 46.

5- Conclusion

The possible use of slow pyrolysis to convert poultry litter to product fractions that may be valorized as energy vectors was investigated. The main product streams were quantified and characterized. Production of liquid condensates, the fraction that may be upgraded to liquid fuels, is the maximum at 550°C. The main identified components of the liquid fraction were fatty acids, N-compounds, phenols and sterols, although water is also present. The char fraction has high energy content, but retains most of the sulphur originally present in the substrate and all of the ashes. A low HHV gas is also associated with the pyrolysis, and it is estimated to be energetically suitable for the self-sufficient operation of the process. The analysis of the energy transfer to the different product fractions showed that roughly a third of the potential combustion energy of the initial feedstock is transferred to the organic liquid product, while about another third is retained in the char. Altogether, the results evidence the main potentialities and critical elements in the use of the slow pyrolysis process for sanitation and waste-to-energy valorization of poultry litter waste.

The possibility of process upgrading by the use of catalyst was also investigated. The yields and composition of the produced gas were obtained, and the results were compared to the non-catalytic one. By use of catalyst, the catalytic cracking of the organic bio-oil is promoted, resulting in a higher formation of char, water and gas. The yield of all measured gaseous compounds in the gas phase was increased by use of catalyst. The fraction of combustibles increases in the gas that also has a higher HHV.

References

1. Abdoulmoumine, N., Kulkarni, A., Adhikari, S., 2014. Effects of Temperature and Equivalence Ratio on Pine Syngas Primary Gases and Contaminants in a Bench-Scale Fluidized Bed Gasifier. Ind. Eng. Chem. Res. 53, 5767–5777.

2. Adam, J., Blazso, M., Meszaros, E., Stocker, M., Nilsen, M., Bouzga, A., Hustad, J., Gronli, M., Oye, G., 2005. Pyrolysis of biomass in the presence of Al-MCM-41 type catalysts. Fuel.

3. Adam, J., Antonakou, E., Lappas, A., Stöcker, M., Nilsen, M.H., Bouzga, A., Hustad, J.E., Øye, G., 2006. In situ catalytic upgrading of biomass derived fast pyrolysis vapours in a fixed bed reactor using mesoporous materials. Microporous Mesoporous Mater. 96, 93–101.

4. Agblevor, F.A., Beis, S., Kim, S.S., Tarrant, R., Mante, N.O., 2010. Biocrude oils from the fast pyrolysis of poultry litter and hardwood. Waste Manag. 30, 298–307.

5. Ahn, H.K., Sauer, T.J., Richard, T.L., Glanville, T.D., 2009. Determination of thermal properties of composting bulking materials. Bioresour. Technol. 100, 3974–3981.

6. Aho, A., Kumar, N., Lashkul, A.V., Eränen, K., Ziolek, M., Decyk, P., Salmi, T., Holmbom, B., Hupa, M., Murzin, D.Y., 2010. Catalytic upgrading of woody biomass derived pyrolysis vapours over iron modified zeolites in a dual-fluidized bed reactor. Fuel 89, 1992–2000.

7. Amutio, M., Lopez, G., Alvarez, J., Moreira, R., Duarte, G., Nunes, J., Olazar, M., Bilbao, J., 2013. Flash pyrolysis of forestry residues from the Portuguese Central Inland Region within the framework of the BioREFINA-Ter project. Bioresour. Technol. 129, 512–518.

8. Antal, M.J.J., Varhegyi, G., 1995. Cellulose pyrolysis kinetics: the current state of knowledge, Ind. Eng. Chem. Res. 34(3) 703-717.

9. Asadullah, M., Ito, S., Kunimori, K., Tomishige, K., 2002. Highly Efficient Catalyst for Biomass Gasification to Produce Hydrogen and Syngas at Low Temperature, in: ABSTRACTS OF PAPERS OF THE AMERICAN CHEMICAL SOCIETY. AMER CHEMICAL SOC 1155 16TH ST, NW, WASHINGTON, DC 20036 USA, pp. U580–U580.

10. Association of Poultry Processors and Poultry Trade in the EU Countries – AS, 2015 Annual Report.
Retrieved from:
http://www.avecpoultry.eu/system/files/archive/newstructure/avec/Annual_Report/2015/Annual%20Report%202015.pdf Last access: 1/1/2016.

11. ASTM International, Standard test method for ash in biomass - E1755(2015), ASTM International, West Conshohocken, PA, USA, 2015.

12. Bak, J., Larsen, A., 1995. Quantitative gas analysis with FT-IR: a method for CO calibration using partial least-squares with linearized data Appl. Spectrosc. 49, 437-443.

13. Bakhshi, N.N., Dalai, A. K., Thring, R. W., 'Biomass char and lignin: potential application ' Chemistry of renewable fuels chemicals. 1999. ANAHEIM 44 (2).

14. Baniasadi, M., Mousavi, S.M., Zilouei, Shojaosadati, S.A., Rastegar, S.O. 2014. Statistical Evaluation and prcess optimization of biotreatment of polycyclic aromatic hydrocarbons in a bioreactor. Env. Eng. Manag. J. In press: http://omicron.ch.tuiasi.ro/EEMJ/pdfs/accepted/510_715_Baniasadi_13.pdf

15. Basile, L., Tugnoli, A., Stramigioli, C., Cozzani, V., 2014. Influence of pressure on the heat of biomass pyrolysis. Fuel 137, 277–284.

16. Basu, P., 2013. Biomass gasification, pyrolysis and torrefaction practical design and theory. Academic Press, Amsterdam.

17. Behainne, J.J.R., Martinez, J.D., 2014. Performance analysis of an air-blown pilot fluidized bed gasifier for rice husk. Energy Sustain. Dev. 18, 75–82.

18. Blamey, J., Anthony, E.J., Wang, J., Fennell, P.S., 2010. The calcium looping cycle for large-scale CO2 capture. Prog. Energy Combust. Sci. 36, 260–279.

19. Brennan, L., Owende, P., 2010. Biofuels from microalgae—A review of technologies for production, processing, and extractions of biofuels and co-products. Renew. Sustain. Energy Rev. 14, 557–577.

20. Brown, J.N., 2009. Development of a lab-scale auger reactor for biomass fast pyrolysis and process optimization using response surface methodology.

21. Bulushev, D.A., Ross, J.R.H., 2011. Catalysis for conversion of biomass to fuels via pyrolysis and gasification: A review. Catal. Today 171, 1–13.

22. Butler, E., Devlin, G., Meier, D., McDonnell, K., 2011. A review of recent laboratory research and commercial developments in fast pyrolysis and upgrading. Renew. Sustain. Energy Rev. 15, 4171–4186.

23. Campanella, A., Harold, M.P., 2012. Fast pyrolysis of microalgae in a falling solids reactor: Effects of process variables and zeolite catalysts. Biomass Bioenergy 46, 218–232.

24. Capareda, S.C., 2011. Biomass Energy Conversion. Tex. AM Univ. USA Www Intechopen Com.

25. CEN, European Standard EN 15148:2009 Solid biofuels — Determination of the content of volatile matter, CEN, Brussels, 2009.

26. Choi, H.S., Meier, D., 2013. Fast pyrolysis of Kraft lignin—Vapor cracking over various fixed-bed catalysts. J. Anal. Appl. Pyrolysis 100, 207–212.

27. Channiwala, S.A., Parikh, P.P., 2002, A unified correlation for estimating HHV of solid, liquid and gaseous fuels, Fuel 81(8) 1051–1063.

28. Conti, R., Rombolà, A.G., Modelli, A., Torri, C., Fabbri, D., 2014. Evaluation of the thermal and environmental stability of switchgrass biochars by Py-GC-MS, Anal. Appl. Pyrol. 110(1) 239-247.

29. Cordella, M., Torri, C., Adamiano, A., Fabbri, D., Barontini, F., Cozzani, V., 2012. Bio-oils from biomass slow pyrolysis: A chemical and toxicological screening. J. Hazard. Mater. 231-232, 26–35.

30. Cozzani, V., Nicolella, C., Petarca, L., Rovatti, M., Tognotti, L., 1995. A fundamental study on conventional pyrolysis of a refuse-derived fuel. Ind. Eng. Chem. Res. 34, 2006–2020.

31. Czernik, S., Bridgwater, A.V., 2004, Overview of applications of biomass fast pyrolysis oil, Energ. Fuels 18(2), 590-598.

32. Dahalquist, E., 2013. Technologies for Converting Biomass to Useful Energy Combustion, gasification, pyrolysis, torrefaction and fermentation.CRC Press, New York.

33. Dalluge, D.L., Daugaard, T., Johnston, P., Kuzhiyil, N., Wright, M.M., Brown, R.C., 2014. Continuous production of sugars from pyrolysis of acid-infused lignocellulosic biomass, Green Chem. 16(9), 4144-4155.

34. Das, D.D., Schnitzer, M.I., Monreal, C.M., Mayer, P., 2009. Chemical composition of acid–base fractions separated from biooil derived by fast pyrolysis of chicken manure. Bioresour. Technol. 100, 6524–6532.

35. Dejong, W., Dinola, G., Venneker, B., Spliethoff, H., Wojtowicz, M., 2007. TG-FTIR pyrolysis of coal and secondary biomass fuels: Determination of pyrolysis kinetic parameters for main species and NOx precursors. Fuel 86, 2367–2376.

36. Design-Expert® Software Version 9 Free Trial - Software [WWW Document], n.d. URL http://www.statease.com/software/dx9-trial.html (accessed 12.18.15).

37. Differential Scanning Calorimetry [WWW Document], n.d. URL http://pslc.ws/macrog/dsc.htm (accessed 12.18.15).

38. European commission directorate general environment, Inventory of manure processing activities in Europe. Retrieved from http://agro-technology-atlas.eu/docs/21010_technical_report_I_inventory.pdf. Last access: 1/1/2016.

39. Eurostat statistic Explained, RENEWABLES-PRIMARY-PRODUCTION-2013. Retrieved from http://ec.europa.eu/eurostat/statistics-explained/index.php/File:RENEWABLES-PRIMARY-PRODUCTION-2013.png#file. Last access: 1/1/2016.

40. Fu, P., Xiang, J., Sun, L., Yang, T., Zhang, A., Wang, Y., Chen, G., 2009. Effects of pyrolysis temperature on characteristics of porosity in biomass chars, in: P. Kellenberger, Proceedings of the 2009 International Conference on Energy and Environment Technology (ICEET '09), The Institute of Electrical and Electronics Engineers, Danvers, MA, USA, 2009, pp. 109–112. Avaliable at: http://dx.doi.org/10.1109/ICEET.2009.33 (Last accessed 01/09/2015).

41. Gauthier, G., Melkior, T., Grateau, M., Thiery, S., Salvador, S., 2013. Pyrolysis of centimetre-scale wood particles: new experimental developments and results, J. Anal. Appl. Pyrol. 104, 521-530.

42. Giuntoli, J., de Jong, W., Arvelakis, S., Spliethoff, H., Verkooijen, A.H.M., 2009. Quantitative and kinetic TG-FTIR study of biomass residue pyrolysis: Dry distiller's grains with solubles (DDGS) and chicken manure. J. Anal. Appl. Pyrolysis 85, 301–312.

43. Glossary - Biomass Energy Data Book [WWW Document], n.d. URL http://cta.ornl.gov/bedb/glossary.shtml (accessed 12.30.15).

44. Grierson, S., Strezov, V., Ellem, G., Mcgregor, R., Herbertson, J., 2009. Thermal characterisation of microalgae under slow pyrolysis conditions. J. Anal. Appl. Pyrolysis 85, 118–123.

45. Guar, S., Reed, T.B., 1995. An atlas of thermal data for biomass and other fuels. NREL.

46. Güngör, A., Önenç, S., Uçar, S., Yanik, J., 2012. Comparison between the "one-step" and "two-step" catalytic pyrolysis of pine bark. J. Anal. Appl. Pyrolysis 97, 39–48. doi:10.1016/j.jaap.2012.06.011

47. Heikkinen, J.M., Hordijk, J.C., Dejong, W., Spliethoff, H., 2004. Thermogravimetry as a tool to classify waste components to be used for energy generation, J. Anal. Appl. Pyrol. 71(2), 883-900.

48. Huber, G.W., Iborra, S., Corma, A., 2006. Synthesis of Transportation Fuels from Biomass: Chemistry, Catalysts, and Engineering. Chem. Rev. 106, 4044–4098.

49. Iliopoulou, E.F., Antonakou, E.V., Karakoulia, S.A., Vasalos, I.A., Lappas, A.A., Triantafyllidis, K.S., 2007. Catalytic conversion of biomass pyrolysis products by mesoporous materials: Effect of steam stability and acidity of Al-MCM-41 catalysts. Chem. Eng. J. 134, 51–57.

50. International biochar initiative, Profile: Using Biochar for Water Filtration in Rural South East Asia. Retrieved from: http://www.biochar-international.org/profile/water_filtration. Last access: 1/1/2016.

51. Inthapanya, s., Preston, T. R., Leng, R. A., 2012. 'Biochar increase biogas production in a batch digester charged with cattel manure' Livestock research for rural development 24 (12).

52. Isahak, W.N.R.W., Hisham, M.W.M., Yarmo, M.A., Yun Hin, T., 2012. A review on bio-oil production from biomass by using pyrolysis method. Renew. Sustain. Energy Rev. 16, 5910–5923.

53. ISO, International Standard ISO 17246:2010 Coal - Proximate analysis, 2nd ed., ISO, Geneva, 2010.

54. Ithaka-Journal for ecology, winegrowing and climate farming, The use of biochar in cattle farming. Retrieved from: http://www.ithaka-journal.net/pflanzenkohle-in-der-rinderhaltung?lang=en. Last access: 1/1/2016.

55. Ithaka institute, Biochar as a building materials. Retrieved from http://www.ithaka-institut.org/en/ct/95-Biochar-Feed-Additives. Last access: 30/1/2015.

56. Jena, U., Das, K.C., 2011. Comparative Evaluation of Thermochemical Liquefaction and Pyrolysis for Bio-Oil Production from Microalgae. Energy Fuels 25, 5472–5482.

57. Joseph, P., Tretsiakova-McNally, S., McKenna, S., 2012. Characterization of cellulosic wastes and gasification products from chicken farms. Waste Manag. 32, 701–709.

58. Kazi, Z.H., Schnitzer, M.I., Monreal, C.M., Mayer, P., 2010. Separation and identification of heterocyclic nitrogen compounds in biooil derived by fast pyrolysis of chicken manure. J. Environ. Sci. Health Part B 46, 51–61.

59. Kelleher, B.P., Leahy, J.J., Henihan, A.M., O'dwyer, T.F., Sutton, D., Leahy, M.J., 2002. Advances in poultry litter disposal technology–a review. Bioresour. Technol. 83, 27–36.

60. Kim, S.-S., Agblevor, F.A., Lim, J., 2009. Fast pyrolysis of chicken litter and turkey litter in a fluidized bed reactor. J. Ind. Eng. Chem. 15, 247–252.

61. Koufopanos, C.A., Maschio, G., Lucchesi, A., 1989. Kinetic modelling of the pyrolysis of biomass and biomass components, Can. J. Chem. Eng. 67, 5-84.

62. Lima, I.M., Boateng, A.A., Klasson, K.T., 2009. Pyrolysis of Broiler Manure: Char and Product Gas Characterization [†] [†] The mention of firm names or trade products does not imply that they are endorsed or recommended by the U.S. Department of Agriculture over other firms or similar products not mentioned. Ind. Eng. Chem. Res. 48, 1292–1297.

63. Lu, Q., Zhang, Y., Tang, Z., Li, W., Zhu, X., 2010a. Catalytic upgrading of biomass fast pyrolysis vapors with titania and zirconia/titania based catalysts. Fuel 89, 2096–2103.

64. Lu, Q., Zhang, Z.-F., Dong, C.-Q., Zhu, X.-F., 2010b. Catalytic Upgrading of Biomass Fast Pyrolysis Vapors with Nano Metal Oxides: An Analytical Py-GC/MS Study. Energies 3, 1805–1820.

65. Ma, B., Agblevor, F.A., Polarity-based separation and chemical characterization of fast pyrolysis bio-oil from poultry litter, Biomass Bioenerg. 64 (2014) 337-347.

66. Mahmood, A.S.N., Brammer, J.G., Hornung, A., Steele, A., Poulston, S., 2013. The intermediate pyrolysis and catalytic steam reforming of Brewers spent grain. J. Anal. Appl. Pyrolysis 103, 328–342.

67. Mante, O.D., Agblevor, F.A., 2010. Influence of pine wood shavings on the pyrolysis of poultry litter. Waste Manag. 30, 2537–2547.

68. Marcilla, A., Gómez-Siurana, A., Gomis, C., Chápuli, E., Catalá, M.C., Valdés, F.J., 2009. Characterization of microalgal species through TGA/FTIR analysis: application to nannochloropsis sp., Thermochimica Acta 484(1-2) 41-47.

69. Marshal, A.J., 2013. Commercial application of pyrolysis technology in agriculture, Retrieved from: http://www.ofa.on.ca/uploads/userfiles/files/pyrolysis%20report%20final.pdf.

70. Miao, X., Wu, Q., Yang, C., 2004. Fast pyrolysis of microalgae to produce renewable fuels. J. Anal. Appl. Pyrolysis 71, 855–863.

71. Miskolczi, N., Buyong, F., Angyal, A., Williams, P.T., Bartha, L., 2010. Two stages catalytic pyrolysis of refuse derived fuel: Production of biofuel via syncrude. Bioresour. Technol. 101, 8881–8890.

72. Moloodi, S., Tzanetakis, T., Nguyen, B., Zarghami-Tehran, M., Khan, U., Thomson, M.J., 2012, Fuel property effects on the combustion performance and emissions of hardwood-derived fast pyrolysis liquid-ethanol blends in a swirl burner, Energ. Fuels 26(9), 5452-5461.

73. Monreal, C.M., Schnitzer, M., 2011. Production of a refined biooil derived by fast pyrolysis of chicken manure with chemical and physical characteristics close to those of fossil fuels. J. Environ. Sci. Health Part B 46, 630–637.

74. Mortensen, P.M., Grunwaldt, J.-D., Jensen, P.A., Knudsen, K.G., Jensen, A.D., 2011. A review of catalytic upgrading of bio-oil to engine fuels. Appl. Catal. Gen. 407, 1–19.

75. Ngo, T.-A., Kim, J., Kim, S.-S., 2013. Fast pyrolysis of palm kernel cake using a fluidized bed reactor: Design of experiment and characteristics of bio-oil. J. Ind. Eng. Chem. 19, 137–143.

76. Nguyen, T.S., Zabeti, M., Lefferts, L., Brem, G., Seshan, K., 2013. Catalytic upgrading of biomass pyrolysis vapours using faujasite zeolite catalysts. Biomass Bioenergy 48, 100–110.

77. Nordgreen, T., Liliedahl, T., Sjostrom, K., 2006. Metallic iron as a tar breakdown catalyst related to atmospheric, fluidised bed gasification of biomass. Fuel 85, 689–694.

78. Oudenhoven, S.R.G., Westerhof, R.J.M., Aldenkamp, N., Brilman, D.W.F., Kersten, S.R.A., 2013. Demineralization of wood using wood-derived acid: towards a selective pyrolysis process for fuel and chemicals production, J. Anal. Appl. Pyrol. 103, 112-118.

79. Pan, P., Hu, C., Yang, W., Li, Y., Dong, L., Zhu, L., Tong, D., Qing, R., Fan, Y., 2010. The direct pyrolysis and catalytic pyrolysis of Nannochloropsis sp. residue for renewable bio-oils. Bioresour. Technol. 101, 4593–4599.

80. Patwardhan, P.R., 2010. Understanding the product distribution from biomass fast pyrolysis.

81. Perry, R.H., Green, D.W., Maloney, J.O. (Eds.), 1997. Perry's chemical engineers' handbook, 7th ed. ed. McGraw-Hill, New York.

82. Prayogo, C., Jones, J.E., Baeyens, J., 2014. Impact of biochar on mineralisation of C and N from soil and willow litter and its relationship with microbial community biomass and structure. Biol. Fert. Soils. 50(4), 695-702.

83. Pu, G., Zhou, H., Hao, G., 2013. Study on pine biomass air and oxygen/steam gasification in the fixed bed gasifier. Int. J. Hydrog. Energy 38, 15757–15763.

84. Pütün, E., Uzun, B.B., Pütün, A.E., 2009. Rapid Pyrolysis of Olive Residue. 2. Effect of Catalytic Upgrading of Pyrolysis Vapors in a Two-Stage Fixed-Bed Reactor. Energy Fuels 23, 2248–2258.

85. Quirk, R.G., Van Zwieten, L., Kimber, S., Downie, A., Morris, S., Rust, J., 2012. Utilization of Biochar in Sugarcane and Sugar-Industry Management. Sugar Tech 14, 321–326.

86. Radlein, D., Piskorz, J., Majerski, P., 1997, Method of producing slow- release nitrogenous organic fertilizer from biomass, U.S. Patent 5,676,727.

87. Rath, J., Wolfinger, M., Steiner, G., Krammer, G., Barontini, F., Cozzani, V., 2002. Heat of wood pyrolysis. Fuel. 82, 81–91

88. Ren, X., Gou, J., Wang, W., Li, Q., Chang, J., Li, B., 2013. Optimization of bark fast pyrolysis for production of phenol rich bio-oil. Bioresour. 8(4), 6481-6492.

89. Renewable Energy Policy Network for the21 century, Renewables 2015 Global Status Report. Retrieved from http://www.ren21.net/wp-content/uploads/2015/07/GSR2015_KeyFindings_lowres.pdf. Last access: 1/1/2016.

90. Rennard, D., French, R., Czernik, S., Josephson, T., Schmidt, L., 2010. Production of synthesis gas by partial oxidation and steam reforming of biomass pyrolysis oils. Int. J. Hydrog. Energy 35, 4048–4059.

91. Rezaiyan, J., Cheremisinoff, N.P., 2005. Gasification technologies: a primer for engineers and scientists. CRC press.

92. Ringer, M., Putsche, V., Scahill, J., 2006. Large-Scale Pyrolysis Oil. Assessment.

93. Rizzo, A.M., Prussi, M., Bettucci, L., Libelli, I.M., Chiaramonti, D., 2013. Characterization of microalga Chlorella as a fuel and its thermogravimetric behavior. Appl. Energy 102, 24–31.

94. Ro, K.S., Cantrell, K.B., Hunt, P.G., 2010. High-Temperature Pyrolysis of Blended Animal Manures for Producing Renewable Energy and Value-Added Biochar. Ind. Eng. Chem. Res. 49, 10125–10131.

95. Sadaka, S. Gasification, Producer Gas and Syngas. Agriculture and natural resources. Reterived from: https://www.uaex.edu/publications/PDF/FSA-1051.pdf.

96. San Miguel, 2012. New Advances in the Fast Pyrolysis of Biomass. J. Biobased Mater. Bioenergy 6.

97. Schnitzer, M.I., Monreal, C.M., Facey, G.A., Fransham, P.B., 2007. The conversion of chicken manure to biooil by fast pyrolysis I. Analyses of chicken manure, biooils and char by [13] C and [1] H NMR and FTIR spectrophotometry. J. Environ. Sci. Health Part B 42, 71–77.

98. Sanchez-Silva, L., López-González, D., Villaseñor, J., Sánchez, P., Valverde, J.L., 2012. Thermogravimetric–mass spectrometric analysis of lignocellulosic and marine biomass pyrolysis. Bioresour. Technol. 109, 163–172.

99. Senneca, O., Salatino, P., Masi, S., 1998, Microstructural changes and loss of gasification reactivity of chars upon heat treatment, Fuel 77(13) 1483-1493.

100. Shackley, S., Sohi, S., Brownsort, P., Carter, S., Cook, J., Cunningham, C., Gaunt, J., Hammond, J., Ibarrola, R., Mašek, O., 2010. An assessment of the benefits and issues associated with the application of biochar to soil. Dep. Environ. Food Rural Aff. UK Gov. Lond.

101. Sharma, A.M., Kumar, A., Madihally, S., Whiteley, J.R., Huhnke, R.L., 2014. Prediction of biomass-generated syngas using extents of major reactions in a continuous stirred-tank reactor. Energy 72, 222–232.

102. Sheth, A.C., Bagchi, B., 2005. Investigation of Nitrogen-Bearing Species in Catalytic Steam Gasification of Poultry Litter. J. Air Waste Manag. Assoc. 55, 619–628.

103. Skoulou, V., Koufodimos, G., Samaras, Z., Zabaniotou, A., 2008. Low temperature gasification of olive kernels in a 5-kW fluidized bed reactor for H2-rich producer gas. Int. J. Hydrog. Energy 33, 6515–6524.

104. Skoulou, V., Zabaniotou, A., 2012. Fe catalysis for lignocellulosic biomass conversion to fuels and materials via thermochemical processes. Catal. Today 196, 56–66.

105. Sohi, S.P., Krull, E., Lopez-Capel, E., Bol, R., 2010. A review of biochar and its use and function in soil. Adv. Agron. 105, 47–82.

106. Srinivas, S.T., Dalai, A.K., Bakhshi, N.N., 2000. Thermal and catalytic upgrading of a biomass-derived oil in a dual reaction system. Can. J. Chem. Eng. 78, 343–354.

107. Sutton, D., Kelleher, B., Ross, J.R., 2001. Review of literature on catalysts for biomass gasification. Fuel Process. Technol. 73, 155–173.

108. Tang, J., Zhu, W., Kookana, R., Katayama, A., 2013. Characteristics of biochar and its application in remediation of contaminated soil. J. Biosci. Bioeng. 116, 653–659.

109. Taufiq-Yap, Y.H., Nur-Faizal, A.R., Sivasangar, S., Hussein, M.Z., Aishah, A., 2014. Modification of Malaysian dolomite using mechanochemical treatment via different media for oil palm fronds gasification: Potential of Malaysian dolomite as a gasification catalysts. Int. J. Energy Res. 38, 1008–1015.

110. Torri, C., Fabbri, D., 2014, Biochar enables anaerobic digestion of aqueous phase from intermediate pyrolysis of biomass, Bioresource Technol. 172, 335-341.

111. Tzanetakis, T., Farra, N., Moloodi, S., Lamont, W., McGrath, A., Thomson, M.J., 2010. Spray combustion characteristics and gaseous emissions of a wood derived fast pyrolysis liquid-ethanol blend in a pilot stabilized swirl burner, Energ. Fuels 24(10) 5331-5348.

112. United State Environmental Protection Agency, Global Greenhouse Gas Emissions Data. Retrieved from http://www3.epa.gov/climatechange/ghgemissions/global.html. Last access: 1/1/2016.

113. United State Department of Energy, 2014 Renewable Energy DataBook. Retrieved from http://www.nrel.gov/docs/fy16osti/64720.pdf. Last access: 1/1/2016.

114. United State Environmental Protection Agency, Global Greenhouse Gas Emissions Data. Retrieved from http://www3.epa.gov/climatechange/ghgemissions/global.html. Last access: 1/1/2016.

115. Van Alfen, N., 2014. Encyclopedia of agriculture and food systems. Academic Press, Amsterdam.

116. van Rossum, G., Kersten, S.R.A., van Swaaij, W.P.M., 2007. Catalytic and Noncatalytic Gasification of Pyrolysis Oil. Ind. Eng. Chem. Res. 46, 3959–3967.

117. Wang, P., Zhan, S., Yu, H., Xue, X., Hong, N., 2010. The effects of temperature and catalysts on the pyrolysis of industrial wastes (herb residue). Bioresour. Technol. 101, 3236–3241.

118. Wongsiriamnuay, T., Kannang, N., Tippayawong, N., 2013. Effect of Operating Conditions on Catalytic Gasification of Bamboo in a Fluidized Bed. Int. J. Chem. Eng. 2013, 1–9. doi:10.1155/2013/297941

119. Wright, L., Boundy, B., Perlack, B., Davis, S., Saulsbury, B., 2006. Biomass Energy Data Book, Volume 1.

120. Wu, C., Huang, Q., Sui, M., Yan, Y., Wang, F., 2008. Hydrogen production via catalytic steam reforming of fast pyrolysis bio-oil in a two-stage fixed bed reactor system. Fuel Process. Technol. 89, 1306–1316.

121. Wu, C., Wang, Z., Dupont, V., Huang, J., Williams, P.T., 2013. Nickel-catalysed pyrolysis/gasification of biomass components. J. Anal. Appl. Pyrolysis 99, 143–148.

122. Xiao, R., Yang, W., 2013. Influence of temperature on organic structure of biomass pyrolysis products. Renew. Energy 50, 136–141.

123. Xie, Q., Kong, S., Liu, Y., Zeng, H., 2012. Syngas production by two-stage method of biomass catalytic pyrolysis and gasification. Bioresour. Technol. 110, 603–609.

124. Yang, H., Yan, R., Chen, H., Lee, D.H., Zheng, C., 2007. Characteristics of hemicellulose, cellulose and lignin pyrolysis, Fuel 86(12–13) 1781-1788.

125. Zhang, H., Xiao, R., Huang, H., Xiao, G., 2009. Comparison of non-catalytic and catalytic fast pyrolysis of corncob in a fluidized bed reactor. Bioresour. Technol. 100, 1428–1434.

126. Zhang, S.-Y., Hong, R.-Y., Cao, J.-P., Takarada, T., 2009. Influence of manure types and pyrolysis conditions on the oxidation behavior of manure char. Bioresour. Technol. 100, 4278–4283.

127. Zhang, S.-Y., Cao, J.-P., Takarada, T., 2010. Effect of pretreatment with different washing methods on the reactivity of manure char. Bioresour. Technol. 101, 6130–6135.

128. Zhang, S.-Y., Wang, J., Cao, J.-P., Takarada, T., 2011. H2 production from fowl manure by low temperature catalytic gasification. Bioresour. Technol. 102, 7561–7566.

129. Zhang, Z., Wang, Q., Tripathi, P., Pittman Jr, C.U., 2011. Catalytic upgrading of bio-oil using 1-octene and 1-butanol over sulfonic acid resin catalysts. Green Chem. 13, 940.

Appendix

APP1- Proximate analysis calculations

For obtaining the proximate analysis values the TGA experiment were carried out at atmospheric pressure, with a flow rate of 60 ml/min of nitrogen purge gas applied to 2-3 mg of chicken manure. In the furnace, the samples were heated up to 105 °C with a rate of 10 °C/min, this temperature was hold constant for 10 minutes in order to be completely dry. Temperature increase at 10 °C/min was continued up to 800 °C followed by an isotherm of 10 minutes. In the next step the purge gas was switched to air (60 ml/min inlet flow), and kept for 10 more minutes so that the combustible fraction can be burned.

The amount of moisture in sample was calculated by Equation APP-1 in which w_0 and w_d refer to initial (fresh) and dry weight percent respectively and %Moisture is the moisture percentage in sample.

$$\%Moisture = \frac{w_0 - w_d}{w_0} \qquad \qquad \text{Equation APP-1}$$

While the amount of w_d used in above equation comes from Figure APP- 1and w_0 is equal to 1 according to definition.
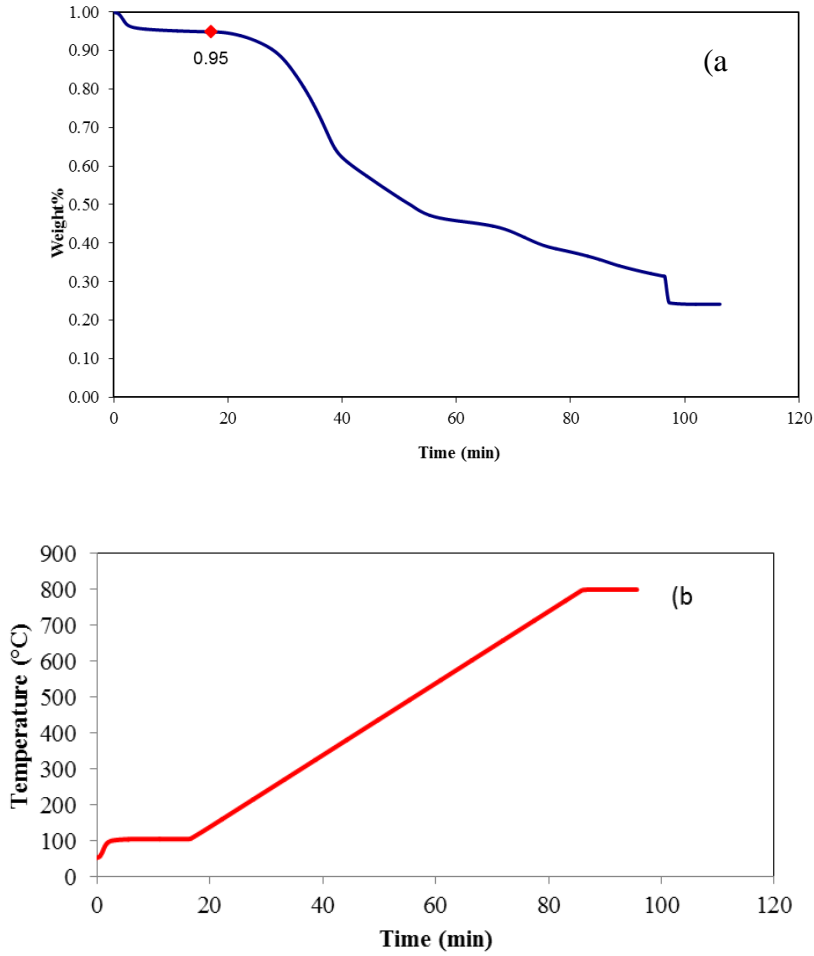
Figure APP- 1- TGA curve obtained from fresh chicken manure using nitrogen indicating the amount of moisture a)

Weight % b) Temperature over time

Knowing the moisture content of the sample, the TGA results can be reported on a dry basis (Figure APP-2). The data in this graph were rearranged with Equation APP-2:

$$w_{x,d} = \frac{w_x}{w_{0,d}}$$
Equation APP-2

In which $w_{x,d}$ refers to moisture free weight at each time, w_x are the recorded data for fresh biomass at different time and $w_{0,d}$ refer to initial weight in dry basis.

The ash content is then equal to the weight of the residue at the end of the test (after combustion), as it is indicated in Figure APP- 2 by w_f symbol.

The volatile fraction is the weight percentage change during thermal degradation up to the final isotherm in nitrogen flow (right before the change of purge gas) and is expressed by EquationAPP-3.

In this equation w_v refers to weight% at the end of isothermal condition at 800 °C, before switching to air, as indicated in Figure APP- 2.

$$\%Volatile = \frac{w_{0,d} - w_v}{w_{0,d}}$$

<div style="text-align:right">Equation APP-3</div>

The fixed carbon is the amount of weight loss during combustion process on moisture free basis and is obtained by the Equation APP-4.

$$Fixed\ carbon = \frac{w_v - w_f}{w_{0,d}}$$

<div style="text-align:right">Equation APP-4</div>

All the above data were obtained from Figure APP- 2.

Knowing the moisture and ash content of the sample, the TGA results can be reported on a DAF basis as it is shown in Figure APP- 3by use of Equation APP-5:

$$w_{x,DAF} = \frac{w_{x,d} - w_f}{w_{0,d} - w_f}$$

<div style="text-align:right">Equation APP-5</div>

In which $w_{x,DAF}$ is the obtained weight% at any time on DAF basis. Figure APP- 3 also depicts the DAF TG curve of biomass.
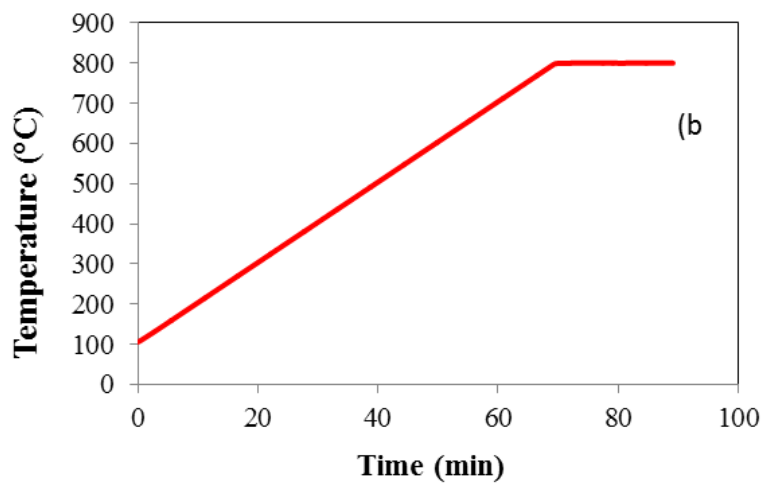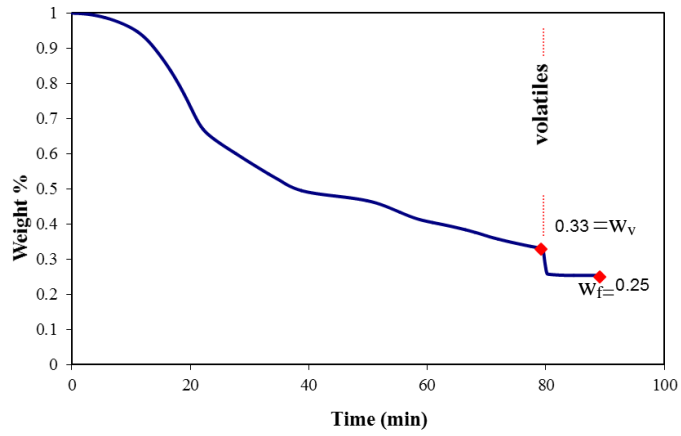
Figure APP- 2- TGA curve in dry basis of chicken manure in nitrogen atmosphere indicating the amount of ash, volatiles

and fixed carbon a) Weight % b) Temperature over time
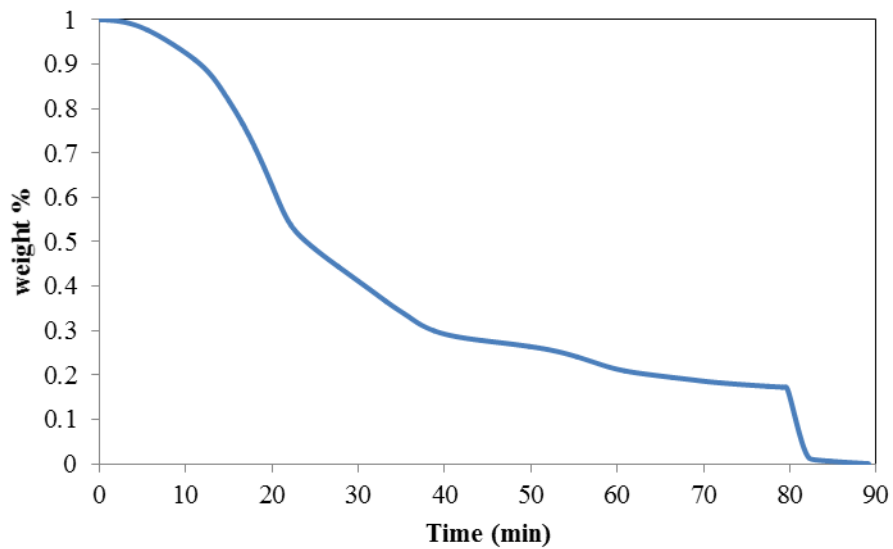
Figure APP-3- TG curve DAF of chicken manure with nitrogen

APP 2- Residence time calculation

a) *Reactor*

The residence time of the decomposition gases in the reactor was calculated from the volume between the holder and the end of the narrow outlet pipe. This volume can be estimated as combination of two contributions: the large diameter reactor tube and the narrow outlet pipe. The coloured (orange) part in Figure APP- 4 shows exactly the considered volume.
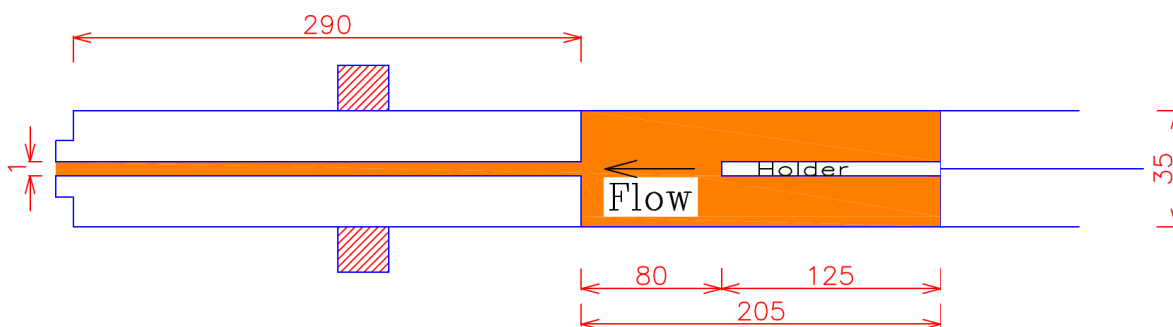
Figure APP-4- Considered reaction volume in retention time calculation

This volume was calculated to be 197 cm^3. The residence time is calculated at different temperatures and is shown in Table APP- 1considering pure nitrogen:

Table APP- 1- Reactor residence time calculation for initial flow rate of 8.5 Nl/hr

Temperature (°C)	Nitrogen density (kg/m3)	Residence time (min)
0	1.251	1.4
400	0.507	0.57
450	0.474	0.53
500	0.441	0.49
550	0.416	0.46
600	0.391	0.44
700	0.351	0.39
800	0.318	0.35

b)Traps

The traps train consist of four traps. The first two are empty, while the last two contain 40 gr of glass beads each. The calculation of traps train volume are mentioned in Table APP- 2.

The data on porosity and bulk density were calculated by pouring 20 cm^3 of beads in one graduated cylinder and then weighting them (30.55 gr). Then gradually the water was added to the cylinder up to the top of the beads by taking care the volume of added water (5.5 cm^3) which is equal to pores volume. Porosity and bulk density are then calculated using Equation APP-6 and Equation APP-7.

$$\text{Porosity} = \frac{\text{Pores volume}}{\text{Bulk beads volume}}$$
<div align="right">Equation APP-6</div>

$$\text{Bulk density} = \frac{\text{Beads bulk weight}}{\text{Beads bulk volume}}$$
<div align="right">Equation APP-7</div>

Table APP- 2- Calculations of traps volume

Volume of traps without beads			Volume of traps with beads		
Height	18.5	cm	Empty volume of trap	104.7	cm^3
Inner diameter	3	cm	Bulk beads density	1.53	gr/cm^3
Total volume of 2 empty traps	261	cm^3	Beads weight in one trap	40	gr
			Bulk beads volume	26.2	cm^3
			Beads porosity	0.275	
			Porous volume	7.34	cm^3
			Total volume of 2 traps containing beads	224	cm^3
Total volume of 4 traps			*485*		*cm^3*

The residence time calculation for the traps is shown inTable APP- 3, considering the approximate amount of beads (80 gr) inside the reactor and neglecting traps connections volume.

The temperature in the ice bath was measured by K type thermocouple and was -4 °C on average. At this temperature, the nitrogen density is equal to 1.271 kg/m^3.

Table APP- 3- Traps residence time calculations considering the temperature (-4 °C)

Flow rate	8.5	Nl/hr
Density at -4 °C	1.271	kg/m^3
Residence time	3.4	min

c) FTIR residence time calculation

The pipe that connected the traps to the FTIR instrument was a plastic pipe, left in the atmosphere without any isolation. Therefore, the temperature of the gas was considered to be equal to ambient temperature which was measured to be 22°C on average. The pipe length is 250 cm and the inner diameter is 4.5 mm. In addition, the gas cell volume must be considered which is 8.7 ml. The flow rate supposed to be the flow of pure nitrogen 8.5 Nl/hr. This causes 0.31 min of residence time in FTIR (Table APP- 4).

Table APP- 4- Delay time in FTIR connection pipe considering ambient temperature (22 °C)

Temperature (°C)	Nitrogen density	Calculated retention time in FTIR pipe and cell (min)
22	1.153	**0.31**

APP 3- Thermal program used in TG runs

The thermal program used in TGA runs are mentioned in Table APP- 5.

Table APP- 5- Thermal program used in TGA runs

Biomass characterization (N_2)	Biomass characterization (air)	Isotherm
Data storage On	Data storage On	Data storage On
Select gas 1	Select gas 2	Select gas 1
Equilibrate at 105°C	Equilibrate at 105 °C	Ramp 10°C/min to 105°C
Isothermal for 10min	Isothermal for 10min	Isothermal for 10.00 min
Ramp 10.00 °C/min to 800 °C	Ramp 10°C/min to 800°C	Jump to (400 *or up to 800* °C)
Isothermal for 10min	Isothermal for 10 min	Isothermal for 60 min
Select gas 2	Data storage Off	Ramp 10 °C/min to 800 °C
Isothermal for 10min		Isothermal for 1 min
Data storage Of		Select gas 2
		Isothermal for 10 min
		Data storage Off

Constant heating rate	Char characterization (air)
Data storage On	Data storage On
Select gas 1	Select gas 1
Equilibrate at 105 °C	Equilibrate at 105°C
Isothermal for 10 min	Isothermal for 10 min
Ramp (from 5-100 °C/min) to 800°C	Ramp 10°C/min to 800°C
Isothermal for 10 min	Isothermal for 10 min
Select gas 2	Select gas 2
Isothermal for 10 min	Isothermal for 10 min
Data storage Off	Data storage Off

The programs used in simulation of FBD temperature with TGA

The temperature curve obtained by Agilent was studied and tried to be reproduced by TG in order to compare the results of TG and FBR. The temperature curves depicted versus time obtained by two methods are shown in Figure APP- 5. In these graphs phase 1 refers to initial step of FBR experiment in which the reactor is being purged while the sample is in the cold zone, and phase 2 refers to reaction step when the sample is in hot zone. Agilent curves were obtained from sample temperature, meanwhile the furnace temperature raised from room temperature (22 °C) to the desired temperature

with ramp of 100 °C/ min, and then kept constant at that temperature. Table APP- 6 summarizes the different temperature program used in TG for simulating FBR conditions.
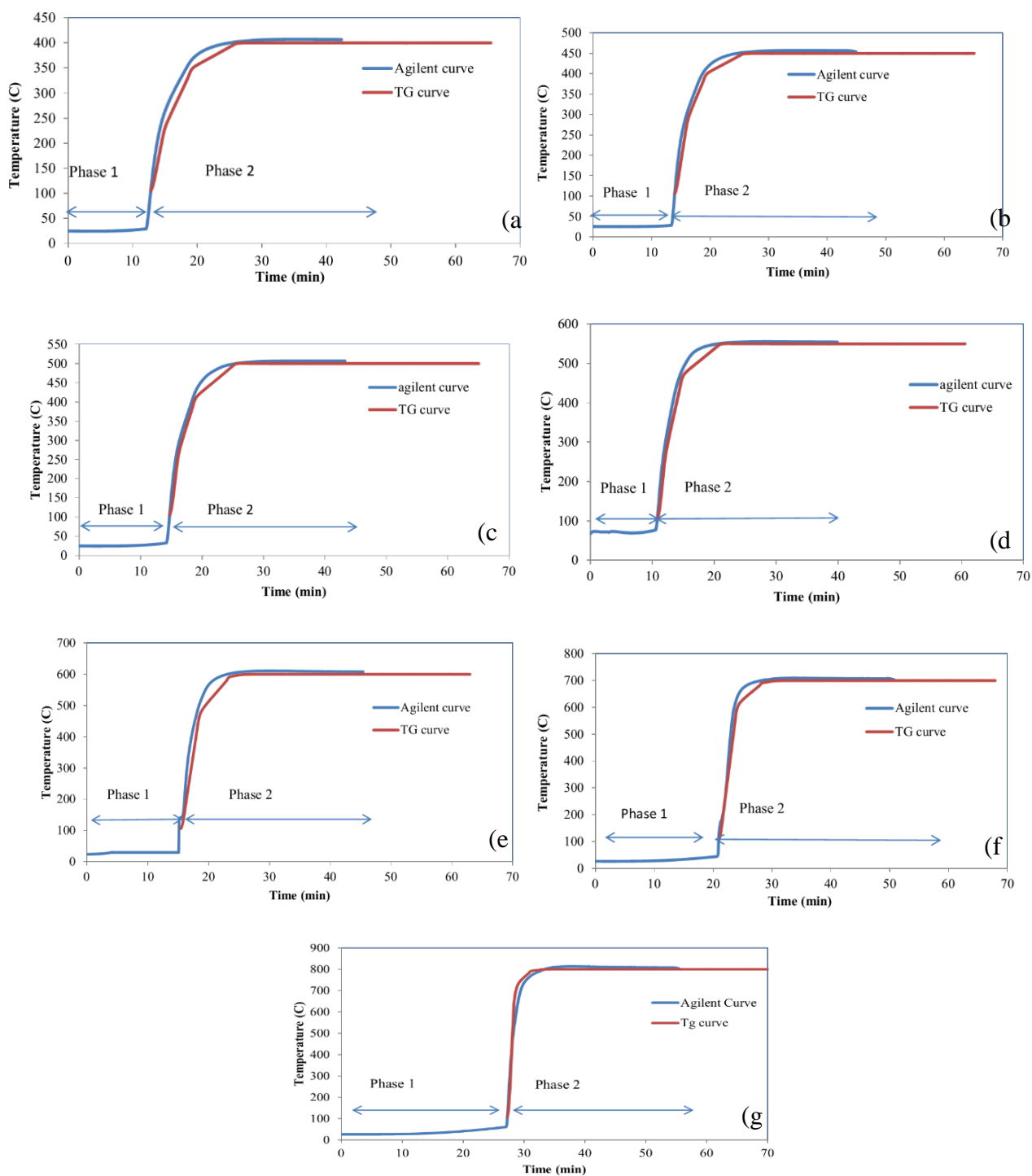

Figure APP-5- TG and FBR temperature condition of sample over time during pyrolysis at a) 400 °C b) 450°C c) 500°C d) 550°C e) 600°C f) 700°C g) 800°C

Table APP-6- Temperature program used in TG for simulating FBR condition

400 °C	450 °C	500 °C
Data storage On	Data storage On	Data storage On
Select gas 1	Select gas 1	Select gas 1
Equilibrate at 105.00 °C	Equilibrate at 105.00 °C	Equilibrate at 105.00 °C
Isothermal for 10.00 min	Isothermal for 10.00 min	Isothermal for 10.00 min
Ramp 68.30 °C/min to 240.00°C	Ramp 95.6 °C/min to 300.00 °C	Ramp 136.90 °C/min to 280.00°C
Ramp 28.10 °C/min to 350.00°C	Ramp 35.0 °C/min to 400.00 °C	Ramp 52.40 °C/min to 410.00 °C
Ramp 7.20 °C/min to 400.00 °C	Ramp 7.80 °C/min to 450.00 °C	Ramp 7.80 °C/min to 500.00 °C
Isothermal for 30.00 min	Isothermal for 30.00 min	Isothermal for 30.00 min
Ramp 10.00 °C/min to 800.00 °C	Ramp 10.00 °C/min to 800.00 °C	Ramp 10.00 °C/min to 800.00 °C
Select gas 2	Select gas 2	Select gas 2
Isothermal for 10.00 min	Isothermal for 10.00 min	Isothermal for 10.00 min
Data storage Off	Data storage Off	Data storage Off

550 °C	600 °C	700 °C
Data storage On	Data storage On	Data storage On
Select gas 1	Select gas 1	Select gas 1
Equilibrate at 105.00 °C	Equilibrate at 105.00 °C	Equilibrate at 105.00 °C
Isothermal for 10.00 min	Isothermal for 10.00 min	Isothermal for 10.00 min
Ramp 157.3 °C/min to 280.00°C	Jump to 490.00 °C	Jump to 622.00 °C
Ramp 74.0 °C/min to 470.00°C	Ramp 23.0 °C/min to 600.00 °C	Ramp 18.5 °C/min to 700.00 °C
Ramp 13.0 °C/min to 550.00 °C	Isothermal for 30.00 min	Isothermal for 30.00 min
Isothermal for 30.00 min	Ramp 10.00 °C/min to 800.00 °C	Ramp 10.00 °C/min to 800.00 °C
Ramp 10.00 °C/min to 800.00 °C	Select gas 2	Select gas 2
Select gas 2	Isothermal for 10.00 min	Isothermal for 10.00 min
Isothermal for 10.00 min	Data storage Off	Data storage Off
Data storage Off		

800 °C
Data storage On
Select gas 1
Equilibrate at 105.00 °C
Isothermal for 10.00 min
Jump to 710.00 °C
Ramp 25.0 °C/min to 800.00°C
Isothermal for 30.00 min
Select gas 2
Isothermal for 10.00 min
Data storage Off

APP 4- Dry and ash free (DAF) TG curve

Since the sample may be heterogeneous at the end of each experiment the sample was heated to 800 °C and the gas changed to oxygen. Therefore, the result of isothermal and FBR simulation TG analysis on DAF basis are depicted here in Figure APP- 6and in Figure APP- 6 for FBR simulation TGA. Graphs in DAF basis were obtained with the same method mentioned in APP1 for proximate analysis.

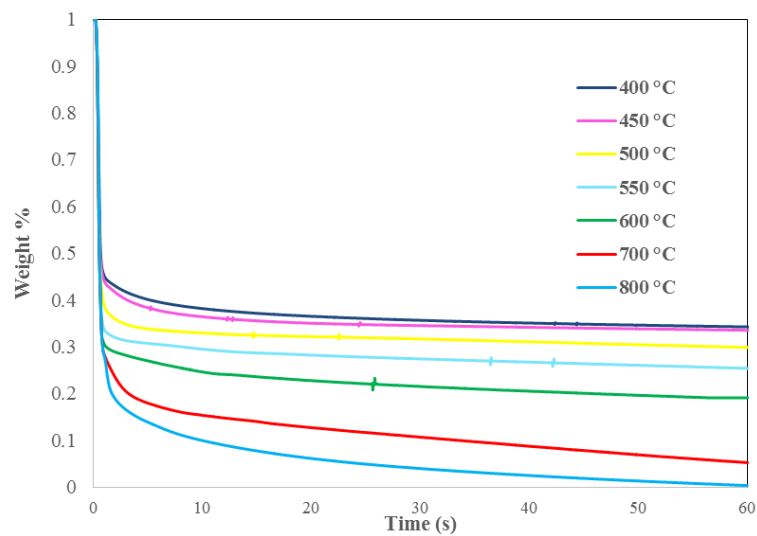

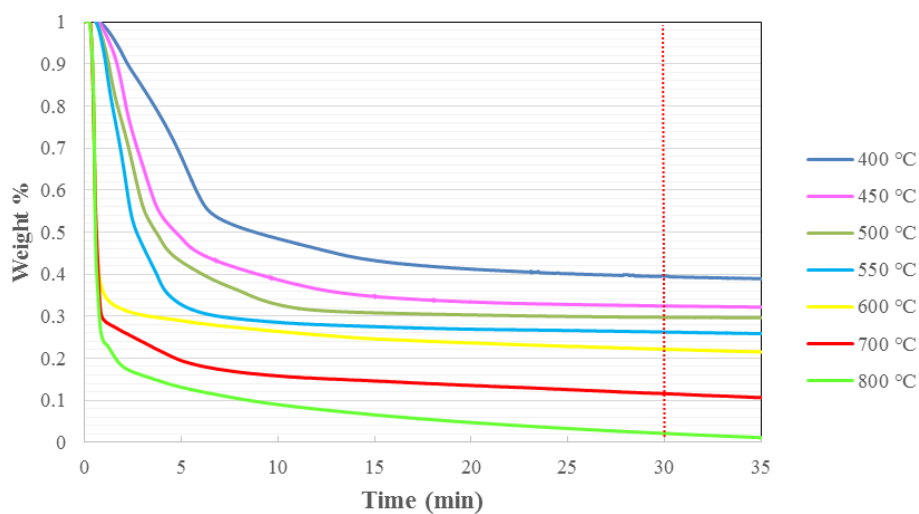*Figure APP- 6- Isothermal weight loss TG curve of chicken manure in N2 at various temperatures (DAF basis)*

Figure APP- 7- TG curves obtained at different temperature in N₂ with chicken manure at FBR thermal conditions (DAF basis)

APP 5- DSC curves

DSC temperature program is mentioned in Table APP- 7. This program was applied to both biomass and char. The DSC curve was obtained for both samples, and the final curve was obtained by subtracting the two curves.
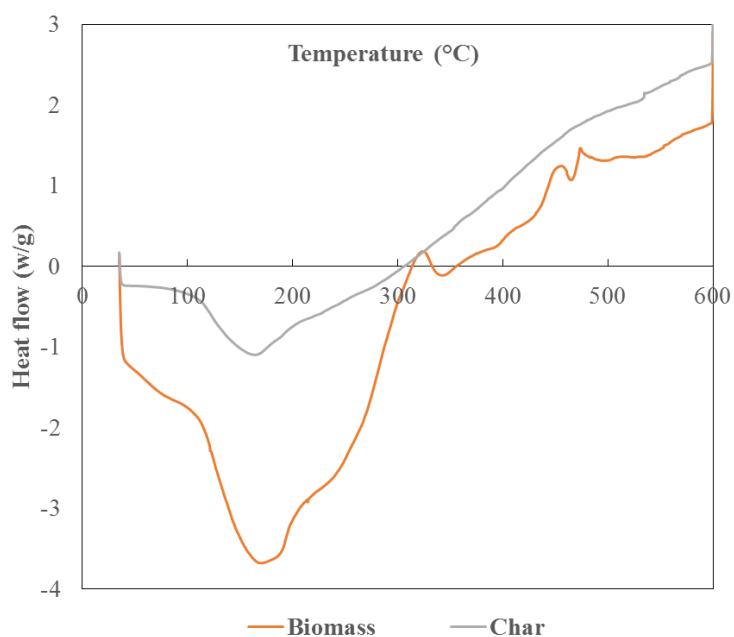
Table APP-7- DSC temperature program

Data storage On
Equilibrate at 35 °C
Isothermal for 10min
Ramp 10 °C/min to 600°C
Isothermal for 5 min
Data storage Off

Figure APP- 9 shows the obtained DSC curve of the char and sample.

Figure APP-8- DSC curve obtained for biomass and char sample

APP 6- Analytic and statistic check of non-catalytic product yields

The amounts of bio-oil in different repeated experiments were measured and they were not always consistent. Different results obtained and their statistical analyses are mentioned in Table APP- 8 and Table APP- 9. The method used here is called analysis of variance (ANOVA) which is a statistical analysis method to evaluate the interaction between the process variables and the response.

Table APP-8- Different amount of bio-oil obtained to check reliability

	400 °C	450 °C	500 °C	550 °C	600 °C	700 °C	800 °C
set 1	26.5	35.6	34.7	40.9	25.6	28.2	27.8
set 2	22.9	31.2	35.5	36.2	31.5	29.7	20.3
set 3	23.2	36.3	32.3	31.8	24.2	24.3	26.3
set 4	27.6	31.2		39.4	30.0	32.6	25.3
set 5	30.0	33.7		29.3	29.4		23.7
set 6				33.9	33.7		29.2
set 7				26.8			
set 8				37.6			
set 9				33.8			
average	26.1	33.6	34.2	35.3	29.1	28.7	25.4
STD	0.031	0.024	0.017	0.046	0.036	0.035	0.032
Number	5	5	3	9	6	4	6
STE	0.014	0.011	0.010	0.015	0.015	0.017	0.013

Total mean	30.3
Total STD	0.059
Total STE	0.009
Number	39

Source	Sum of Squares	DF	F-ratio	F-critical	Probability	
between groups	569.9	6				
within groups	395.2	31	7.45	2.6807	0.00	significant
Total	965.1	37				

The parameters in table were calculated with following equations: (j refers to different temperatures and i to different set of experiments)

$$\text{Mean} = \bar{x}_i = \frac{\sum x_i}{n} \qquad \text{(n=number of data in each group (variable for each group)} \qquad \text{Equation APP-8}$$

$$SD = \sqrt{\frac{\sum(x_i - \bar{x})^2}{n-1}} \qquad\qquad \text{Equation APP-9}$$

$$SE = \frac{SD}{\sqrt{n}} \qquad\qquad \text{Equation App-10}$$

$$\bar{\bar{x}} = \frac{\sum \bar{x}_i}{m} \qquad\qquad \text{m= number of tested temperatures=7} \qquad \text{Equation APP-11}$$

$$SD_T = \frac{\sum(\bar{x}_i - \bar{\bar{x}})^2}{m-1} \qquad\qquad \text{EquationAPP-12}$$

$$SSB = \text{sum of square between group} = \sum(\bar{x}_i - \bar{\bar{x}})^2 \times n_j \qquad \text{Equation APP-13}$$

$$SSW = \text{Sum of square within group} = \sum(x_{ij} - \bar{\bar{x}})^2 \qquad \text{Equation APP-14}$$

$$SST = SSB + SSW \qquad\qquad \text{Equation APP-15}$$

$$DFW = \text{Total number of data} - m \qquad\qquad \text{Equation APP-16}$$

$$DFB = m - 1 \qquad\qquad \text{Equation APP-17}$$

$$F - ratio = \frac{\frac{SSB}{DFB}}{\frac{SSw}{DFW}} \qquad\qquad \text{Equation APP-18}$$

Probability was red from F-table values with knowing DFW, DFB and F-ratio and was equal to 0.00.

If Probability< 0.05 the data are significant.

The results of TGA on chars of different set of experiments were compared in Table APP- 10. Suitable consistency between the char yields was observed.

Table APP-10- Different amount of char obtained to check reliability

	400 °C	450 °C	500 °C	550 °C	600 °C	700 °C	800 °C
set 1	53.3	48.4	46.7	45.1	43.6	39.1	37.3
set 2	53.3	47.9	47.1	45.5	43.1	38.1	36.6
set 3	55.1	47.7	45.5	45.5	44.5	38.6	36.5
set 4	52.9	49.5		44.9	45.1	38.5	36.4
set 5	53.1	46.1		46.3	41.6		36.1
set 6				43.9	42.6		37.1
set 7				45.5			
set 8				43.3			
set 9				44.8			
average	53.6	47.9	46.5	45.0	43.4	38.6	36.7
STD	0.009	0.012	0.009	0.009	0.013	0.004	0.004
Number	5	5	3	9	6	4	6
STE	0.004	0.006	0.005	0.003	0.005	0.002	0.002

Total mean	44.5
Total STD	0.053
Total STE	0.009
Number	38

App 7- Second order calibration curve

In order to obtain more precise calibration, the second order calibration curve was assigned for methane and carbon monoxide, for which the lack of fit was observed for linear regression. Here is an example of the calculations done for methane at 600 °C by using second order data fitting. The calibration curve and the volumetric results are shown in Figure APP- 9 to Figure APP- 11. The final yield result is mentioned in Table APP- 11. As it is shown in the Table 10 the final result do not change significantly.
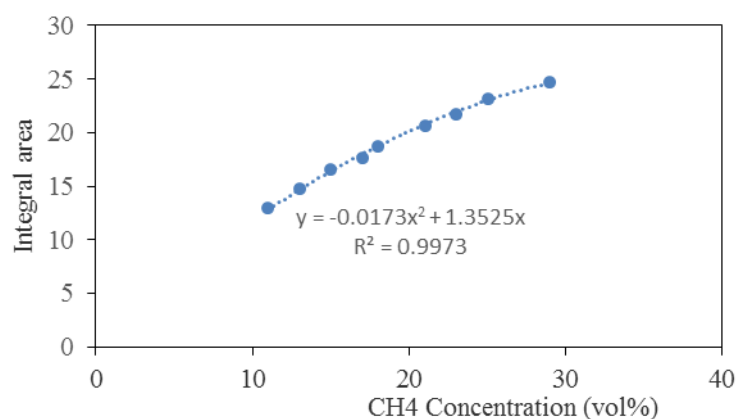

$$y = -0.0173x^2 + 1.3525x$$
$$R^2 = 0.9973$$

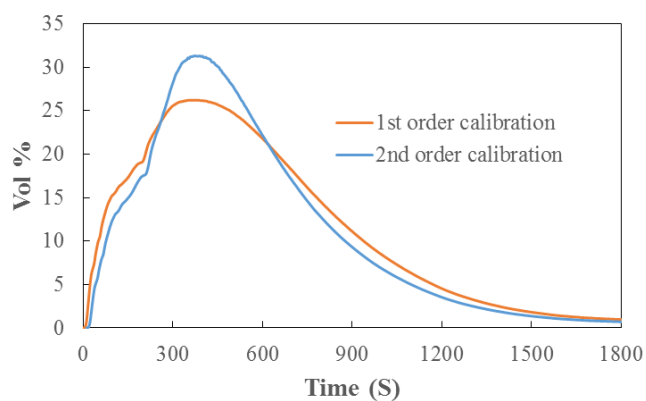*Figure APP-9- Second order calibration curve for methane*

Figure APP- 10- Methane concentration over time from slow pyrolysis of chicken manure at 600 °C (obtained by second order calibration curve)
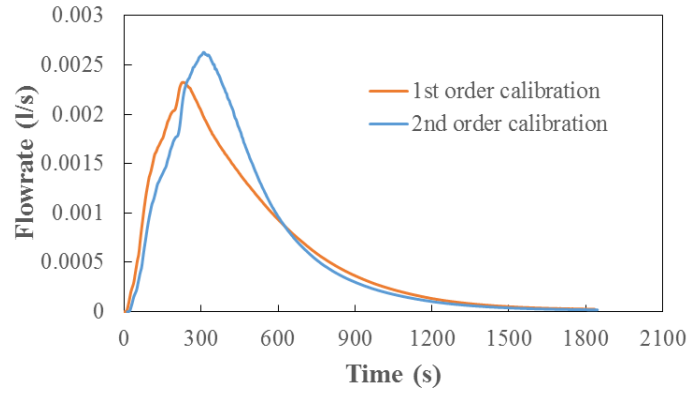
Figure APP- 11- Methane flow rate over time from slow pyrolysis of chicken manure at 600°C (obtained by second order calibration curve)

Table APP-11- CH$_4$ yield from slow pyrolysis of chicken manure at 600 °C with different calibration

	1st order	2nd order
CH$_4$ yield (gr/gr dry biomass)	0.0518	0.0527

APP 8- FTIR outlet flow measured from bubble flow meter

Despite serious attempts to seal all the compartments of the system, there was always some leakage specially from the reactors connections. Therefore the idea of having 8.5 Nl/hr of nitrogen during the whole experiment in FTIR may be deviate from reality. This problem was even more sever for the runs that produced more bio-oil, since the bio-oil could condense in the pipes and blocks the gas path. Therefore, outlet flow from FTIR was measured periodically using bubble flow meter during the process. This was done to check two facts. First, checking the presence of flow during the whole process and second, to assure that the flow loss from reactor connections are negligible. Total flow calculated from FTIR results by assuming fixed nitrogen flow of 8.5 Nl/hr and negligible amount of other compounds except CO_2 and CO and CH_4, is mentioned in Figure APP- 12.
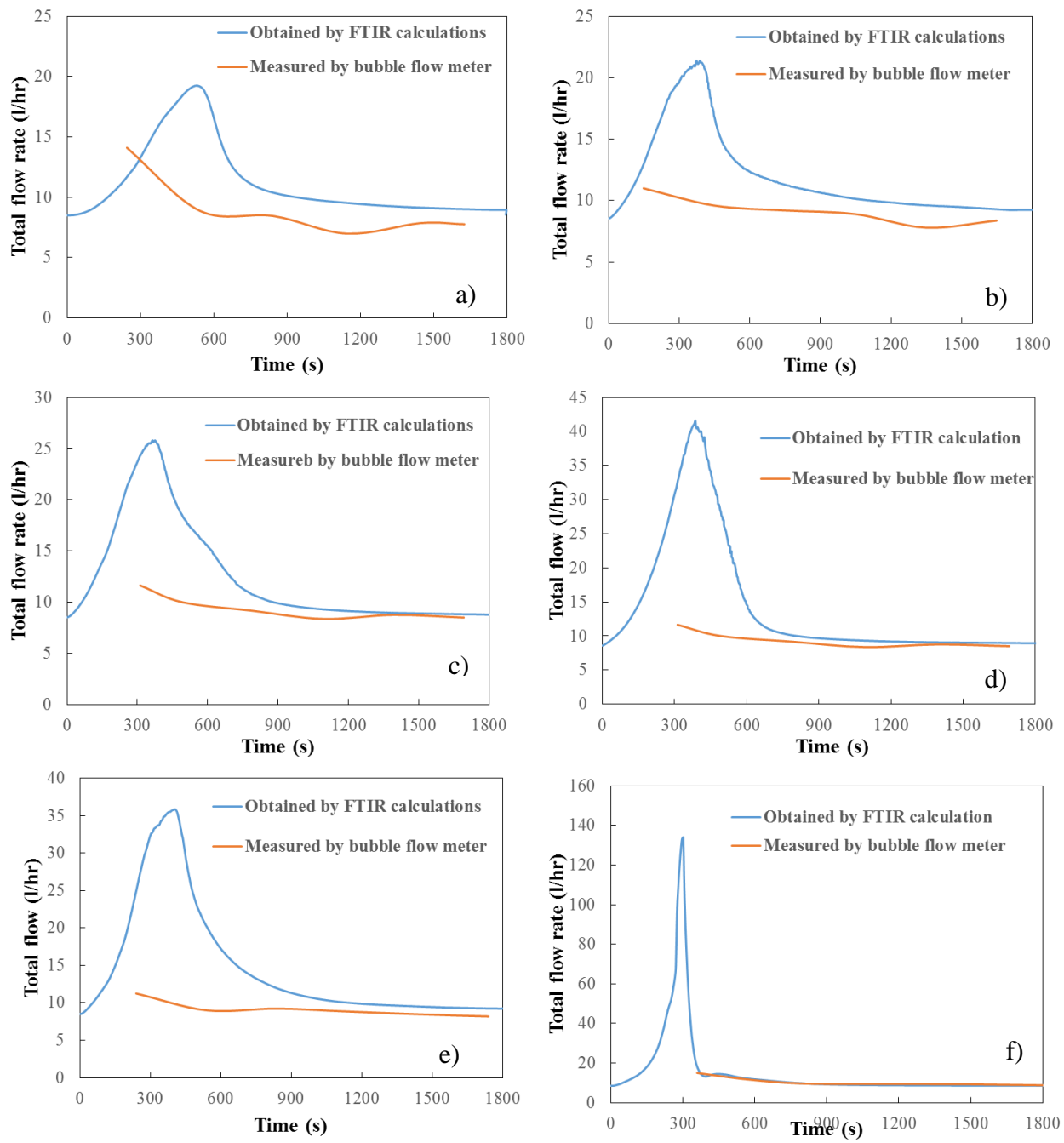
Figure APP- 12- Gas flow rate from FTIR outlet during the pyrolysis process at a) 400°C b) 450°C c) 500 °C d) 550 °C e) 600 °C f) 800 °C

APP 9- Investigating the consistency of the FTIR results

The FTIR calculation was performed for all the temperatures and for all the three compounds. Each experiment was repeated several times and at least two consistent results were obtained for each temperature. Table APP- 12 shows the result of all the repeats

Figure APP- 13 shows the consistency of the total gas production obtained by summation of the different gaseous compounds yields with the gaseous FBR yield. It can be observed that at each temperature, at least two repeats with consistent results with each other and FBR results were obtained. The result, which has the closest results to FBR, was reported as the final result in Table 4-7. The selected reported repeats at each temperature is shown with asterisk in Table APP- 12.
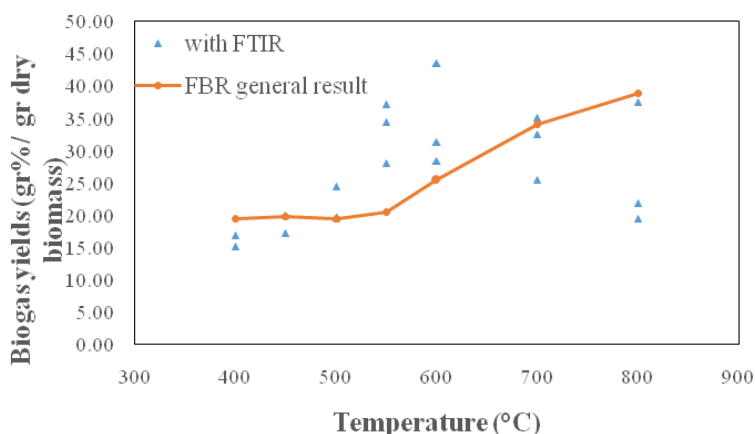

Figure APP- 13- Total biogas yield results over temperature in different repeats

Table APP-12- FTIR result of all runs

Temperature (°C)	Repeat	CO_2 gr/gr dry biomass	CH_4 gr/gr dry biomass	CO gr/gr dry biomass	Total gr/gr dry biomass	FBR gas yield gr/gr dry biomass
400	1*	0.12	0.01	0.03	0.15	0.203
	2	0.14	0.01	0.03	0.17	
450	1	0.15	0.02	0.03	0.20	0.185
	2*	0.13	0.02	0.03	0.17	
500	1	0.18	0.03	0.04	0.24	0.193
	2*	0.14	0.03	0.03	0.20	
550	1	0.24	0.05	0.06	0.34	0.197
	4	0.21	0.04	0.12	0.37	
	5*	0.19	0.04	0.05	0.28	
600	1*	0.18	0.05	0.06	0.28	0.275
	2	0.30	0.05	0.08	0.43	
	3	0.20	0.05	0.06	0.31	
700	1	0.21	0.04	0.10	0.35	0.327
	2	0.14	0.04	0.07	0.25	
	3*	0.18	0.05	0.09	0.33	
800	1*	0.17	0.06	0.15	0.38	0.379
	2	0.09	0.07	0.06	0.22	
	3	0.09	0.04	0.06	0.19	
	4	0.11	0.04	0.06	0.22	

APP 10- Comparison of the results of different analytic techniques

Equation APP-19 to Equation APP-27are used for calculating how much carbon, oxygen and hydrogen are available in gas phase regarding to FTIR results. Figure APP- 15 and Table APP- 13 show the comparison of the elemental carbon in gas obtained by FTIR and elemental analysis.

$$Carbon\ in\ biogas = carbon\ as\ CO_2 + Carbon\ as\ CO + Carbon\ as\ CH_4 \qquad \text{Equation APP-19}$$

$$Carbon\ as\ CO_2 = Total\ CO_2 \times \frac{12}{44} \qquad \text{Equation APP-20}$$

$$Carbon\ as\ CO = Total\ CO \times \frac{12}{28} \qquad \text{Equation APP-21}$$

$$Carbon\ as\ CH_4 = Total\ CH_4 \times \frac{12}{16} \qquad \text{Equation APP-22}$$

$$Oxygen\ in\ biogass = oxygen\ as\ CO_2 + Oxygen\ as\ CO \qquad \text{Equation APP-23}$$

$$Oxygen\ as\ CO_2 = Total\ CO_2 \times \frac{32}{44} \qquad \text{Equation APP-24}$$

$$Oxygen\ as\ CO = Total\ CO \times \frac{16}{28} \qquad \text{Equation APP-25}$$

$$Hydrogen\ in\ biogass = Hydrogen\ as\ CH_4 \qquad \text{Equation APP-26}$$

$$Hydrogen\ as\ CH_4 = Total\ CH_4 \times \frac{4}{16} \qquad \text{Equation APP-27}$$

Table -APP-13- FTIR and elemental analysis results comparison

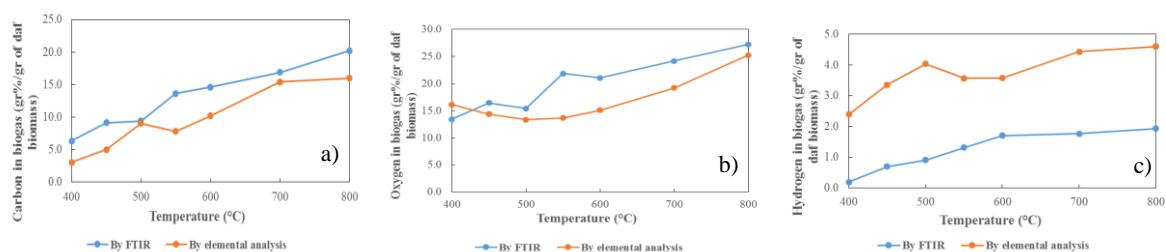| Temperature (°C)	Carbon in gas (gr%/gr DAF biomass)		Oxygen in gas (gr%/gr DAF biomass)		Hydrogen in gas (gr%/gr DAF biomass)	
	FTIR	Elemental analysis	FTIR	Elemental analysis	FTIR	Elemental analysis
400	6.3	3.2	13.4	16.2	0.2	2.4
450	9.1	5.0	16.4	14.4	0.7	3.3
500	9.4	9.0	15.4	12.5	0.9	3.9
550	13.6	7.4	21.9	13.3	1.3	3.5
600	14.6	10.2	21.1	15.1	1.7	3.4
700	16.9	15.4	24.2	19.2	1.8	4.4
800	20.2	14.8	27.2	25.3	1.9	4.7

Figure- APP-14- Comparison between the results of FTIR and elemental analysis a) carbon b) oxygen c) hydrogen